THE UNIVERSITY *of* EDINBURGH

Understanding the effects of drought upon carbon allocation and cycling in an Amazonian rain forest

by

Daniel Benjamin Metcalfe

Thesis

Submitted to the University of Edinburgh
for the degree of

Doctor of Philosophy

School of GeoSciences

December 2006

Declaration

I composed this thesis, the work is my own. No part of this thesis has been submitted for any other degree or qualification.

Name…Daniel Benjamin Metcalfe…….Date…11th May 2007 ……..……

Acknowledgements

The research in this thesis contributes to the Brazil-led Large Scale Biosphere - Atmosphere Experiment in Amazonia. Work was supported by a Natural Environment Research Council (U.K.) PhD studentship and a Standard Research Grant (NER/A/S/2003/1609), a Royal Society (U.K.) Dudley Stamp Memorial Fund award, and an Elizabeth Sinclair Fund award (School of Geosciences, University of Edinburgh, U.K.). I would like to thank Leonardo Sá and Ima Vieira for their scientific support and collaboration, the Museu Paraense Emilio Goeldi for the use of its field station and laboratory facilities, and Bene and Joca for committed field work assistance.

The following people made valuable contributions to this thesis by providing comments on the manuscript and assisting with field work: Patrick Meir, Mathew Williams, Yadvinder Malhi, Luiz Aragão, Antonio da Costa, Samuel Almeida, Alan Braga, Paulo Gonçalves, Joao de Athaydes and Lorna Dawson. In particular, I am grateful to my PhD supervisors- Patrick Meir, Mathew Williams and Yadvinder Malhi- for their beneficial support and advice throughout the studentship.

I would like to thank all of my friends in Edinburgh with whom I have shared so many excellent times over the last three years. In particular, I would like to thank Charlie for her morning coffee sessions, and for generally being my partner in crime.

Finally, I would like to thank my mother, father, brother and all my aunts, uncles, cousins and granparents for their unconditional love and support. I would never have got anywhere near this stage without such a great family.

Abstract

The Amazon rain forest plays an important role in regional and global biogeochemical cycling, but the region may undergo an increase in the frequency and severity of drought conditions driven by global climate change, regional deforestation and fire. The effects of this drought on carbon cycling in the Amazon, particularly below-ground, are potentially large but remain poorly understood. This thesis examines the impacts of seasonal and longer-term drought upon ecosystem carbon allocation and cycling at an Amazon rain forest site with a particular focus upon below-ground processes. Measurements are made at three one-hectare forest plots with contrasting soil type and vegetation structure, to observe responses across a range of Amazon primary forest types. A fourth plot is subjected to partial rainfall exclusion to permit measurement of forest responses to a wider range of soil moisture levels than currently exists naturally.

An analysis of the number of samples required to accurately quantify important ecosystem carbon stocks and fluxes is used to guide the sampling strategy at the field site. Quantifying root dynamics, in particular, presents methodological challenges. Thus, I critically review existing methods, and develop techniques to accurately measure root standing biomass and production. Subsequently, these techniques are used to record root responses, in terms of standing biomass, production, morphology, turnover and nutrient content, to variation in soil moisture across the four rain forest plots. There is substantial environmental variation in root characteristics. However, several responses remain consistent across plots: root production of biomass, length, and surface area, is lower where soil is dry, while root length and surface area per unit mass show the opposite pattern.

The other major component of the below-ground carbon cycle is soil carbon dioxide efflux. I partition this efflux, on each plot, into contributions from organic ground surface litter, roots and soil organic matter, and investigate abiotic and biotic

causes for observed differences within and between plots. On average, the percentage contribution of soil organic matter respiration to total soil carbon dioxide efflux declines during the dry season, while root respiration contribution displays the opposite trend. However, spatial patterns in soil respiration are not directly attributable to variation in either soil moisture or temperature. Instead, ground surface organic litter mass and root mass account for 44 % of observed spatial heterogeneity in soil carbon dioxide efflux.

Finally, information on below-ground carbon cycling is combined with above-round data, of canopy dynamics and stem wood production and mortality, to analyze the potential effects of drought upon carbon cycling in an Amazon forest ecosystem. Comparison of the rainfall exclusion plot with a similar, but unmodified, control plot reveals potentially important differences in tree carbon allocation, mortality, reproduction, soil respiration and root dynamics. The apparent net consequence of these changes is that, under drier conditions, the amount of CO_2 moving out of the forest and into the atmosphere is diminished. This synthesis of above-ground and below-ground data advances understanding of carbon cycling in rain forests, and provides information which should allow more accurate modelling of the response of the Amazon region to future drought. Additional measurements at other sites, and of other ecosystem carbon fluxes, should further refine modelling predictions.

Contents

Tables and Figures

Chapter 1.

Chapter 2. section 2.1

Chapter 2. section 2.2

Chapter 2. section 2.3

Chapter 3.

Chapter 4.

Chapter 5.

Chapter 7.

Common abbreviations used in text

Anthropogenic dark earth	ADE
Autotrophic respiration	R_a
Carbon	C
Carbon dioxide	CO_2
Carbon use efficiency	CUE
Coefficient of variation	CV
General linear model	GLM
Gross primary production	GPP
Ground surface litter respiration	R_l
Heterotrophic respiration	R_h
Infra-red gas analyzer	IRGA
Leaf area index	LAI
Net ecosystem production	NEP
Net primary production	NPP
Percentile	Pc
Petagram	Pg
Root respiration	R_r
Sample size	n
Soil organic matter	SOM
Soil organic matter respiration	R_{som}
Soil respiration	R_s
Specific litter respiration	SLR
Specific root length	SRL
Specific root respiration	SRR
Specific root surface area	SRA
Statistical significance value	P

Chapter 1

1. Introduction

1.1. Climate and Amazon carbon cycling

'Separation of temperature, CO_2, moisture and nutrient effects on below-ground processes is a prerequisite for predictive understanding of ecosystem C cycling.' (Pendall *et al*., 2004).

Tropical forests play an important role in regional and global biogeochemical cycles and climate. The Amazon rain forest alone contains up to 84 - 114 petagrams (Pg, 1 Pg = 1×10^9 tonnes) of carbon (C) in vegetation (60 - 90 Pg C: Houghton *et al*., 2000; Malhi *et al*., 2005) and the surface 30 cm soil layer (24 Pg C: Batjes *et al*., 2005). Emissions from fossil fuel burning represent an annual flux of approximately 6.3 Pg C into the atmosphere (House *et al*., 2003). So even a minor change in Amazonian C cycling could significantly alter atmospheric carbon dioxide (CO_2) levels, and hence climate. However, the frequency and severity of drought may increase in the Amazon, both due to a possible increase in the frequency of El Niño-Southern Oscillation related events driven by global climate changes (Trenberth & Hoar, 1997; Timmermann *et al.*, 1999, Cubasch *et al*., 2001; Tudhope *et al*., 2001; Schöngart *et al*., 2005), and reductions in rainfall caused by regional deforestation (Shukla *et al.*, 1990; Nobre *et al.*, 1991; Costa & Foley, 2000; Werth & Avissar, 2002) and fire (Rosenfeld, 1999; Andreae *et al.*, 2004). The effects of drought upon ecosystem structure and function in the Amazon are potentially large, but remain poorly defined. For example, El Niño related drought events appear to coincide with large CO_2 effluxes from the Amazon (Tian *et al*., 1998, Tian *et al*., 2000), which model analyses estimate to be as much as 0.6 Pg C $year^{-1}$ from 1980 to 1994 (Tian *et al*., 1998; Prentice and Lloyd 1998; Foley *et al*., 2002). However, relatively little information from field studies are available to test whether the modelled representation of drought effects in the region (i.e.: decreased forest photosynthesis and increased soil respiration) is realistic. In addition, most, but not all, climate models predict that the Amazon will switch from a net sink of C to a source around the middle of the century, due to progressive changes in temperature and rainfall (e.g. Cox *et al*., 2000;

Dufresne *et al*., 2002; Cramer *et al*., 2001; Cox *et al*; 2004). The accuracy of these projections is limited particularly by a lack of detailed knowledge about the physical controls upon ecosystem C allocation and soil respiration. Recent research has yielded valuable insights into drought-induced changes in above-ground C cycling and soil respiration (e.g.: Carswell *et al*., 2002; Nepstad *et al*., 2002; Davidson *et al*., 2004; Nepstad *et al*., 2004; Sotta *et al*., 2004; Fisher *et al*., 2006; Meir *et al*., 2006) in the Amazon. However, without additional information about below-ground plant growth it remains difficult to interpret observed patterns.

The overall purpose of this thesis, therefore, is to examine the impacts of seasonal and medium-term drought upon Amazon ecosystem C cycling, with a particular focus upon below-ground processes, over a full seasonal cycle at two one-hectare (100 × 100 meter) rain forest plots in the eastern Amazon. The impacts of medium-term (~ 4 years) soil drought have been simulated by restricting the amount of rainfall received by one of the plots since 2002 (for a detailed field site description see section 1.4.), using plastic panels placed at two meters above the ground. I present data from the fourth year of the drought treatment, and compare them to data from a floristically and structurally similar, but unmodified, control plot located nearby. In addition, I present data from two other one-hectare plots located nearby with contrasting soil type and vegetation structure, to provide an insight into spatial heterogeneity among primary forests within the Amazon. Understanding the extent and causes of this heterogeneity represents an important step towards accurately modelling ecosystem C cycling, and up-scaling localized measurements across larger spatial scales for comparison with top-down measurement systems (e.g.: satellites, flux towers). The following broad science questions are addressed:

1) How does soil moisture deficit affect above- and below-ground C stocks and fluxes?
2) What will increased soil moisture deficit mean for the allocation of C in above- and below-ground plant biomass, and the net flux of CO_2 into the atmosphere?

3) How much variation in C cycling and allocation is there within- and between four forest sites with contrasting vegetation and soil types?

Within these general questions, I use the following results from existing research to develop specific hypotheses about the potential effects of drought upon below-ground C cycling in the Amazon, which provide the focus for the subsequent Chapters of this thesis.

1.2. Drought and below-ground carbon cycling

1.2.1. Soil respiration

Soil is composed of a number of distinct fractions which store different quantities of C (Figure 1), and vary in terms of their sensitivity to environmental change. Soil respiration expels 75-80 billion tones of C annually into the atmosphere (Schlesinger 1977; Raich & Potter 1995) which is more than 11 times the recent rate of C production by anthropogenic combustion of fossil fuels (Marland & Boden 1993). So even a slight fractional change in soil C dynamics could significantly alter atmospheric CO_2 levels, and hence the climate. Soil respiration is derived from two principal sources: autotrophic respiration by roots and associated mycorrhizae, and heterotrophic respiration by microorganisms that decompose leaf litter and soil organic matter (Figure 1). Important factors affecting respiration include: 1) temperature (Winkler *et al.,*1996; Rustad *et al.,*1998; Melillo 2002), 2) soil moisture (Gulledge & Schimel 2000; Xu & Qi 2001), 3) vegetation and substrate quality (Tewary *et al.,*1982; Raich & Schlesinger 1992), 4) net ecosystem productivity (Schlesinger 1977; Raich & Potter 1995), 5) plant assimilation and allocation of C (Boone *et al.,* 1998; Högberg *et al*., 2001; Högberg & Read, 2006), 6) community dynamics of flora and fauna (Raich & Schlesinger 1992), 7) land use and/or disturbance regimes (Gordon *et al.,* 1987; Weber 1990).

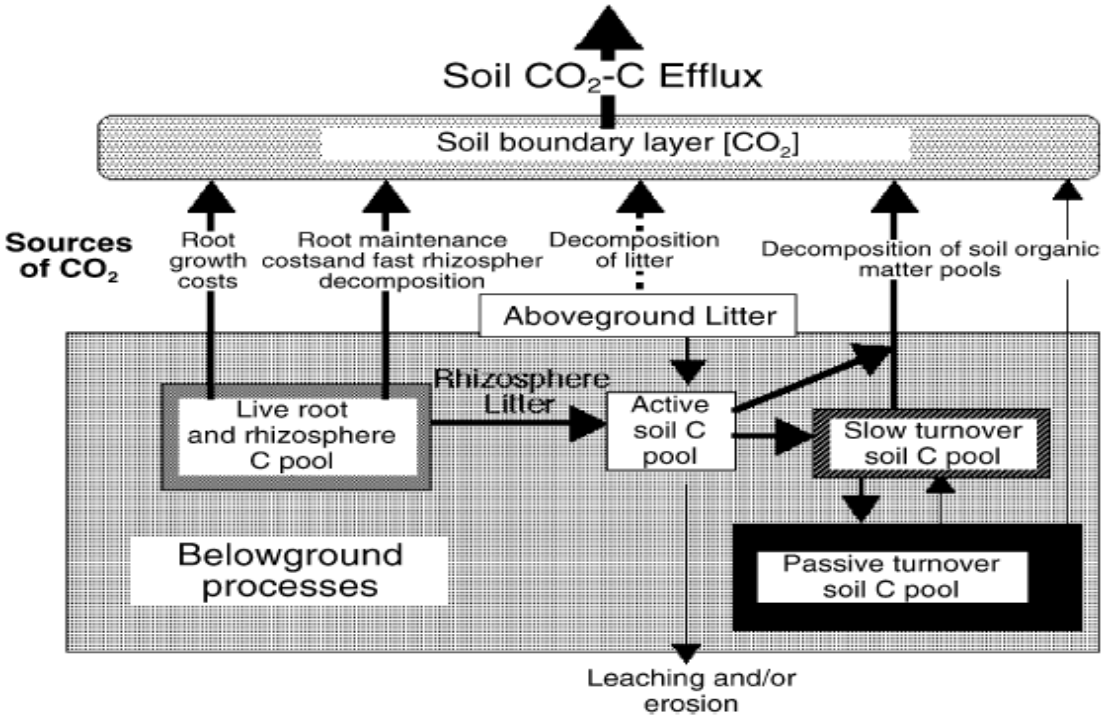

Figure 1. Below-ground C stocks and fluxes affected by environmental change, from Pendall *et al*., (2004). Soil organic matter is represented in simplified terms by three main pools: active, slow, and passive. The active pool is sustained by inputs from root exudates and decay of root and above-ground litter, and turns over relatively rapidly (years). The slow pool receives inputs mainly from the active pool and turns over on decadal to century time scales. The passive pool consists of recalcitrant C compounds with turnover times of millennia. Soil CO_2 efflux is derived from decomposition of the various soil organic matter pools, as well as live root respiration and above-ground litter decay. Other potentially important fluxes, not quantified in this thesis, are erosion of particulate C and leaching of dissolved organic C.

A large number of studies have recorded soil respiration in the Amazon (Table 1). Available data from the Amazon shows substantial spatial (Sotta *et al*., 2004) and temporal variation in soil respiration, potentially caused by heterogeneity of soil type and seasonal changes in soil water content (Tian *et al*., 1998; Sotta *et al*., 2004). Soil CO_2 efflux is often the largest component of ecosystem respiration in Amazon rain forests, accounting for 50 – 84 % of total respiration (Meir 1996; Malhi *et al*., 1999;

Chambers *et al*., 2004). Several studies in the Amazon have recorded a distinct asymptotic response of soil respiration to soil moisture (e.g.: Davidson, et al., 2000; Schwendenmann et al., 2003; Sotta et al., 2006): with soil CO_2 efflux increasing as soil moisture rises, then reaching an optimum and subsequently declining as the soil becomes waterlogged. Dry conditions inhibit microbial decomposition of labile C in organic litter and soil organic matter, with an associated decline in CO_2 production (Davidson *et al*., 1998), but waterlogged soil is a sub-optimal environment for aerobic respiration, and also blocks the transport of CO_2 produced within the soil matrix to the surface (Sotta *et al*., 2004).

Location	**Season**	**Mean efflux** μmol m^{-2} s^{-1}	**Reference**
Barcelos, Brazil	Dry	2.78	Coutinho & Lamberti, 1971
Manaus Brazil	Dry	1.39 ± 0.5	Martins & Matthes, 1978
San Carlos Venezuela	2 years	3.09 ± 0.5	Medina *et al*., 1980
Manaus, Brazil	2 years	4.48	Wofsy *et al*., 1988
Manaus, Brazil	Wet	5.87	Fan *et al*., 1990
Reserva Jaru, Brazil	Wet	5.49 ± 1.58	Meir *et al*., 1996
Fazenda Vitoria, Brazil	1 year	5.3	Davidson *et al*., 2000
Manaus, Brazil	1 year	3.79	Chambers *et al*., 2004
Rio Branco, Brazil.	1 year	4.86 ± 0.13	Salimon *et al*., 2004
Rio Branco, Brazil.	1 year	6.94 ± 0.06	Salimon *et al*., 2004
Rio Branco, Brazil.	1 year	6.00 ± 0.13	Salimon *et al*., 2004
Rio Branco, Brazil.	1 year	7.26 ± 0.13	Salimon *et al*., 2004
Manaus, Brazil	1 year	6.38 ± 0.32	Sotta *et al*., 2004
Caxiuana, Brazil	2 years	3.91 ± 0.19	Sotta *et al*., 2006
Caxiuana, Brazil	2 years	3.09 ± 0.25	Sotta *et al*., 2006

Table 1. Summary of soil respiration values from the Amazon rain forest, adapted from Sotta *et al*., (2004). Values represent mean ± standard deviation (where available). To convert respiration units of μmol m^{-2} s^{-1} into g m^{-2} hr^{-1} divide by 6.312. To convert CO_2 flux into C multiply by 0.27.

1.2.2. Root dynamics

A significant fraction of gross primary production (GPP) is allocated below-ground in the form of root growth, respiration and exudates. Jackson *et al.,* (1997) estimated that fine roots account for at least 33% of global annual terrestrial net primary production (NPP). This C store is highly dynamic and sensitive to changes in both the soil environment (Eissenstat *et al*., 2000) and above-ground C assimilation and allocation (Högberg *et al*., 2001; Högberg & Read, 2006). A wide variety of studies have documented that plants in dry ecosystems tend to allocate a greater proportion of their resources below-ground, compared to vegetation in wetter climates (see Joslin *et al*., 2000, and references therein). These observations of general plant community characteristics shaped over an evolutionary time-scale have contributed to the development of the concept that plants may respond to short-term drought conditions by increasing growth of below-ground biomass relative to above-ground components. According to the functional balance theory, as water becomes limiting, plants should preferentially allocate C to roots where photosynthate can be used to increase water uptake (Thornley, 1972; Cannell & Dewar, 1994). The product of this shift in allocation should be an increase in the production of root tissue relative to foliage and stem wood. However, attempts to test this hypothesis, either by surveying vegetation along a rainfall gradient or using large-scale irrigation experiments, have yielded conflicting results (Joslin *et al*., 2000, and references therein) possibly because any changes in allocation predicted by the functional balance theory may be offset by drought induced reductions in GPP (Williams *et al*., 1998; Schwarz *et al*., 2004) or localised changes in the structure of drying soil which impede root growth (Whalley *et al*., 1998; Bingham & Bengough, 2003; Bengough *et al*., 2006).

There is also evidence that drought may impact upon the dynamics of C stored within roots. Some studies indicate that root mortality is likely to accelerate in response to drought (Klepper *et al*., 1973; Hayes & Seastedt, 1987; Huck *et al*., 1987). However, decomposition of dead root tissue may be inhibited by dry conditions. It remains unclear what the net effect of these two processes, responding independently to drought, means for the efflux of C into, and out of, the soil via roots.

Root characteristic	Summary reference	value
Total root mass (kg m^{-2})	Jackson *et al*., 1996	4.9
Fine root mass (kg m^{-2})	Jackson *et al*., 1997	0.57
Live fine root mass (kg m^{-2})	Jackson *et al*., 1997	0.33
Live fine root length (km m^{-2})	Jackson *et al*., 1997	4.1
Live fine root area (m^2 m^{-2})	Jackson *et al*., 1997	7.4
Total root mass in surface 30 cm (%)	Jackson *et al*., 1996	69
Fine root mass in surface 30 cm (%)	Jackson *et al*., 1997	57
Root : shoot ratio	Jackson *et al*., 1996	1 : 19
Annual total root turnover (%)	Gill & Jackson, 2000	10
Annual fine root turnover (%)	Gill & Jackson, 2000	78

Table 2. Summary of important root characteristics for the tropical evergreen forest ecosystem. Fine roots are defined here as roots less than 2 mm in diameter. Summary values are means of data from the following sources. (Jackson *et al*., 1996): Berish, 1982; Gower, 1987; Greenland & Kowal, 1960; Huttel, 1975; Klinge, 1973; Klinge & Herrera, 1978; Mensah & Jeník, 1968; Vance & Nadkarni, 1992; Nepstad *et al*., 1994. (Jackson *et al*., 1997): Cavalier, 1992; Arunachalam *et al*., 1996; Berish, 1982; Gower, 1987; Huttel, 1975; Klinge, 1973; Lugo, 1992; Mensah & Jeník, 1968; Nepstad *et al*., 1994; Silver & Vogt, 1993; Vance & Nadkarni, 1992. (Gill & Jackson, 2000): Arunachalam *et al*., 1996; Cuevas & Medina, 1988; Cuevas *et al*., 1991; Jordan & Escalante, 1980; Kummerow *et al*., 1990; Lehman & Zech, 1998; Schroth & Zech, 1995; Singh & Singh, 1981.

Information about root characteristics, and responses to environmental changes, are relatively scarce in tropical forests. A number of global reviews of root characteristics have summarized available knowledge about the tropical evergreen forest ecosystem (Table 2). Information available from the Amazon region indicates that roots account for a substantial proportion of total ecosystem NPP, contribute ~ 50 % (24 – 73 %) to total soil CO_2 efflux (Subke *et al*., 2006), turnover on seasonal to annual timescales, and are sensitive to a range of environmental factors including soil moisture and texture (Silver *et al*., 2000; Silver *et al*., 2005).

1.3. Measuring below-ground carbon fluxes

The main contribution of this thesis is to present and analyze data on below-ground C cycling in the Amazon. Despite the importance of below-ground processes to understanding of Amazon ecosystem functioning, relatively little information exists because of the difficulties inherent in sampling and processing below-ground C stocks and fluxes. There exist a range of methods for quantifying most components of the below-ground C cycle, but no clear consensus on which are the most reliable and accurate. Therefore, I provide here a brief review of the methods available for quantifying two important below-ground fluxes (soil respiration, and root dynamics), in order to provide some context to the methods and results presented in the subsequent Chapters.

1.3.1. Soil respiration

The most common approach to measuring soil respiration is to place a chamber over the soil and measure the rate of increase in CO_2 concentration within the chamber with an infra-red gas analyzer. Chamber-based systems may distort the pressure gradient from the soil to the atmosphere or directly disturb the soil itself (Livingston & Hutchinson 1995; Rayment *et al*., 2000). Quantifying the degree of measurement error is also difficult. All of these approaches assume that the amount of CO_2 produced at the soils surface is solely a function of the rate of respiration throughout the soil, when in fact changes in the diffusivity of the soil may also have an important effect (Sotta *et al*., 2004). Methods to overcome these problems include using vented or dynamic chambers to reduce pressure changes, allowing the effects of soil disturbance to fade before measurements begin, and constructing a diffusivity model of the soil at different times of the year (Davidson *et al*., 2002, and references therein).

The following methods have been developed to separate the contribution of different soil fractions to total respiration (see reviews by Hanson *et al.,* 2000; Subke *et al*., 2006): 1) component integration (Edwards & Harris 1977; Davidson *et al.,* 2002), 2) litter manipulation (Sotta *et al*., 2006), 3) root removal (Wiant 1967; Bowden *et al.,* 1993), 4) root regression (Subke *et al*., 2006, and references therein) 5) isotopic labelling (see references below). Component integration involves separating each soil fraction (e.g.: soil organic matter, roots, leaf litter) and measuring respiration rate per unit mass for each fraction. The sum of all components can then be checked against values of total soil respiration. A potential problem with this approach is that samples may undergo disturbance which could alter their respiration rate. For example, root excision could alter root respiration rate (see Amthor 1994, for a discussion of wound respiration). The relative importance of this effect may be quantified by recording root respiration over time since root excision.

An additional approach for quantifying ground surface litter respiration is litter manipulation, where soil respiration from a location where litter has been removed is compared to an unmodified location. Organic litter respiration is calculated as the difference in soil CO_2 efflux between the two locations. The main advantage of this method is that a large number of samples may be taken to capture the substantial spatial and temporal variation in litter respiration. Similarly, roots may be removed from soil at one site and compared with soil CO_2 efflux from another, unmodified site, to estimate root respiration. Removal is usually achieved through trenching; severing all the roots within a plot by inserting metal plates around the plot edges. However, this method may often overestimate root respiration because the level of root decay in trenched plots is still elevated compared to the un-trenched control and/or not all of the roots within the plot have been severed. An additional complication is that trenching may alter physical conditions within the soil (Vogt *et al.,* 1998).

If there is a positive linear relationship between soil respiration and root or litter mass, then the intercept of the line indicates the likely value of soil respiration where

root or litter mass equals zero. An advantage of this 'root regression' method (see discussion by Subke *et al.*, 2006) is that it involves less disturbance to the soil, litter and roots which could affect respiration estimates. However, this method assumes that variation in soil respiration is entirely attributable to roots and litter, which is unlikely to be true. Instead, variation in soil organic matter respiration may display considerable spatial and temporal variation.

Finally, isotopic labelling of different soil components provides a means of partitioning total soil respiration in situ, with minimal disturbance to the soil system. The following isotopic methods have been used in ecosystem C cycling studies 1) pulse labelling (Cheng *et al.,* 1993), 2) continuous labelling (Liljeroth *et al.,* 1994), 3) atomic bomb-derived ^{14}C (Dorr & Munnich 1987), 4) stable isotope techniques (Lin *et al.,* 1999), 5) free air CO_2 enrichment (Ellsworth 1999). However, the principal problem with isotopic methods is the large amount of time, effort and money required to conduct studies, particularly in remote field locations which have limited access to laboratories, chemicals and equipment.

1.3.2. Root dynamics

The following methods have been developed to sample fine root growth, mortality and distribution (see review in Vogt *et al.,* 1998): 1) sequential soil coring (Vogt & Persson 1991), 2) ingrowth cores (Flower-Ellis & Persson 1980), 3) rhizotrons or minirhizotrons (Hendrick & Pregitzer 1993; King *et al.,* 2002). Sequential coring is the most common method for determining biomass of roots and associated mycorrhizae. The data produced from this method can be analyzed in several different ways to yield estimates of growth and mortality. This method requires a large amount of effort to clean and sort roots from the cores, and yields raw data which is not easily converted into root growth data. An important flaw is that sequential coring does not account for simultaneous root growth and mortality. The ingrowth core method involves inserting a core of soil without roots into the ground,

then removing it after a specified amount of time and measuring root biomass. This is a relatively simple way of ascertaining biomass changes over time, though caution should be applied when interpreting ingrowth core data because it is possible that root growth within the core may not be representative of growth in the surrounding soil environment. Even the initial absence of roots in the soil core could distort the results (Friend *et al.,* 1990). In addition, ingrowth cores are usually used to provide root growth information at intervals of several months. Such a low temporal resolution may miss rapid, transient periods of root growth and senescence. It is possible to have a system of cores installed at different times so that data is available more often but this would be difficult to sustain given the large amount of effort required to install and process cores. Minirhizotrons or rhizotrons are clear glass/plastic chambers inserted into the soil which allow direct visual analysis of root growth dynamics at high temporal frequency. After the initial disturbance associated with insertion these chambers allow continuous *in situ* data collection. They can be used to determine rooting patterns and elongation rates, and provide qualitative information on root colour, branching patterns, senescence and parasitism (Taylor 1987; Lussenhop *et al.,* 1991; Hendrick & Pregitzer 1993). Though rhizotrons only yield information on root length per unit area of observation window, several methods exist to convert these units into root biomass production and mortality (Taylor *et al*., 1970; Itoh, 1985 Tingey *et al*., 2000; Bernier & Robitaille, 2004; Hendricks *et al*., 2006), and potentially to avoid much of the bias introduced when roots grow preferentially along the soil-rhizotron interface (Bernier & Robitaille, 2004).

1.4. Field site

The research site is located in the Caxiuanã National Forest, Pará State, north-eastern Brazil (1º43’3.5”S, 51º27’36”W). The ecosystem is a lowland *terra firme* rain forest with a high annual rainfall (~ 2272 mm) and a pronounced dry season (Fisher *et al.*,

2005). The most widespread soil type is a highly weathered yellow Oxisol (Brazilian classification: Latosol), though there is substantial spatial variation in the relative proportion of sand and clay (Ruivo & Cunha 2003). There are also patches of relatively fertile soil, called anthropogenic dark earths (ADE) or *Terra Preta do Indio*, which mark areas which were intensively managed by indigenous populations of pre-Columban inhabitants (da Costa & Kern 1999; Lehmann *et al*., 2003).

To represent existing variation in soil type at the site, three one-hectare plots (see Table 3 for additional plot details) were established on a well drained sandy Oxisol (OX_{sand} plot), a clay-rich Oxisol (OX_{clay} plot), and an ADE ($OX_{fertile}$ plot). A fourth plot, on sandy Oxisol soil, was modified by the installation of plastic panels placed at two meters above the ground in order to exclude a proportion of incident rainfall (OX_{dry} plot, Figure 2). Data from the OX_{dry} plot was combined with data from the other, unmodified, plots to examine ecosystem C cycling over a wider range of soil moisture than currently exists naturally. The boundaries of the OX_{dry} plot were trenched to a depth of one meter to minimize lateral flow of water into the plot, and the rainfall exclusion began in January 2002. The OX_{sand}, OX_{dry} and OX_{clay} plots are located about 15 m above river water level, the water table has occasionally been observed at a depth of 10 m during the wet season, and excavation confirms that the soil and live roots extend to at least 10 m depth. Less information is available for the $OX_{fertile}$ plot: the ADE forms a surface soil layer of approximately 40 cm, below this layer a clay-rich Oxisol extends to at least 60 cm depth (total recorded soil depth of at least 1 metre), the plot is located approximately 6-10 m above river water level, and during the wet season the water level rises near the soil surface of some parts of the plot (da Costa & Kern 1999).

Plot characteristics	OX_{sand}	OX_{dry}	OX_{clay}	$OX_{fertile}$
Vegetation				
Tree number ha^{-1}	434	421	419	544
Stem basal area (m^2 ha^{-1})	23.9	24.0	25.1	36.8
Leaf area index (m^2 m^{-2})	5.3 (4, 7)	5.3 (3, 6)	5.5 (4, 7)	
Soil				
Clay content (%)	18	13	42	20
Silt content (%)	5	4	14	22
Sand content (%)	77	83	44	57
pH	4	4	5	5
Carbon content (g kg^{-1})	9	12	22	46
Nitrogen content (g kg^{-1})	0.4	0.3	2	3
Carbon:Nitrogen ratio	23	35	9	15
P (mg kg^{-1})	3	3	4	36
Ca^{2+} (mg kg^{-1})	63	–	65	2213
Mg^{2+} (mg kg^{-1})	43	–	39	313
Carbon stocks				
Total	81.2 (68, 98)	44.8 (35, 62)	106.7 (97, 121)	199.6 (191, 215)
Ground litter (t ha^{-1})	2.1 (1, 4)	1.7 (1, 3)	1.9 (1, 3)	3.0 (1, 6)
Roots (t ha^{-1})	15.5 (4, 31)	11.4 (2, 40)	14.1 (6, 27)	10.0 (3, 23)
Soil (t ha^{-1})	63.6	31.7	90.7	186.6

Table 3. Key vegetation and soil features for each plot surveyed. Values indicate mean and, where possible, 5th percentile, 95th percentile around mean (in brackets). Tree number and basal area represents all individuals over 10 cm diameter at breast height, measured in January 2005. Leaf area index values are means of 25 replicate measurements taken each month at each plot in 2005 (25 ×12 = 300 replicates), no data are available for the $OX_{fertile}$ plot. Soil type values are collated from data in Ruivo & Cunha (2003) and Sotta (2006). Percentiles could not be calculated for soil C stocks because Ruivo & Cunha (2003) present no error estimates. Root and soil C stocks are estimated only for the surface 30 cm and 100 cm soil layers respectively.

Figure 2. View **(a)** above and **(b)** below the plastic panels on the OX_{dry} plot.

1.5. Overview of thesis

The overall objective of this thesis is to examine the relationships between soil moisture and C stocks and fluxes, across a range of different rain forest and soil types at a site in the Amazon. Measurements of all major C stocks and fluxes, and potential environmental drivers, at the research site are used to address a number of specific scientific questions that are detailed below, and relate to the broad science questions introduced in section 1.1. The core of the thesis is designed as a series of four independent, but interlinking, Chapters (Chapters 2 - 5) which have been prepared for submission as articles to peer-reviewed scientific journals. Around this core text is a general introduction (Chapter 1) and discussion (Chapter 6), an appendix with a detailed explanation of field equipment and methodology (Chapter 7), and a full reference list (Chapter 8).

1.5.1. Chapter 2. Methodological considerations

This Chapter is comprised of three brief articles concerning methodological issues which required special consideration during the course of this research.

1.5.1.1. Required sample size for estimating important ecosystem parameters in a tropical rain forest

In the first analysis, the number of samples required to estimate values for all major C stocks, fluxes and environmental drivers at the site within specified confidence intervals and probability levels are calculated. This information is useful both for experimental design to calculate the sample size required to estimate mean (± confidence interval) values of chosen variables, and after data collection to estimate confidence intervals around measurements for a chosen sample size. These values have not been reported frequently for variables like root standing mass and production, especially in the tropics.

Key science questions

1) How many samples are required to quantify different ecosystem parameters within specified confidence intervals and probability levels?
2) Are there any variables which are relatively over-, or under-sampled?

Conclusions

Measurements of soil properties- temperature, moisture, C and nitrogen (N) content- show the least spatial heterogeneity: requiring a maximum of 8 samples to estimate a mean value within 10 % confidence intervals with 95% probability. In contrast, to attain the same confidence intervals and probability levels around estimates of mean ground surface litter mass, standing crop root mass, and root production require 113 - 140, 143 – 236 and 29-154 samples. Thus, more sampling effort should be invested in quantifying ground surface litter mass, standing crop root mass, and root production

compared to soil properties. These results were used to guide the sampling strategy of measurements which provide the basis for Chapters 3 -5.

1.5.1.2. A comparison of methods for converting rhizotron root length measurements into estimates of root biomass per unit ground area

Rhizotrons are increasingly used to quantify root production and mortality because they record *in situ* root activity at relatively high temporal frequency compared to alternative methodologies. However, the principal disadvantage of rhizotrons is that root measurements are recorded in units (root length per unit surface area of observation window surface) which are not directly comparable with above-ground plant production, usually quantified as biomass per unit ground area. Several methods have been presented in the literature to convert rhizotron length measurements into units of biomass per unit area but there has been no review and comparison of these different conversion methods.

This analysis applies five different conversion methods to the same dataset of rhizotron measurements. These data are used to assess differences in temporal variation in, and annual magnitude of, root biomass production estimates derived from the various methods. Potential biases inherent in each approach are briefly considered.

Key science questions

1) Are there differences between methods, in terms of the temporal variation in, and annual magnitude of root mass production estimates?

2) What are the flaws in each technique? Is there a single methodology which is likely to lead to the most accurate, un-biased estimate of root mass production?

Conclusions

Application of the different conversion methods result in root biomass production estimates ranging from 4.1 to 18.9 t ha^{-1} yr^{-1}, while temporal variation in root mass production also varies between methods. I propose that one conversion method in particular- the 'plane intersect' approach proposed by Bernier & Robitaille, (2004) - is likely to produce the most reliable estimates of root biomass production. The plane intersect conversion method is applied to estimate root biomass production and mortality in Chapter 5.

1.5.1.3. A method which corrects for underestimates when removing plant roots from soil

The lack of data on roots in the literature, relative to above-ground data, is due partly to the large amount of time required to process root samples, combined with the large sample size necessary to capture spatial and temporal variation in root mass. No current approaches entirely resolve this trade-off between investing sufficient effort in each soil sample to derive an accurate measurement of root mass, and taking enough samples to capture the majority of spatial and temporal variation in root mass. In this paper, a new technique is described and tested whereby the period of manual root removal from soil cores is split into time steps, to reveal the cumulative pattern of extraction over time. The observed pattern can then be used to estimate the amount of root material remaining in the soil sample after manual collection has finished.

Key science questions

1) Can the pattern of root retrieval over time from soil cores be modelled?
2) How much estimated root material remains in the soil sample after the period of manual removal has finished? How long would it take to manually remove this 'missing fraction'?

Conclusions

Cumulative root extraction over 120 minutes may be accurately modelled with a logarithmic curve (mean r^2 of 0.97 between observed and predicted). Predictions underestimate observed extraction by 1.9 %, on average, but there is no systematic change in the extent of this underestimate over time. Between 21 – 32 % of the total root mass present in samples remains uncollected after 40 minutes of manual root extraction. To manually collect this extra root material would take 13 hours per sample on average (ranging between 1 – 18 hours). The prediction method does introduce uncertainties, but these are small compared to uncertainties caused by spatial heterogeneity in root mass. In conclusion, this method provides a useful way of increasing the number of soil/root samples processed per unit time, without compromising measurement accuracy.

1.5.2. Chapter 3. Root responses to soil moisture variation at an eastern Amazon rain forest site.

Despite their importance to understanding of biogeochemical cycling in the Amazon, there is little information about root characteristics (e.g.: standing crop, production, morphology, turnover, nutrient content), and how they might be affected by increased drought in the Amazon. Therefore, this article examines the relationships among root

standing crop, productivity, morphology, turnover, nutrient content, and soil moisture in four Amazon rain forest plots with contrasting vegetation and soil type.

Key science questions

1) What is the effect of soil moisture upon the root characteristics measured?
2) How do observed responses fit with existing theories of how plants and their root systems are likely to respond to drought?
3) Does natural environmental variation in vegetation and soil type mask any effect of soil moisture on root characteristics?

Conclusions

Growth of root mass, length and surface area is consistently lower in drier soils, while root length and surface area per unit mass display the opposite response. The pattern of root production observed is consistent with a decline in GPP and/or changes in soil texture which impede the ability of roots to penetrate the soil under drier conditions. Observed changes in root length and surface area per unit mass suggest that alteration of root morphology may provide an important additional strategy for plants to increase water uptake. There is no clear evidence that a decline in soil moisture is linked with changes in either root turnover or root C and N content. There is substantial spatial heterogeneity in standing crop root mass, root production and morphology, but these variables respond to changes in soil moisture in a similar way across different vegetation and soil types. Whilst there is a significant relationship between root characteristics and soil moisture at this study site, none of the environmental variables measured can explain the majority of within-plot spatial variation.

1.5.3. Chapter 4. Factors controlling spatio-temporal variation in respiration from litter, roots and soil organic matter at four contrasting rain forest sites in the eastern Amazon.

In addition to root production (Chapter 3), another important soil C flux is soil respiration. Little information is available about the proportional contribution of surface organic litter, roots and soil organic matter to soil respiration, and the controls upon each of these sources of CO_2. This article, therefore, presents monthly estimates of litter, root and soil organic matter respiration over the course of 1.5 years from four Amazon rain forest plots with contrasting vegetation and soil type. Potential abiotic (soil temperature, soil moisture) and biotic (ground surface organic litter and root mass) controls upon observed spatial and temporal patterns in respiration are explored.

Key science questions

1) How does the annual magnitude of, and seasonal variation in, soil respiration vary between rain forest plots with contrasting vegetation and soil types?
2) What is proportional contribution of ground surface organic litter, roots, and soil organic matter to total soil respiration? Does this vary substantially within and between plots?
3) Which factors cause spatial and seasonal changes in respiration?

Conclusions

Across the four plots, estimated mean annual soil CO_2 efflux varies between 12.5 - 16.6 t C ha^{-1} yr^{-1}, which is partitioned into 0.1 – 1.7 t C ha^{-1} yr^{-1} from litter, 6.2 – 9.3 t C ha^{-1} yr^{-1} from roots, and 4.7 – 5.8 t C ha^{-1} yr^{-1} from soil organic matter. Respiration from all components displays a high degree of spatial variation, both within and between plots, which is not explained by either soil moisture or temperature. Instead, surface litter mass and root mass account for 44% of observed variation in soil respiration. Specifically, variation in litter respiration per unit mass and root mass account for much of the recorded variation in litter and root respiration respectively, and hence total soil respiration. There appears to be a seasonality to soil organic matter respiration: peaking in the wet season and declining during the dry season. In comparison, root and litter respiration do not show consistent seasonal changes. Though, rainfall exclusion over the OX_{dry} plot is associated with a ten-fold reduction in litter respiration relative to the other, unmodified, plots. Despite large differences in soil C stocks, CO_2 fluxes on the plots are not very different, which suggest that the amount of labile C is similar on all plots.

1.5.4. Chapter 5. Carbon cycling and allocation in an eastern Amazonian rain forest after four years of an experimental drought.

This article synthesizes information about below-ground C fluxes considered in Chapters 3 and 4, with additional data on above-ground plant mass and production. A number of hypothetical responses of forests to seasonal and medium-term drought (~ 4 years of through fall exclusion at the OX_{dry} plot) are tested. Patterns observed at his site are compared to existing results obtained from other research in the region.

Key science questions

1) How does seasonal and medium-term (~ 5 years) drought affect above- and below-ground C stocks and fluxes?
2) What do drought-induced changes in C cycling mean for forest net ecosystem production (NEP) of C?
3) How is seasonal and long-term drought likely to affect tree demography, through shifts in reproduction and tree mortality?
4) How, and why, do results differ from existing information about the effects of drought in the Amazon and elsewhere?

Conclusions

Four years of artificial soil drought on the OX_{dry} plot elicited several important responses in terms of forest growth dynamics and soil respiration. The apparent net consequence of these changes is that the forest of the OX_{dry} plot was a C sink of 0.5 t C ha^{-1} yr^{-1} over the period of measurement, whereas on the forest on the OX_{sand} plot was an estimated net C source of 0.9 t C ha^{-1} yr^{-1}. There was little difference between plots in terms of GPP (~ 29 t C ha^{-1} yr^{-1} on both plots), and the proportion of GPP invested in NPP was low (~ 28% of total assimilated C) compared with many temperate forest sites. The forest canopy appeared to be relatively resilient to drought with little change in either leaf area index of leaf litter N content. Tree reproduction appeared to be inhibited by the OX_{dry} treatment, but seasonal reproduction on the OX_{sand} plot was highest during the dry season. The strong response of reproduction to drought is consistent with the hypothesis that under water deficit plants divert resources away from non-essential tissues, and towards organs responsible for water uptake and transport (i.e.: roots). Root production was higher on the OX_{dry} plot relative to the OX_{sand} plot, but production on both plots coincided with the annual maximum of soil moisture (with an additional peak in the OX_{dry} plot at the initiation of the wet season). Tree mortality, quantified in mass terms, was highest in the OX_{dry} plot, while root mortality was lower and peaked on both plots during the wet season.

It is likely that observed patterns of root mortality reflected changes in not only root longevity, but also rates of decomposition. Annual soil CO_2 efflux was slightly lower on the OX_{dry} plot compared to the OX_{sand} plot. There was no clear seasonal pattern on either plot. In the OX_{dry} plot, this lack of seasonality disguised an increase in heterotrophic respiration during the wet season, with a rise in autotrophic respiration when conditions became drier. Autotrophic and heterotrophic respiration showed no clear seasonality on the OX_{sand} plot.

1.6. Publication status of thesis Chapters

Chapter	Status	Journal
2, section 1.5.1.1.	Conditionally accepted	Forest Ecology and Management
2, section 1.5.1.2.	In Review	Plant and Soil
2, section 1.5.1.3.	Published	New Phytologist
3	In Review	Journal of Ecology
4	Conditionally accepted	Journal of Geophysical research- Biogeosciences
5	In preparation	Global Change Biology

Chapter 2

2. Methodological considerations

2.1. Required sample size for estimating important ecosystem parameters in a tropical rain forest

2.1.1. Abstract

This study estimated required measurement sample size for several soil and vegetation characteristics at three rain forest plots in the eastern Amazon. The most spatially heterogeneous variables were measurements of ground surface litter mass, standing crop root mass, and root production that required 113 - 140, 143 – 236 and 29-154 samples respectively to estimate mean values within 10 % confidence intervals with 95 % probability. In contrast, for the same confidence and probability level only 16, 34 – 90 and 27 – 43 samples were required when measuring leaf area index, litter fall rate, and soil respiration respectively. Measurements of soil properties- temperature, moisture, C and N content- displayed the lowest degree of spatial variation: requiring a maximum of 8 samples to estimate mean values within 10 % confidence intervals with 95 % probability. My results indicate that most sampling effort should be invested in quantifying below-ground processes such as root biomass and production, and soil respiration. This information will help researchers to design field experiments and interpret collected data, particularly in tropical forests.

2.1.2. Introduction

Terrestrial ecosystems play an important role in the global C cycle and climate system (IPCC 2001). The Amazon rain forest alone contains 70-80 billion tones of C in plant biomass, and is responsible for up to 10 % of global terrestrial NPP (Houghton *et al.,* 2001; Malhi *et al*., 2006). Current attempts to quantify terrestrial C cycle components in the Amazon, and elsewhere, have been limited by the considerable time and labour costs associated with measurements, together with the high degree of spatial heterogeneity in many C stocks and fluxes.

In this context, sample size analysis is important both at the experimental design stage to calculate the sample size required to estimate mean (± confidence interval) values of chosen variables, and after data collection to estimate confidence intervals around measurements for a chosen sample size. However, given the high costs associated with even preliminary measurements of some variables (e.g.: root standing mass and production) few studies estimate required sample size for most major C stocks and fluxes simultaneously.

The purpose of this analysis, therefore, is to provide sample size data to aid decision-making by researchers designing and interpreting field experiments, particularly in tropical forests. To do this, required sample size is estimated for the following ecosystem parameters at three rain forest plots with contrasting soil and vegetation type in the eastern Amazon:

1) Soil properties (moisture, temperature, C and N content).
2) Plant biomass and production (leaf area index, litter fall, ground surface litter, root standing crop, root production estimated from ingrowth cores and rhizotrons).
3) Soil respiration.

2.1.3. Methods

The experimental site is located in the Caxiuanã National Forest, Pará State, north-eastern Brazil (1º43'3.5"S, 51º27'36"W). The forest is a lowland *terra firme* rain forest with a high annual rainfall (~ 2272 mm) and a pronounced dry season (Fisher *et al.,* 2005). The most widespread soil type is a highly weathered yellow Oxisol (Brazilian classification: Latosol), though there is substantial spatial variation in the relative proportion of sand and clay. There are also areas of relatively fertile soil, called anthropogenic dark earths (ADE), which mark locations which were intensively managed by indigenous populations of pre-Columban inhabitants (da Costa & Kern 1999; Ruivo & Cunha, 2003). To represent existing variation in soil type at the site one-hectare plots were established (see Table 1 for additional plot details) on a well drained sandy Oxisol (OX_{sand} plot), a clay-rich Oxisol (OX_{clay} plot), and an ADE ($OX_{fertile}$ plot). The OX_{sand} and OX_{clay} plots are located about 15 m above river water level, the water table has occasionally been observed at a depth of 10 m during the wet season, and excavation confirms that the soil and live roots extend to at least 10 m depth. Less information is available for the $OX_{fertile}$ plot: the ADE forms a surface soil layer of approximately 40 cm, below this layer a clay-rich Oxisol extends to at least 60 cm depth (total recorded soil depth of at least 1 metre), the plot is located approximately 6-10 m above river water level, and during the wet season the water level rises near the soil surface of some parts of the plot (da Costa & Kern 1999).

Plot characteristics	OX_{sand}	OX_{clay}	$OX_{fertile}$
Vegetation			
Tree number ha^{-1}	434	419	544
Stem basal area (m^2 ha^{-1})	23.9	25.1	36.8
Leaf area index (m^2 m^{-2})	5.3 (4, 7)	5.5 (4, 7)	
Soil			
Clay content (%)	18	42	20
Silt content (%)	5	14	22
Sand content (%)	77	44	57
pH	4	5	5
Carbon content (g kg^{-1})	9	22	46
Nitrogen content (g kg^{-1})	0.4	2	3
Carbon:Nitrogen ratio	23	9	15
P (mg kg^{-1})	3	4	36
Ca^{2+} (mg kg^{-1})	63	65	2213
Mg^{2+} (mg kg^{-1})	43	39	313
Carbon stocks			
Total	81.2 (68, 98)	106.7 (97, 121)	199.6 (191, 215)
Ground litter (t ha^{-1})	2.1 (1, 4)	1.9 (1, 3)	3.0 (1, 6)
Roots (t ha^{-1})	15.5 (4, 31)	14.1 (6, 27)	10.0 (3, 23)
Soil (t ha^{-1})	63.6	90.7	186.6

Table 1. Key vegetation and soil features for each plot surveyed. Values indicate mean and, where possible, 5th percentile, 95th percentile around mean (in brackets). Tree number and basal area represents all individuals over 10 cm diameter at breast height, measured in January 2005. Leaf area index values are means of 25 replicate measurements taken each month at each plot in 2005 (25 ×12 = 300 replicates), no data are available for the $OX_{fertile}$ plot. Soil type values are collated from data in Ruivo & Cunha (2003) and Sotta (2006). Percentiles could not be calculated for soil C stocks because Ruivo & Cunha (2003) present no error estimates. Root and soil C stocks are estimated only for the surface 30 cm and 100 cm soil layers respectively.

All measurements were made along a regularly spaced grid at 20 m intervals, marked within each plot (see Table 2 for a summary of measurements). Soil moisture (CS616 probe, Campbell Scientific, U.K.) and soil temperature (Testo 926 probe, Testo Ltd., U.K.) were recorded at a soil depth of 30 cm. Soil samples were taken from the OX_{sand} plot with opposable semi-circular cutting blades, dried in a desiccating chamber, and stored in plastic bags for C and N content analysis.

Images of the canopy were recorded with a digital camera and fish-eye lens (Nikon Coolpix 900, Nikon Corporation, Japan). Measurements on all plots were taken in the late afternoon when direct sunlight was at a minimum. The images were then analyzed with image analysis software (Hemiview 2.1 SR1, Delta-T Devices Ltd, U.K.) to calculate LAI (Hale and Edwards, 2002).

	Date	Replicates
Soil properties		
Soil moisture	June 05	25
Soil temperature	June 05	25
Soil C content	November 04	16 *
Soil N content	November 04	16 *
Vegetation properties		
Leaf area index	June 05	25
Litterfall	April 05	20
Surface litter	June & November 05	16 #
Root standing crop	June & November 05	16 #
Root mass production	April 05	16 ‡
Root length extension	April 05	9 ‡
Soil respiration	June 05	25

Table 2. Measurement date and replicate number. * Measurements made only in the OX_{sand} plot. Data was collected on two separate dates and pooled to calculate CV. There is no significant difference in values measured between dates (P = 0.38, n = 18). ‡ Root mass production estimated from ingrowth cores, length production calculated from rhizotrons.

Litter fall rate was measured using mesh traps (area = 1 m^2), placed 1 m above the ground surface. Organic litter was also removed from 115 cm^2 areas of the ground surface. Collected samples of litter fall and ground surface litter were cleaned of inorganic debris, dried at 70 ^oC to constant mass and weighed.

Soil cores (diameter = 15 cm, depth = 30 cm) were extracted using opposable semi-circular cutting blades. Roots were carefully removed by hand from the soil cores, cleaned of inorganic debris, dried at 70 ^oC to constant mass and weighed. Two mass measurements were made for standing crop root samples: 1) only roots less than 5 mm in diameter, and 2) all roots. Measurements of standing crop root mass and

surface litter mass were made in June and November 2005. There was no significant difference in values of either measurement between the two periods (P = 0.38, n = 18), and so the data were pooled.

Root production was estimated using both the ingrowth core (Steingrobe *et al.,* 2000) and rhizotron (e.g.: Sword *et al.,* 1996) methods. At the beginning of November 2004, soil cores were extracted from locations on each plot using opposable semi-circular cutting blades, the roots were removed by hand and the remaining soil was reinserted into the holes surrounded by plastic mesh bags (mesh aperture diameter = 1 cm). After a three month interval the process was repeated, and retrieved root material was cleaned of inorganic debris, dried at 70 ^{o}C to constant mass and weighed. The amount of root material which grew into the mesh bags was used to calculate production for each three-month interval. The sum of production from four intervals provided an estimate of annual root mass production. Rhizotrons were constructed from frames, supporting vertically orientated transparent plastic sheets (width = 21 cm, length = 30 cm). Rhizotrons were installed in August 2004 and measurement began in November 2004. Incremental root length extension was recorded every 15 days by tracing over roots visible at the transparent plastic face with a permanent marker. Traced roots were annotated with numbers to denote root growth from successive measurement sessions. Mean rhizotron root length extension per plot between November 2005 and November 2005 was calculated, to give an additional estimate of annual root production.

Soil respiration was measured with a closed dynamic infra-red gas analyzer (EGM-4 and SRC-1 chamber, PP Systems, U.K.). Plastic collars were inserted into the soil at each measurement location, to a depth of approximately 2 cm, to ensure a good seal between the IRGA chamber and soil. Soil respiration was calculated from the change in CO_2 concentration over time within the IRGA chamber (Blanke 1996).

Sample size analysis assumes that data is normally distributed (for a detailed description of sample size analysis see Hammond and McCullagh, 1978). This assumption was tested with the Kolmogorov-Smirnov test. Data that were not

distributed normally were subjected to a natural logarithmic transformation, and retested. After transformation all variables were normally distributed. The equation of Hammond and McCullagh (1978) was used to estimate sample size (n) for a given confidence interval and probability level:

$$n = \frac{t_\alpha{}^2 \bullet CV^2}{D^2} \quad (1)$$

Where t_α is the Student's t statistic with degrees of freedom at the α probability level (for α = 0.05, t_α = 1.96; for α = 0.1, t_α = 1.79), CV is the sample coefficient of variation (standard deviation of the sample as a percentage of the mean value), and D is the specified confidence interval (%). Confidence interval refers to the percentage margin of error in the estimate of the variable mean, while probability level specifies the percentage probability that the measurement falls within the confidence interval. At a fixed probability level, sample size was determined by:

$$n = \gamma \bullet D^{-2} \quad (2)$$

Where γ is a measurement-specific power curve parameter which specifies the relationship between n and D. To facilitate simple calculation of sample sizes by other researchers even in the absence of data to calculate standard deviation, I provided the γ parameters for all of the measured variables, at a 95 % probability level (Table 3).

2.1.4. Results and discussion

	Coefficient of variation (%)			γ parameter		
	OX_{sand}	OX_{clay}	$OX_{fertile}$	OX_{sand}	OX_{clay}	$OX_{fertile}$
Soil properties						
Soil moisture	7	11	12	198.71	471.83	511.86
Soil temperature	1	1	1	4.3954	1.4328	1.7097
Soil C content	15	—	—	809.79	—	—
Soil N content	9	—	—	296.35	—	—
Plant growth						
Leaf area index	20	—	—	1597.5	—	—
Litterfall	30	37	53	3383.7	5293.9	10807
Surface litter	54	60	60	11266	13988	13806
Fine root standing crop	53	49	64	10835	9228.2	15796
Total root standing crop	61	70	78	14315	18787	23550
Root mass production	63	28	34	15379	2930.2	4387.5
Root length extension	40	21	22	6122.3	1623.6	1868.1
Soil respiration	33	27	32	4303.2	2698.9	3891.8

Table 3. Coefficient of variation and sample size equation 2 γ parameter for all measured variables, on each plot. The γ parameter describes the following relationship between sample size (n) and confidence interval (D; %): $n = \gamma \times D^{-2}$. Parameter values presented here assume 95 % probability levels.

At this site, there was substantial between-plot variation, in terms of the amount of spatial variation in the measurements (Table 3). There were, however, several discernable trends for the site as a whole. Methods used in this study were able to quantify soil properties to a high degree of precision relatively easily. All soil characteristics recorded had a CV less than 15 % (Table 3), which means that a maximum sample size of 8 was required to estimate the true plot mean within 10 % confidence intervals, at the 95 % probability level (Table 4). In contrast, measurements of variables relating to vegetation mass and growth and soil respiration were more spatially heterogeneous (Table 3), and hence required more samples to achieve the same level of precision (Table 4). In general, measurements of root and surface litter dynamics (mass and production) displayed high CV, relative to measurements of above-ground vegetation characteristics such as LAI and litter fall (Table 3).

	OX_{sand}		OX_{clay}		$OX_{fertile}$	
	90 %	95 %	90 %	95 %	90 %	95 %
Soil properties						
Soil moisture	2	2	4	5	4	5
Soil temperature	< 1	< 1	< 1	< 1	< 1	< 1
Soil C content	7	8	—	—	—	—
Soil N content	2	3	—	—	—	—
Plant growth						
Leaf area index	13	16	—	—	—	—
Litterfall	28	34	44	53	90	108
Surface litter	94	113	117	140	115	138
Fine root standing crop	90	108	77	92	132	158
Total root standing crop	119	143	157	188	196	236
Root mass production	128	154	24	29	37	44
Root length extension	51	61	14	16	16	19
Soil respiration	36	43	23	27	32	39

Table 4. Required sample size for estimating variables within 10 % confidence intervals at both 90 % and 95 % probability levels, on each plot.

These differences between variables measured, in terms of CV, likely reflected not only genuine differences in spatial heterogeneity, but also differences in the methodology and equipment used to measure each variable. For example, LAI consistently had a lower CV than root biomass and production probably because the hemispherical camera integrated measurements of LAI over a large spatial area, whereas root standing crop mass was estimated from soil cores taken from a relatively small area. For this reason, estimates of CV provided in this study are, to an extent, specific to the methodology and equipment used. However, given that the methods and equipment used in this study are widespread, CV and sample size estimates should still prove useful.

In this study, the sample size required to estimate soil respiration within 10 % confidence intervals and at a 95 % probability level, ranged from 27 – 43 (Table 4). These values for soil respiration are consistent with other published estimates. For example, for the same confidence interval and probability level, Davidson *et al.,* (2002) estimated required sample size of 41, at a temperate forest ecosystem. While

Yim *et al.,* (2003) reported sample sizes ranging from 27 - 33, for a temperate plantation site. In contrast, Adachi *et al.,* (2005) reported much higher sample size values of 67 – 85, to estimate mean soil respiration in several Asian tropical forests with the same confidence interval and probability level used in this study. Relatively few studies provide CV for other vegetation and soil characteristics. Hendricks *et al.,* (2006) reported CV of 44.5 – 62.2 % for root standing crop recorded at a subtropical pine forest site, which are similar to my estimates of 61 – 78 % (Table 3), while Aragão *et al.,* (2005) estimated CV for LAI within several plots in the Amazon forest of 5.2 – 23 %, compared my single plot estimate of 20 %.

Results from this study suggest that most sampling effort should be spent quantifying below-ground processes such as root biomass and production, and respiration from soil. Attempts to quantify these variables, which do not take enough samples, may find that the large degree of uncertainty surrounding estimates impedes detection and interpretation of existing patterns. This is a problem because soil respiration and roots play an important, but poorly understood, role in terrestrial ecosystems (Jackson *et al.,* 1997; Davidson *et al.,* 1998; Roderstein *et al.,* 2005). In conclusion, sample size analysis provides a valuable tool for designing effective sampling strategies that yield accurate data which advance understanding of terrestrial ecosystems.

2.2. A comparison of methods for converting rhizotron root length measurements into estimates of root biomass per unit ground area

2.2.1. Abstract

Rhizotrons provide valuable information about plant root production, but measurements are made in units that are not easily comparable to above-ground plant growth. To address this deficiency several techniques have been developed to convert rhizotron measurement units into root mass production per unit ground area. In this study, four different conversion methods were applied to the same dataset of rhizotron measurements. This data was used to reveal the effect of conversion method upon estimates of the temporal variation in, and annual magnitude of, root mass production. Application of four different conversion methods resulted in root production estimates ranging from 4.1 to 18.9 t ha^{-1} yr^{-1}, while temporal variation in root mass production also varied between methods. In conclusion, researchers should carefully consider the relative merits of each conversion technique before choosing one. Based upon an assessment of each technique I propose that one in particular- the 'plane intersect' approach (Bernier *et al*. 2004)- is likely to produce the most reliable rhizotron estimates of root mass production per unit ground area.

2.2.2. Introduction

A significant fraction of C assimilated by plants is allocated below-ground to sustain growth and maintenance of root tissue (Jackson *et al*., 1997; Högberg *et al*., 2001). As a store of C and other nutrients, roots are relatively dynamic (Eissenstat *et al*., 2000), responding quickly to environmental changes with potentially large consequences for biogeochemical cycling. Several methodologies have been developed to record root production and turnover (see reviews by Vogt *et al*., 1998, Hendricks *et al*., 2006), but most face significant problems inferring root activity based upon occasional measurements. In this context, root observation chambers or rhizotrons are increasingly popular because they record *in situ* root production and turnover at high temporal frequency. However, an important limitation of the rhizotron methodology is that root measurements are recorded in units (root length per unit surface area of observation window surface) which are not directly comparable with above-ground plant production, usually quantified as biomass per unit ground area. Several methods have been presented in the literature to convert rhizotron length measurements into units of biomass per unit area (see references and further details in the methods section). However, to the authors' knowledge, there has been no review of these different conversion methods.

The purpose of this study, therefore, is to perform a review of four different conversion methods by applying them to the same dataset of rhizotron measurements to estimate fine root biomass. This data is used to reveal differences in temporal variation in, and annual magnitude of, root biomass production estimates (t ha^{-1}) derived from the various methods, and briefly assess potential biases inherent in each approach.

2.2.3. Methods

The study site is a one-hectare (100 × 100 m) plot located in the Caxiuanã National Forest, Pará State, north-eastern Brazil (1º43'3.5"S, 51º27'36"W). The forest is a lowland *terra firme* rain forest with high annual rainfall (~ 2272 mm) and a pronounced dry season between July and December (Fisher *et al*., 2005). The soil type is a highly weathered yellow Oxisol or Latosol according to the Brazilian classification (see Table 1 for further plot details). The study plot is located about 15 m above river water level, the water table has occasionally been observed at a depth of 10 m during the wet season, and excavation confirms that the soil and live roots extend to at least 10 m depth.

Plot characteristics	OX_{clay}
Vegetation	
Tree number ha^{-1}	419
Stem basal area (m^2 ha^{-1})	25.1
Leaf area index (m^2 m^{-2})	5.5 (4, 7)
Soil	
Clay content (%)	42
Silt content (%)	14
Sand content (%)	44
pH	5
Carbon content (g kg^{-1})	22
Nitrogen content (g kg^{-1})	2
Carbon:Nitrogen ratio	9
P (mg kg^{-1})	4
Ca^{2+} (mg kg^{-1})	65
Mg^{2+} (mg kg^{-1})	39
Carbon stocks	
Total	106.7 (97, 121)
Ground litter (t ha^{-1})	1.9 (1, 3)
Roots (t ha^{-1})	14.1 (6, 27)
Soil (t ha^{-1})	90.7

Table 1. Key vegetation and soil features for each plot surveyed. Values indicate mean and, where possible, 5th percentile, 95th percentile around mean (in brackets). Tree number and basal area represents all individuals over 10 cm diameter at breast height, measured in January 2005. Leaf area index values are means of 25 replicate measurements taken each month at each plot in 2005 (25 ×12 = 300 replicates). Soil type values are collated from data in Ruivo & Cunha (2003) and Sotta (2006). Percentiles could not be calculated for soil C stocks because Ruivo & Cunha (2003) present no error estimates. Root and soil C stocks are estimated only for the surface 30 cm and 100 cm soil layers respectively.

Soil cores (diameter = 15 cm, depth = 30 cm) were extracted using opposable semi-circular cutting blades at nine replicate points in the plot, at the beginning of November 2004, and the roots were carefully removed by hand. From these samples, mean plot standing crop fine root (≤ 5 mm diameter) mass in the surface 30 cm soil layer was recorded. In addition to rhizotrons, ingrowth cores were used to estimate root production. At the beginning of November 2004, soil cores were extracted from 16 points in each plot (using the equipment described above), the roots were carefully

removed by hand and the remaining soil was reinserted into the holes surrounded by plastic mesh bags (mesh aperture diameter = 1 cm). This was repeated four times (every three months) between November 2004 and November 2005. The amount of root material which grew into the mesh bags was used to calculate new root production for each three-month interval. Roots were retrieved from the soil by hand and placed into plastic bags to minimize desiccation. Root samples were then cleaned of residual soil and detritus with a soft brush and scanned at high resolution (600 dpi) within 48 hours of removal from the soil. From the scans, root length (divided into 0. 1 mm diameter categories) and volume was calculated using image analysis software (WinRHIZO Pro version 2003b, Regent Instruments, Canada). Root samples from both the standing crop and ingrowth cores were dried at 70 ^{o}C to constant mass and weighed.

In August 2004, nine rhizotrons were installed in the plot. The rhizotrons were constructed from wooden frames, supporting vertically orientated transparent plastic sheets (width = 21 cm, length = 30 cm). Incremental root length extension was recorded every 15 days by tracing over roots visible at the transparent plastic screen with a permanent marker. Traced roots were annotated with numbers to denote root diameter and growth from successive measurement sessions. Measurements commenced in November 2004, after a 3 month equilibration period, and continued for one year. Tracings were scanned and root length in each diameter category was recorded for each measurement session using image analysis software (WinRHIZO Tron, Regent Instruments, Canada). Root length was converted to root mass per unit ground area using the following different techniques:

Method 1) The depth of field 'sampled' by the rhizotrons (1.9 mm in this study, but see Taylor *et al*., 1970; Itoh, 1985) was selected because it resulted in a mean value of root length production per unit ground area equal to that derived from ingrowth cores (Tingey *et al*., 2000). Rhizotron root length per unit ground area was then converted to mass using mean root mass per unit length, calculated from ingrowth core sample root length and mass measurements.

Method 2) Adjacent to the plot, 15 ingrowth cores were established in close proximity to rhizotrons in November 2004. Using these paired ingrowth cores and rhizotrons, the following linear relationship (R^2 = 0.43) between root between root length (R_{le}, cm cm^{-2}) and root mass (R_m, t ha^{-1}) was derived:

$$R_m = R_{le} \bullet 8.43 \tag{1}$$

This linear relationship was subsequently applied to the 9 rhizotrons in the study plot, to convert length measurements into estimates of root mass production.

Method 3) From the soil cores extracted (see above), mean plot mass of roots finer than 5 mm diameter was calculated for the period immediately before the initiation of the rhizotron measurement campaign. Subsequently, percentage rhizotron root length increase over time was used to estimate percentage increase in my initial estimates of standing crop root mass (Hendricks *et al*., 2006).

Method 4) The number of roots contacting the rhizotron screen at each time-step, together with root diameter, was used to calculate the total cross-sectional surface area of intersecting roots (R_{xs}), using the following equation (Bernier *et al*., 2004):

$$\sum R_{xs} = \frac{\pi^2 \bullet \sum r^2}{\sqrt{2}} \tag{2}$$

Where r is root radius. Roots which branched after contact with the rhizotron observation screen were not counted. Using the product of equation 2, root production (P_r, g m^{-2}) for each rhizotron measurement session was computed as:

$$P_r = 2 \times 10^6 \bullet D_r \bullet (1 - F_c) \bullet R_{xs} \bullet \frac{\sin\alpha \bullet \cos\gamma}{W} \tag{3}$$

Where D_r is root tissue density (g mm^{-3}), F_c is the soil coarse fraction, α is the angle of the rhizotron observation screen relative to the ground, γ is the ground angle relative to the horizontal, and *W* is the width of the rhizotron observation screen. Root density was calculated by dividing ingrowth core sample root volume by mass (see Bernier *et al* 2005 for further details about calculating root density). The 10^6 value converts mm^2 ground area into m^2. The additional multiplication factor of 2 was used because roots can only intersect with the rhizotron screen from the front. It was assumed that if the rhizotron did not form a solid barrier an equal amount of roots would intersect from behind as well as from the front.

2.2.4. Results and discussion

Using different conversion methods on the same rhizotron data caused changes in estimates of both the temporal pattern and overall magnitude of root mass production per unit ground area. For example, methods 1, 2 and 4 estimated root production of 4.1 – 7.4 t ha^{-1} yr^{-1}, while method 3 estimated much higher production of 18.9 t ha^{-1} yr^{-1} (Figure 1 & Table 2). Method 4 resulted in a different temporal trend in root production, compared to the other methods (Figure 1), because it was the only method which did not use root length extension at the rhizotron observation screen to calculate production. It is, therefore, important to consider the following points before applying any of these methods.

	annual root production (t ha^{-1})	standard error
method 1	7.35	0.58
method 2	5.02	0.39
method 3	18.89	1.06
method 4	4.07	0.51

Table 2. Plot mean ± standard error of annual root mass production for each method. $n = 9$.

Method 3 resulted in much higher estimates of production probably because percentage increases in root stock, derived from rhizotron length measurements, were applied to standing crop estimates which included relatively coarse, heavy roots that were unlikely to grow so fast. Hendricks *et al*., (2006) applied percentage stock increases only to standing crop roots finer than 0.5 mm in diameter. Their estimates of production were, therefore, much lower. It is, however, clearly a simplification to project uniform growth rates for standing crop roots beneath a certain diameter, and zero growth of thicker roots. In addition, there is no clear consensus on the link between root diameter and growth rate, which could provide an objective basis for deciding which portion of root standing crop is likely to grow at the rates projected by the rhizotron length extension measurements.

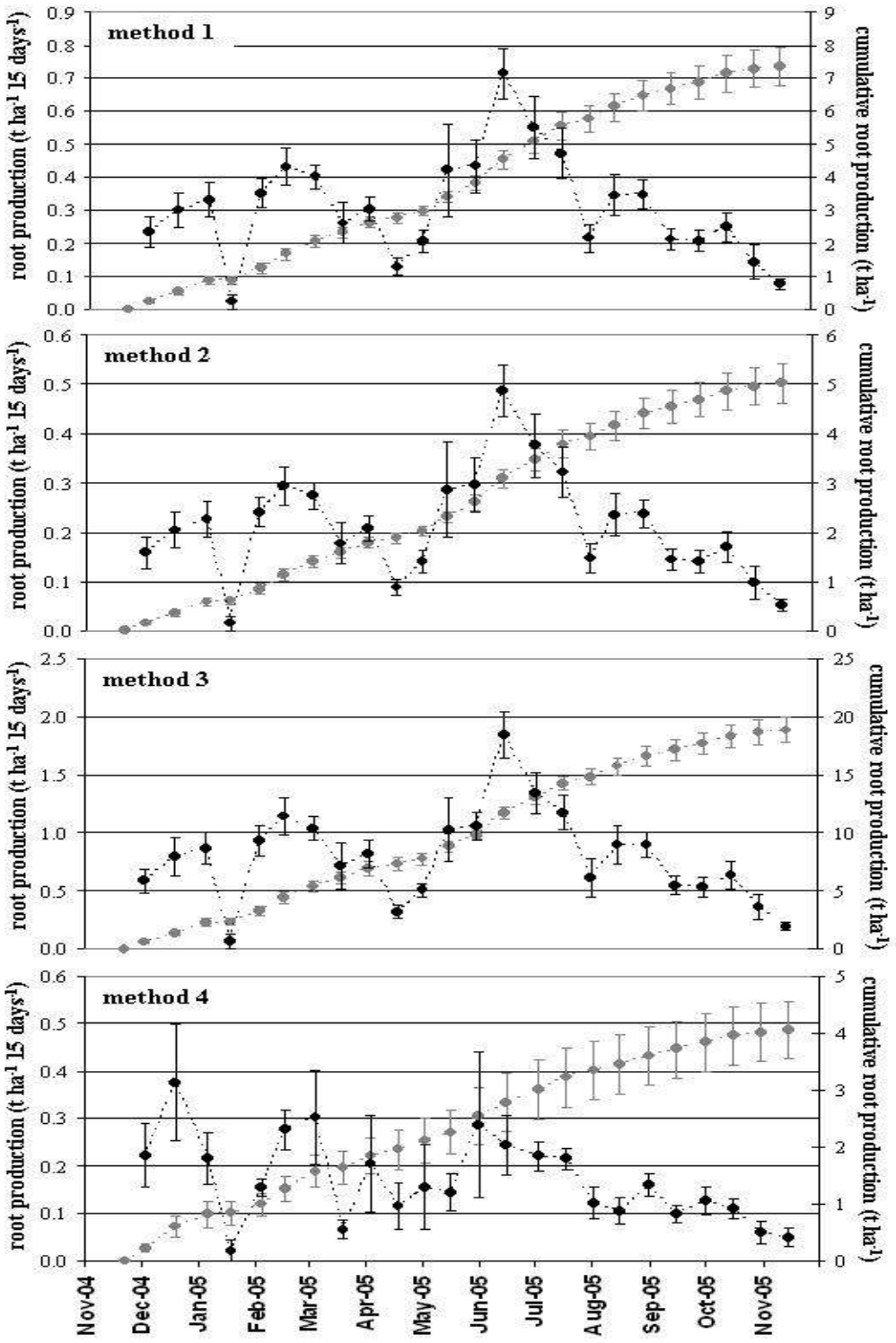

Figure 1. Plot mean dry root biomass production presented cumulatively, and every 15 days, for each method. Error bars indicate standard error of the mean, $n = 9$.

Methods 1 and 2 were calibrated with data from ingrowth cores. They were not, therefore, independent rhizotron estimates of root production. Also, they relied upon the, sometimes questionable (Vogt *et al*., 1998, Steingrobe *et al*., 2000), accuracy of production estimates from ingrowth cores. Methods 1, 2 and 3 all estimated production based upon the amount of root length visible at the rhizotron screen, and the rate of root length extension. However, both total length and length extension rate are likely to be influenced by the rhizotron itself (Withington *et al*., 2003), and therefore may not be representative of root production in the surrounding soil.

Method 4 was quite distinct in several respects. Firstly, it was not inter-calibrated with any other measurements. There was, therefore, no *a priori* reason to expect that production estimates from method 4 would agree with values from other methods. Secondly, production estimates were not derived from root growth at the rhizotron observation screen. Instead, production was calculated solely from the rate of root appearance at the rhizotron screen, growth subsequent to this appearance may be biased by the proximity of the rhizotron material and was not considered.

Based upon the results of this study, and for the reasons outlined above, I make the following conclusions. The different methods available for converting rhizotron measurement units resulted in contrasting estimates of root biomass production. Therefore, researchers should carefully consider the relative merits of each conversion technique before choosing one. Method 4 avoided many potential pitfalls inherent in the other methods, and was therefore likely to give more reliable estimates of the temporal variation in, and annual magnitude of, root mass production per unit ground area.

2.3. A method which corrects for underestimates when removing plant roots from soil.

2.3.1. Abstract

This study evaluated a novel method for removing roots from soil samples and applied it to estimate root standing crop mass (± confidence intervals) at an eastern Amazon rain forest. Roots were manually removed from soil cores over a period of 40 minutes, which was split into 10 minute time intervals. The pattern of cumulative extraction over time was used to predict root retrieval beyond 40 minutes. A maximum likelihood approach was used to calculate confidence intervals. The prediction method added 21–32 % to initial estimates of standing crop root mass. According to predictions, complete manual root collection from 18 samples would have taken ~239 hours, compared to 12 hours using the prediction method. Uncertainties (percentage difference between mean and 10^{th} and 90^{th} percentiles) introduced by the prediction method were small (12–15%), compared to uncertainties caused by spatial variation in root mass (72–191%, for 9 samples per plot surveyed). This method provided a way of increasing the number of root samples processed per unit time, without compromising measurement accuracy.

2.3.2. Introduction

Trees allocate a considerable portion of C fixed through photosynthesis to fine roots (4-69%; Vogt et al., 1996 and references therein), and the amount of C and nutrient inputs to soil via root mortality and decay often equals or exceeds that of leaf litter fall (Hendrick & Pregitzer, 1993, Nadelhoffer & Raich, 1992, Roderstein *et al.*, 2005). Root growth, mortality and decay are also dynamic processes that are highly sensitive to environmental change (Gill & Jackson, 2000, Majdi & Ohrvik, 2004). Yet despite their importance to understanding of ecosystem nutrient cycling and global biogeochemistry there is relatively little information about the amount and spatial distribution of roots in terrestrial ecosystems. For example, Houghton *et al*., (2001) stated that 'Given the Kyoto Protocol and imminent need to determine sources and sinks of C resulting from land-use change (and, perhaps, from natural processes as well), methods that can determine biomass accurately, repeatedly, and inexpensively are desperately needed'.

This gap in knowledge is due primarily to the large amount of effort, in terms of time and labour, required to extract roots from the surrounding soil (particularly non-woody, fine roots). For example, Bernier *et al*. (2005) reported that complete manual extraction of roots from soil cores (with a diameter of 4.5 cm, to a depth of 25 cm) takes up to 24 hours per core. There is a clear trade-off between investing sufficient effort in each soil sample to derive an accurate measurement of root mass and taking enough samples to capture the majority of spatial and temporal variation in root mass.

The most common approach for isolating roots is to extract a soil core and then separate roots from the surrounding soil over a sieve, either by hand (e.g.: Prathapar *et al.*, 1989) or using some type of elutriation system (Chotte *et al*., 1995, Benjamin & Nielsen, 2004). However, all of these methods are likely to underestimate the amount of root material in soil samples, because a proportion of the roots inevitably pass through the sieve, or remain uncollected by hand (Sierra *et al*., 2003).

Using sieves with finer mesh diameter will retrieve more root material, but then a relatively larger quantity of mineral grains and organic detritus will not pass through the sieve, and so the researcher is still left with the difficult task of separating roots from detritus. For example, Benjamin & Nielsen (2004) designed an automatic root sieve-washing system which processes up to 24 samples in 1.5 hours. However, after washing, samples are still contaminated with detritus, and to then manually extract roots requires an additional 20 hours per washed sample.

One method of compensating for root mass underestimates is to exhaustively remove all root material from a subset of soil samples, and then use this data to derive a generic correction factor which is applied to the rest of the dataset (see, for example, recommended protocol in MacDicken 1997). A problem with this approach is that the degree of underestimate is likely to vary between samples and locations, and therefore applying a generic correction factor will lead to inaccurate estimates of root mass. To my knowledge, no current methods provide a simple and quick way of quantifying, and correcting for, root mass underestimates on a sample by sample basis.

Finally, with current methods it remains difficult to determine whether observed differences in root amount between studies and sites reflect not only real biological differences, but also differences in site characteristics (e.g.: soil texture) and equipment (e.g.: sieve mesh diameter). For example, soil clay content could genuinely affect root structure and function (Silver *et al*., 2005), but additionally it may also alter the efficiency of root sample extraction from the soil matrix. Thus, the confounding influence of site and equipment differences hinders attempts to interpret and understand the role that roots play in different ecosystems.

These problems can be minimized however, if current methods are modified so that root collection per sample is divided into separate time intervals to reveal the pattern of root extraction over time for each sample. If the amount of roots retrieved over time changes in a predictable way, then, even after sample processing has finished, the amount that would have been retrieved had processing continued can be

estimated. The rate of root retrieval specific to each sample, and the estimated amount of roots remaining in the soil sample after a set period of processing, will depend both on the amount of roots present in the sample and on other factors such as the equipment used, the dexterity of the person manually removing root material, and soil texture. This means not only that more replicate samples can be processed per unit time without compromising measurement accuracy, but also that the confounding effect of variation between samples in terms of root removal rate can be corrected for. Since a different curve is calculated for every single soil sample, based upon the unique pattern of root extraction observed from each sample, this method should prove applicable for a wide range of vegetation and soil types.

The amount of roots retrieved at each time interval has an associated measurement error. Using a maximum likelihood approach, this measurement error can be incorporated into an estimate of the total amount of root matter in soil samples, and thus provides confidence intervals on the estimate. The objectives of this study, therefore, were to:

1) Evaluate whether root mass retrieval from soil cores can be accurately predicted.
2) Quantify measurement error for root mass collected at each time interval.
3) Use maximum likelihood techniques to estimate mean (± confidence intervals) standing crop root mass (t ha^{-1}) in two rain forest plots in the eastern Amazon.

In this study, the prediction method was applied to provide estimates of root mass but there is nothing, in principle, to prevent application of the same approach to estimate root length, surface area or volume from soil samples. The only change necessary is that roots collected from soil samples, instead of being weighed, should be scanned and analyzed with commercially available software (e.g.: WinRhizo, Regent Instruments, Canada) to record root morphology. Further, root samples collected each time interval may be sub-divided into categories (e.g.: live/dead, mycorrhizal/non-

mycorrhizal, fine/coarse, different species) to derive a more detailed assessment of root material present in soil samples.

2.3.3. Materials and methods

2.3.3.1. Field site and sampling

The experimental site is located in the Caxiuanã National Forest, Pará state, eastern Brazil (1º43'3.5"S, 51º27'36"W). The forest is a lowland *terra firme* rain forest with high annual rainfall (~ 2500mm) but a pronounced dry season (Fisher *et al.*, 2006). The most widespread soil type is a highly weathered yellow Oxisol (Brazilian classification: Latosol), though there is substantial spatial variation in the relative proportion of sand (> 0.05 mm particle diameter) and clay (< 0.02 mm particle diameter). Two one-hectare (100 × 100 meter) plots were established at locations with different vegetation and soil characteristics (Table 1). The plots are located about 15 m above river water level, the water table has occasionally been observed at a depth of 10 m during the wet season, and excavation confirms that the soil and live roots extend to at least 10 m depth. For further details of soil texture and chemistry at the site see Ruivo and Cunha (2003).

Plot characteristics	OX_{sand}	OX_{clay}
Vegetation		
Tree number ha^{-1}	434	419
Stem basal area (m^2 ha^{-1})	23.9	25.1
Leaf area index (m^2 m^{-2})	5.3 (4, 7)	5.5 (4, 7)
Soil		
Clay content (%)	18	42
Silt content (%)	5	14
Sand content (%)	77	44
pH	4	5
Carbon content (g kg^{-1})	9	22
Nitrogen content (g kg^{-1})	0.4	2
Carbon:Nitrogen ratio	23	9
P (mg kg^{-1})	3	4
Ca^{2+} (mg kg^{-1})	63	65
Mg^{2+} (mg kg^{-1})	43	39
Carbon stocks		
Total	81.2 (68, 98)	106.7 (97, 121)
Ground litter (t ha^{-1})	2.1 (1, 4)	1.9 (1, 3)
Roots (t ha^{-1})	15.5 (4, 31)	14.1 (6, 27)
Soil (t ha^{-1})	63.6	90.7

Table 1. Key vegetation and soil features for each plot surveyed. Values indicate mean and, where possible, 5th percentile, 95th percentile around mean (in brackets). Tree number and basal area represents all individuals over 10 cm diameter at breast height, measured in January 2005. Leaf area index values are means of 25 replicate measurements taken each month at each plot in 2005 (25 ×12 = 300 replicates), no data are available for the $OX_{fertile}$ plot. Soil type values are collated from data in Ruivo & Cunha (2003) and Sotta (2006). Percentiles could not be calculated for soil C stocks because Ruivo & Cunha (2003) present no error estimates. Root and soil C stocks are estimated only for the surface 30 cm and 100 cm soil layers respectively.

2.3.3.2. Quantifying prediction accuracy

Eight soil cores (diameter = 12 cm, depth = 30 cm) were extracted from an area adjacent to the OX_{sand} plot, with matching vegetation and soil characteristics, using opposable semi-circular cutting blades. Conventional cylindrical soil corers were not used because they could not sever coarse roots encountered, and caused considerable

soil compaction. The opposable semi-circular cutting blades were retracted, to remove discrete portions of the core at a time (thus minimizing compaction), and a knife was used to sever coarse roots encountered within the core hole. Roots were removed from the soil cores by hand over a period of 120 minutes, which was split into 10-minute time intervals. Subsequently, roots retrieved at each interval were cleaned of residual soil and detritus, dried at 70 Cº to constant mass and weighed. Cumulative sample dry root mass retrieved at each time interval was plotted against time for each core (Fig. 2). Two different curve types (saturation and logarithmic) were fitted to the observed pattern of retrieval from each soil core to predict root mass retrieved beyond the period of manual collection (Fig. 2). The saturation curve was described by:

$$R_t = \frac{R_c \bullet t}{k_r + t} \quad (1)$$

Where R_t is the root mass retrieved at time t, R_c is the total root mass in the sample, and k_r is a half saturation constant. The logarithmic curve was described by:

$$R_t = a\log(t) + b \quad (2)$$

Where a is a constant defining the shape of the curve and b is the intercept. The accuracy of each curve type was evaluated by fitting the two curve types to the first 40 minutes of root collection for each sample, then using them to predict the pattern of retrieval up to 120 minutes. Predicted root mass collected between 50 - 120 minutes was then compared to the actual amount of root material manually collected over the same period (Fig. 2).

2.3.3.3. Estimating measurement error

There is likely to be some uncertainty around root mass retrieved each time interval for each soil sample, caused by measurement error. This cannot be assessed with live root material because root tissue dries, and therefore loses mass, over time. To avoid this problem the following experiment was devised. A single soil core was extracted (diameter = 14 cm, depth = 30 cm), the majority of roots were removed with a sieve, and the soil was homogenized. Forty five grams of wire segments of different colours (black, brown, and white), thicknesses (0.5, 1, 2 and 5 mm diameter) and lengths (0.5, 1, 3 and 5 cm) were thoroughly mixed into the soil sample. Wire segments were then manually removed from the soil over a period of 40 minutes, which was split into 10 minute time intervals. Segments retrieved from each interval were weighed. At the end of the collection period the segments retrieved were then mixed back into the same soil sample, and the process was repeated a further nine times (Fig. 3). This data was used to estimate sample-specific mean and variation in the cumulative mass of segments collected at each time interval (Table 2).

2.3.3.4. Field application & data analysis

In June 2005, nine soil cores (diameter = 14 cm, depth = 30 cm) were removed at locations along a regular grid within each plot, using opposable semi-circular cutting blades. Roots were removed from the soil cores by hand over a period of 40 minutes, which was split into 10-minute time intervals. The cumulative increase in roots retrieved over time was used to fit a curve which predicted root extraction rate. There was some measurement error around mass collected at each time interval. There was, therefore, unlikely to be only one optimal parameter combination and curve which fitted observed data. Instead, multiple parameter combinations and curves fitted within the error limits of the observed data for each sample (Fig. 1).

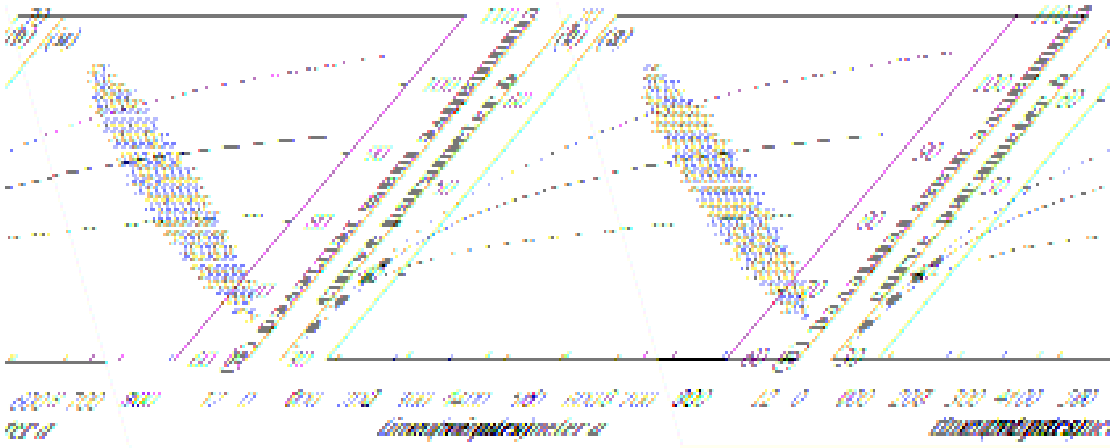

Figure 1. (a) Parameter combinations which adequately describe the observed pattern of root retrieval within specified measurement error limits, and **(b)** the resulting range in predicted cumulative mass collected until the cut-off point at 740 minutes. Data are taken from core 4, OX_{sand} plot. Black crosses = parameter combinations, black closed circles = manually retrieved mass, solid black line = mean predicted retrieval curve beyond 40 minutes, dotted black lines = 10^{th} and 90^{th} percentiles around mean predicted curve. Means and percentiles are calculated from the range of curves specified by the parameter combinations in Fig. 1a.

A maximum likelihood approach was used (van Wijk *et al*., 2002, Williams *et al*., 2006) to fit a range of acceptable curves, based upon the observed cumulative increase in roots collected over 40 minutes for each sample together with estimates of measurement error around each data point (see methods: estimating measurement error), which predict root mass retrieval (± confidence intervals) beyond 40 minutes. The optimal parameters were found by minimizing the following objective function ($O(p)$):

$$O(p) = \sum_{i=1}^{n} \frac{1}{\sigma^2_{Yi}} \left[y_{i,meas}(x_i) - y_{i,\mathrm{mod}}(x_i : p) \right]^2 \qquad (3)$$

Where n is the total number of measurements, p is the number of model parameters, $y_{i,meas}(x_i)$ is the measured value of output variable y at the value x_i of the driving

variable x, $y_{i,mod}(x_i : p)$ is the modelled value of the output variable at the value x_i of the driving variable x given the parameters p, and σ^2_{yi} is the measurement error variance for each of the observations. The minimal sum-of-squares followed a chi-squared distribution with n-p degrees of freedom. A Monte-Carlo approach was used to generate parameter confidence regions, varying the two unknown parameters at 100 points linearly arranged between specified maximum and minimum values ($8 < R_c < 80$ and $0.01 < k_r < 10$; $0.1 < a < 20$ and $0.0 < b < 100$). A chi-squared test was used to determine which of the 10000 parameter combinations which could possibly explain the pattern of root extraction from each soil sample lay within a 95 % confidence interval of the observations.

Due to the nature of a logarithmic curve, the predicted amount of root material retrieved never saturated and it was, therefore, necessary to select a cut-off point to determine the maximum root biomass**.** In this study, this point was when root mass retrieved in a single 10-minute time interval was less than 1 % of the cumulative total mass already collected. Differences in mean uncorrected (roots manually collected within the first 40 minutes) and corrected (roots manually collected plus the predicted amount of roots gathered until the cut-off point) mass were assessed with the paired sample t-test (output = test statistic t and significance p-value). Mass values were square root transformed to conform to the assumptions of parametric analysis. Statistical analysis was carried out using SPSS 13.0 for Windows (SPSS Inc., Chicago, U.S.A).

2.3.4. Results

2.3.4.1. Prediction accuracy assessment

The curve equations fitted to the first 40 minutes of root collection showed a close fit to the pattern of root removal between 50 – 120 minutes (Fig. 2; mean r^2 of 0.97 and

0.96 for the logarithmic and saturation equations respectively). On average, both equations provided conservative estimates of the total amount of root mass retrieved between 50 – 120 minutes (Fig. 2); the logarithmic equation underestimated collection by 1.9 %, which falls within the likely range of measurement error (2 %; see results: measurement error assessment), while the saturation equation underestimated by 8.2 %. The saturation equation not only underestimated by a greater amount compared to the logarithmic equation, but also the extent of the underestimate increased with each consecutive time interval (Fig. 2). Thus, the underestimate was on average only 4 % between 40 – 50 minutes but increased linearly over time such that by the 110 – 120 minute time interval the underestimate was 11 %. In contrast, there was no systematic change in the fit between the logarithmic predictions and observed data over time (Fig. 2).

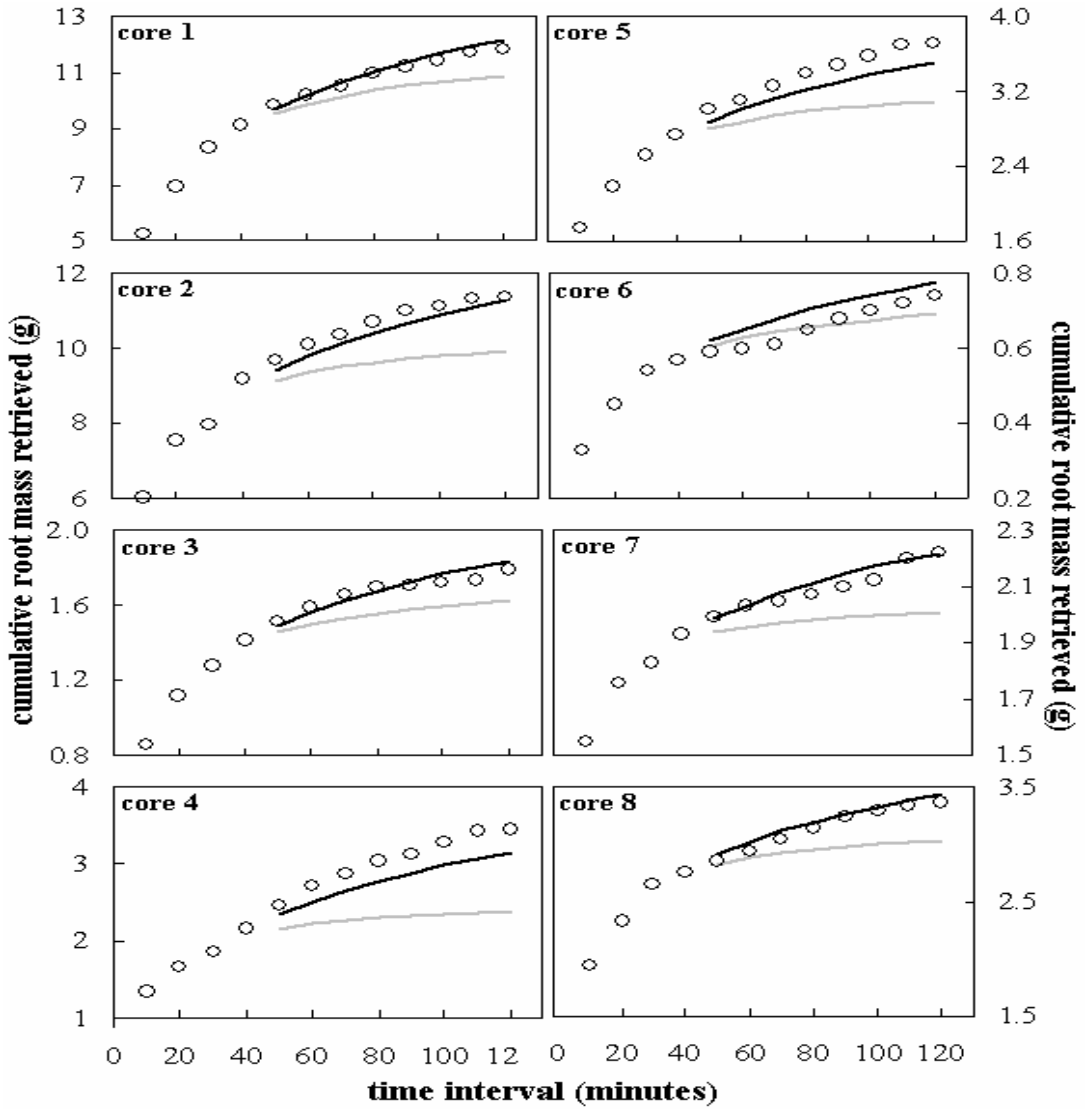

Figure. 2 Observed and predicted cumulative root mass retrieval over 120 minutes, from 8 different soil cores. Predictions are based upon the pattern of retrieval observed between 0-40 minutes. Black open circles = manually collected root mass, black line = mass retrieval predicted by the logarithmic equation, grey line = mass retrieval predicted by the saturation equation.

2.3.4.2. Measurement error assessment

There was little measurement error around replicated measurements of wire segment removal from a soil sample (Fig. 3 & Table 2); standard deviation as a percentage of the mean mass removed each time interval did not rise above 2 % (average for all intervals is 1.6 %). There was no systematic change in measurement error over time (Fig. 3 & Table 2).

Time interval	Mean root mass (grams)	Range	Variance	Standard deviation
0 – 10	22.80	1.46	0.21	0.45
10 – 20	32.52	1.79	0.54	0.73
20 – 30	37.27	0.62	0.03	0.17
30 – 40	40.59	2.62	0.63	0.80

Table 2. Results of the measurement error assessment. Mean and variation of cumulative wire segment mass collected for each time interval. Means and measures of variation are derived from 10 replicated measurements for the same soil sample, for each time interval.

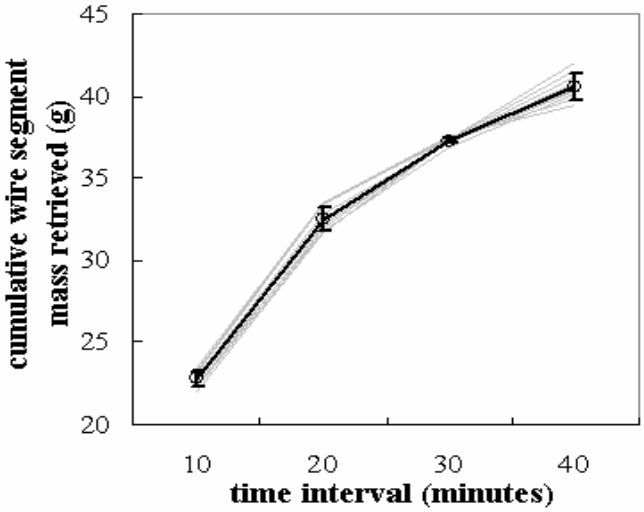

Figure 3. Cumulative wire segment mass retrieval over 40 minutes from 10 replicated measurements for the same soil sample. Grey lines = individual measurements, black open circles and black line = mean of 10 measurements. Error bars = standard deviation of the mean.

2.3.4.3. Field application of method

Based upon the prediction accuracy assessment, the logarithmic equation was chosen to predict root retrieval from all soil cores extracted from plots A and B, though the equation parameters varied between soil cores. Using results from the measurement error assessment, a generic within-sample measurement error (standard deviation as a percentage of mean) of 3 % was assigned around values of mass retrieved at every time interval, for all samples. This measurement error value was larger than that calculated directly from the measurement error assessment (2 %), but ensured that uncertainty around predicted mass was not underestimated. The number of curves per sample which could account for the observed pattern in cumulative root mass retrieved ranged from 3 to 429, out of the 10000 parameter sets that were tested on each sample. Considering only root mass retrieved in the first 40 minutes, estimated mean root standing crop in the surface 30 cm soil depth was 38.7 and 32.6 t ha^{-1}, for the OX_{sand} plot and the OX_{clay} plot respectively (see estimates from individual cores in Fig. 4).

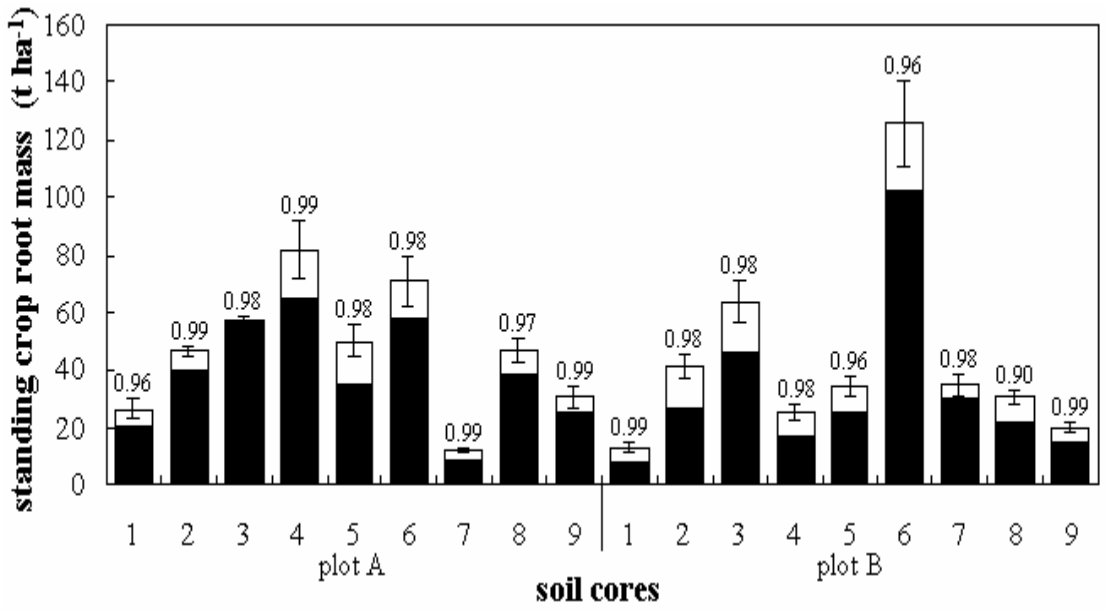

Figure 4. Standing crop root mass estimated from soil cores extracted in each plot. Values above each bar represent the R^2 of the fit between the predicted and observed root mass extracted in the first 40 minutes, for each sample. Black columns = uncorrected mass (roots manually collected within the first 40 minutes), white columns = additional mass from incorporating the prediction method. Error bars = 10th and 90th percentiles around mean predicted mass collected.

Incorporating the predictions of the curves significantly increased these initial estimates of mean plot root standing crop mass by 21 % for the OX_{sand} plot and 32 % for the OX_{clay} plot ($t = 10.1$, d.f. = 16, $p < 0.001$). Thus, the corrected estimates of standing crop mass in the surface 30 cm soil depth on plots A and B were 47.0 and 43.2 t ha^{-1} respectively (see estimates from individual cores in Fig. 4). According to the prediction method, it would have taken, on average, an additional 12.6 hours per sample (ranging between 1.0 – 18.3 hours) to manually collect this extra root material.

The proportion of root standing crop mass added through prediction rises as root mass collected manually increases (Fig. 5a). However, there was substantial variation around this general linear relationship. This indicates that there were other factors,

other than the amount of root mass within the soil samples, which determined the proportional increase in mass when using the prediction method proposed here. In addition, the predicted amount of time taken for complete root removal from soil samples decreased as the amount of roots collected in the first 40 minutes from each sample increased (Fig. 5b).

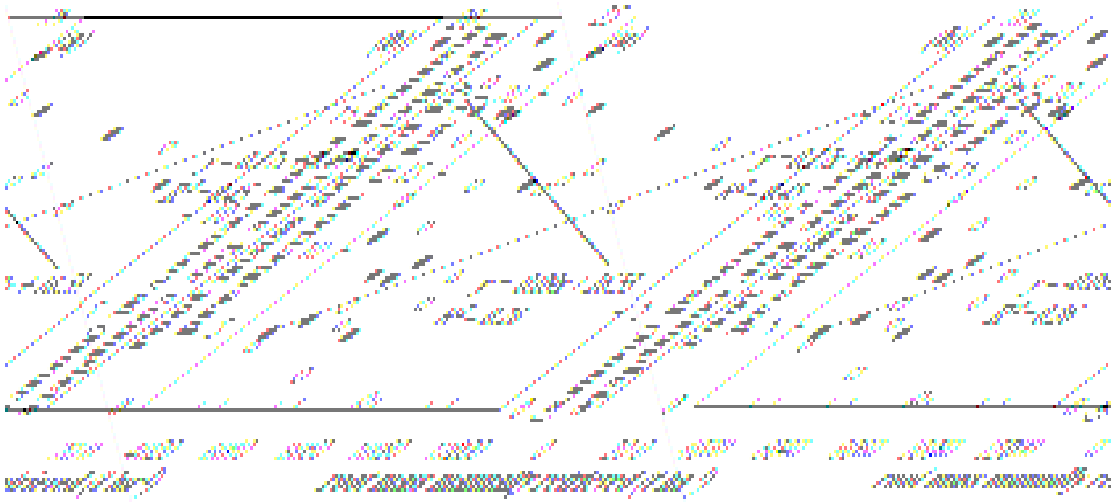

Figure 5. The relationship between root mass manually collected and (a) mass subsequently added with the prediction method, and (b) the predicted time taken for complete manual root removal. Black open circles = plot A, black closed circles = plot B.

Measurement error did lead to uncertainty around the predictions, since the range of acceptable parameter combinations and curves per sample resulted in a range of values for the predicted root mass retrieved (see error bars in Fig. 4). However, the uncertainty (quantified as the percentage difference between the mean and 10^{th} and 90^{th} percentiles) caused by measurement error was relatively small (3 % for uncorrected mass, and 12 – 15 % for corrected mass) compared to uncertainty introduced by spatial heterogeneity in standing crop root mass (72 – 191 %, see the variation in standing crop root mass between cores in Fig. 4).

2.3.5. Discussion

2.3.5.1. Method assessment

Division of the processing period into time intervals provided a simple way of checking how thoroughly a chosen processing method removed root material from the soil. Furthermore, results of the prediction accuracy assessment indicated that this method could also be used to correct for mass underestimates when removing roots from soil (Fig. 2). Though it was only possible to verify predictions over a time period of 120 minutes for 8 soil samples, further work, checking predictions against root collection over longer periods of time, could reinforce the preliminary conclusions of this study. I can think of no reason to expect that the degree of within-sample measurement error should vary between samples. Though, this issue could be directly addressed by repeating the measurement error assessment (Fig. 3) on soil samples with different characteristics (e.g.: different soil texture). According to the curve predictions, the corrected values would have taken a prohibitively long period of time to obtain solely through manual removal of root material (1.6 – 18.9 hours per sample). The prediction method, therefore, potentially allows high measurement accuracy, for a relatively large number of samples. Applying the prediction methodology to field data significantly increased my estimate of standing crop root mass by 21 – 32 %. However, these estimates were likely to be conservative because logarithmic curves generated from 40 minutes of manual sampling consistently underestimated the actual amount of root material retrieved (Fig. 2).

While there is a positive correlation between root mass manually recovered in the first 40 minutes and the proportion subsequently added by the prediction method (Fig. 5a), there was substantial variation around this general trend. There were samples which yielded either less or more root mass than would be expected from the first 40 minutes of sampling. This may be explained by variations in root removal rate caused not by the amount of root material present in the sample, but by differences in factors such as soil texture, and dexterity of the person manually removing roots from the

soil. I propose that the proportion of the total amount of root material present in a clay-rich soil sample which is not manually collected in the first 40 minutes could be relatively greater compared to an otherwise similar sample of sandy soil. This interpretation is supported by my results which showed that the degree of underestimate is greatest, on average, in soil core samples taken from the OX_{clay} plot (32 %) which occurred on clay-rich soil, compared to the sandier soil samples of the OX_{sand} plot (21 %).

I predict that the time taken for complete manual root removal is longest in soil samples where initial root mass collection (i.e.: in the first 40 minutes) is low (Fig. 5b). This may be because the soil samples which exhibited low initial root collection rates contained mainly fine roots with relatively low mass, which were difficult to remove compared to coarser roots. Thus, soil texture may impact upon root retrieval rate indirectly, by altering root structure and morphology which then directly affects manual retrieval efficiency.

2.3.5.2. Estimates of root standing crop mass

In this study, estimates of mean standing crop root mass in the top 30 cm soil layer were 47.0 and 43.2 t ha^{-1} on plots A and B respectively (see estimates from individual cores in Fig. 4). To estimate standing crop mass for the entire soil column, I used data and equations derived from root profiles taken from tropical evergreen forests to estimate that 28 % (intermediate to values of 31 % and 24 % reported by Jackson *et al.*, 1996 and Schenk & Jackson, 2002 respectively) of the total root mass present at this site occurs below the depth sampled. Thus, estimates of standing crop mass for the entire soil column are 60.2 t ha^{-1} on the OX_{sand} plot and 55.3 t ha^{-1} on the OX_{clay} plot. These estimates are higher than most values reported from similar ecosystems (49 t ha^{-1}, Jackson *et al.,* 1996) This difference may be partly due to underestimates of root mass in previous studies which do not use the prediction method proposed here,

although the extent of this effect is difficult to assess because of additional differences among studies in terms of vegetation type and methods.

At this site, root standing crop mass showed considerable spatial variation, and data frequently exhibited a right-skewed distribution. A large number of samples were required to capture this spatial heterogeneity, to estimate mean standing crop mass accurately. For example, 119 and 157 soil core samples are required to estimate standing crop root mass in plots A and B respectively, within 10 % confidence intervals with 95 % probability (D. B. Metcalfe, unpublished). To achieve these recommended sample sizes would have taken approximately 66 and 87 days (sample size multiplied by mean sample processing time per person, estimated using the prediction method, of 13.3 hours) of manual root collection per person for plots A and B respectively. In contrast, to process the same number of samples using the combined manual collection and subsequent prediction approach would have taken only ~ 3 days per person for the OX_{sand} plot and ~ 4 days per person for the OX_{clay} plot (sample size multiplied by 40 minutes). In this study, uncertainty caused by spatial variation (quantified as percentage difference between the mean and 10^{th} and 90^{th} percentiles) was 72 – 191 %, because sample size per plot is nine. In contrast, uncertainty introduced by using the prediction approach proposed here, quantified in the same terms, was 12 – 15 %. The prediction method proposed here, therefore, provided a means to obtain the large sample sizes required to quantify root standing crop mass with high precision.

2.3.6. Conclusion

Current understanding of terrestrial ecosystem processes is impaired by the relative paucity of information about root abundance and activity. This gap in knowledge is due primarily to the large amount of effort required to gather roots from soil. A novel, relatively quick method was proposed for separating roots from soil samples which produces reliable results, and was applied to estimate root standing crop mass on two

rain forest plots in the eastern Amazon. This preliminary work could be advanced by further testing of the method, with other equipment and techniques commonly used for removing roots from soil.

Chapter 3

3. Root responses to soil moisture variation at an eastern Amazon rain forest.

3.1. Abstract

Root responses to drought may impact upon ecosystem structure and function but remain poorly understood. This study, therefore, examined variation in root standing crop, productivity, morphology, turnover, nutrient content, and soil moisture over one year in four rain forest plots with contrasting soil type and vegetation structure in the eastern Amazon. Root production was assessed using ingrowth cores. Soil moisture, soil temperature and leaf litter mass of each core were recorded prior to extraction. Length and surface area of roots from cores were calculated using image-analysis software. Total standing crop root mass ranged between 30 – 45 t ha^{-1}. Production of root mass, length and surface area was lower where soil water was depleted (P<0.001), root length and surface area per unit mass showed the opposite pattern (P<0.001). Neither root turnover nor nutrient content were clearly associated with mean plot soil moisture. Root responses to soil moisture remained consistent across all four plots, despite substantial between-plot environmental variation. It may, therefore, be valid to extend these localised measurements to larger spatial scales.

3.2. Introduction

Roots play an important role in terrestrial biogeochemical cycling (Nadelhoffer & Raich, 1992; Hendrick & Pregitzer, 1993; Jackson *et al.*, 1997; Roderstein *et al.*, 2005) but are relatively understudied compared to components of above-ground plant growth (see reviews by Jackson *et al*., 1997; Norby & Jackson, 2000; Trumbore & Gaudinski, 2003). To address this deficiency a large body of research has accumulated, examining C allocation and cycling at an ecosystem scale (See reviews by Atkin *et al.,* 2000; Fitter *et al.,* 2000; Pregitzer *et al.,* 2000; Zak *et al.,* 2000, and references therein). However, the majority of these studies have focused upon the effects of increasing CO_2 and temperature, in temperate or boreal regions. Information about the effects of changes in soil moisture in tropical regions is scarcer, but potentially has important implications for the terrestrial C balance (IPCC 2001; Houghton *et al.,* 2001). While it is acknowledged that the effect of decreased water availability upon tropical rain forests is an important consideration for understanding land – climate interactions, there are relatively few field data available to support current model analyses (Wigley *et al*., 1984; Cox *et al*., 2000; Meir & Grace, 2005).

There are several different, though not necessarily mutually exclusive, mechanisms whereby soil water availability may affect root growth. The functional balance theory suggests that plants actively adjust growth of different organs to maximise uptake of the most limiting resource (Thornley, 1972; Cannell & Dewar, 1994). When water is limiting, plants should shift allocation of C away from leaves and stems, where photosynthate is used for light capture, to the roots where photosynthate can be used to increase water uptake. The product of this shift in plant allocation would be a relative increase in root mass production (and possibly standing crop) as soil moisture declines. This theory does not consider limitation by multiple resources simultaneously (Mooney *et al*., 1991), but it is supported by a substantial

body of empirical evidence (Robinson, 1986; Ingestad & Agren, 1991; Marschner *et al*., 1996; King *et al*., 1999; Giardina *et al*., 2003).

Plants may also respond to water deficit by closing their stomata (Farquhar & von Caemmerer, 1982). Decreased stomatal conductance reduces not only water transpiration from the plant, but also CO_2 diffusion into the plant. Thus plants faced with soil moisture deficit may assimilate less CO_2 compared to their counterparts growing in wetter soils (Williams *et al*., 1998; Schwarz *et al*., 2004). The product of this change in the total amount of labile C available to the plant would likely be a decline in root mass production as soil moisture falls.

The processes outlined above have focused upon plant level C fixation or allocation, but local soil conditions may also lead to a mechanism for altering root production. As the soil dries, root turgor pressure can fall and the soil may become denser. Together these factors decrease the ability of root systems to penetrate soil (Whalley *et al*., 1998; Bingham & Bengough, 2003; Bengough *et al*., 2006). Thus, a decline in soil moisture could impede root production mainly through localised changes in soil physical properties or root turgor and independently of plant C capture or growth strategy.

Additionally, an alternative plant strategy may be to stimulate water uptake not by increasing the total mass of root material, but by producing finer roots (Sharp *et al*., 1998) with relatively greater length and surface area per unit mass. This would lead to an increase in root specific length (SRL; km kg^{-1}) and root specific area (SRA; m^2 kg^{-1}) under drier conditions. However, information on root length and surface area is even scarcer than for root mass. A global review by Jackson *et al*., (1997) estimated root standing crop length and surface area in 10 major terrestrial biomes based upon 11 studies that presented root length, and just seven studies that reported values for root surface area. No data existed for half of the biomes surveyed. This lack of data hinders attempts to accurately model the behaviour of terrestrial ecosystems, and their potential responses to climate change.

The overall objective of this study, therefore, was to improve understanding of how plants alter root characteristics to adapt to changes in water availability, and whether any responses may be dependent upon, or confounded by, landscape-scale environmental variation. Data are presented from a site in the Amazon rain forest because the region plays an important role in global biogeochemical cycling and climate (IPCC, 2001; Houghton *et al*., 2001), but may experience an increase in drought conditions over this century (Shukla *et al*., 1990; Trenberth & Hoar 1997; Costa & Foley 2000; Dias *et al.*, 2002; Andreae *et al.*, 2004; Schoengart *et al.*, 2004). Landscape-scale heterogeneity in root responses was characterized by measurements from three one-hectare *terra firme* forest plots with contrasting vegetation and soil types. An additional one-hectare plot, from which incident rainfall has been largely excluded, was also surveyed to record root responses over a wider range of soil moisture than currently exists naturally in the region. Hypothetical root responses to future drought were inferred from three distinct lines of evidence. Firstly, the correlation between spatial variation in root characteristics and soil moisture (i.e.: space-time substitution). Secondly, changes in root characteristics across the dry and wet seasons. Finally, differences in root characteristics between the rainfall exclusion plot, and the other, unmodified, plots. To place any observed responses within a broader ecological context, I assessed whether the results were consistent with the general mechanisms discussed above (changes in GPP, allocation, soil structure/root turgor, root morphology). My specific aims were to:

1) Quantify root standing crop mass, production rate of root mass, length, and surface area, SRL, SRA, root nutrient content and turnover at each plot.
2) Investigate the following hypothetical responses of roots to soil moisture deficit: H_1) increase in standing crop root mass, H_2) increase in production rate of root mass, length and surface area, H_3) increase in SRL and SRA, H_4) altered root turnover, H_5) altered root chemistry.
3) Examine to what extent landscape-scale environmental variation masks any effect of soil moisture upon root characteristics.

3.3. Materials and methods

3.3.1. Site and experimental design

The experimental site is located in the Caxiuanã National Forest, Pará State, north-eastern Brazil (1º43'3.5"S, 51º27'36"W). The forest is a lowland *terra firme* rain forest with a high annual rainfall (~ 2272 mm) and a pronounced dry season (Fisher *et al.*, 2006). The most widespread soil type is a highly weathered yellow Oxisol (Brazilian classification: Latosol), though there is substantial spatial variation in the relative proportion of sand and clay. There are also patches of relatively fertile soil, called anthropogenic dark earths (ADE), which mark areas that were intensively managed by indigenous populations of pre-Columban inhabitants (da Costa & Kern 1999; Lehmann *et al*., 2003).

Plot characteristics	OX_{sand}	OX_{dry}	OX_{clay}	$OX_{fertile}$
Vegetation				
Tree number ha^{-1}	434	421	419	544
Stem basal area (m^2 ha^{-1})	23.9	24.0	25.1	36.8
Leaf area index (m^2 m^{-2})	5.3 (4, 7)	5.3 (3, 6)	5.5 (4, 7)	–
Soil				
Clay content (%)	18	13	42	20
Silt content (%)	5	4	14	22
Sand content (%)	77	83	44	57
pH	4	4	5	5
Carbon content (g kg^{-1})	9	12	22	46
Nitrogen content (g kg^{-1})	0.4	0.3	2	3
Carbon:Nitrogen ratio	23	35	9	15
P (mg kg^{-1})	3	3	4	36
Ca^{2+} (mg kg^{-1})	63	–	65	2213
Mg^{2+} (mg kg^{-1})	43	–	39	313
Carbon stocks				
Total	81.2 (68, 98)	44.8 (35, 62)	106.7 (97, 121)	199.6 (191, 215)
Ground litter (t ha^{-1})	2.1 (1, 4)	1.7 (1, 3)	1.9 (1, 3)	3.0 (1, 6)
Roots (t ha^{-1})	15.5 (4, 31)	11.4 (2, 40)	14.1 (6, 27)	10.0 (3, 23)
Soil (t ha^{-1})	63.6	31.7	90.7	186.6

Table 1. Key vegetation and soil features for each plot surveyed. Values indicate mean and, where possible, 5th percentile, 95th percentile around mean (in brackets). Tree number and basal area represents all individuals over 10 cm diameter at breast height, measured in January 2005. Leaf area index values are means of 25 replicate measurements taken each month at each plot in 2005 (25 ×12 = 300 replicates), no data are available for the $OX_{fertile}$ plot. Soil type values are collated from data in Ruivo & Cunha (2003) and Sotta (2006). Percentiles could not be calculated for soil C stocks because Ruivo & Cunha (2003) present no error estimates. Root and soil C stocks are estimated only for the surface 30 cm and 100 cm soil layers respectively.

To represent existing variation in soil type at the site, one-hectare plots (see Table 1 for additional plot details) were established on a well drained sandy Oxisol (OX_{sand} plot), a clay-rich Oxisol (OX_{clay} plot), and an ADE ($OX_{fertile}$ plot). A fourth plot (OX_{dry} plot), on a sandy Oxisol soil, was modified by the installation of plastic panels placed at two meters above the ground in order to exclude a proportion of incident rainfall (Fisher *et al.*, 2006). Data from the OX_{dry} plot were combined with data from

the other, unmodified, plots to examine root responses over a wider range of soil moisture than currently exists naturally. The boundaries of the OX_{dry} plot were trenched to a depth of one meter to minimize lateral flow of water into the plot, and the rainfall exclusion began in January 2002. The OX_{sand}, OX_{dry} and OX_{clay} plots are located about 15 m above river water level, the water table has occasionally been observed at a depth of 10 m during the wet season, and excavation confirms that the soil and live roots extend to at least 10 m depth. Less information is available for the $OX_{fertile}$ plot: the ADE forms a surface soil layer of approximately 40 cm, below this layer a clay-rich Oxisol extends to at least 60 cm depth (total recorded soil depth of at least 1 metre), the plot is located approximately 6-10 m above river water level, and during the wet season the water level rises near the soil surface of some parts of the plot (da Costa & Kern 1999).

3.3.2. Measurements

All measurements were made along a regularly spaced grid, marked within each plot. If a grid point was obstructed by a tree, a new location was chosen one meter away in a random direction. No other obstructions were encountered. No upper size limit of root diameter was imposed when measuring standing crop root mass (i.e.: coarse, structural roots were included) since this would bias estimates of total standing crop. Standing crop root mass was recorded at nine replicate points in each plot, at the end of May and November 2005 (Fig. 1). Soil cores (diameter = 15 cm, depth = 30 cm) were extracted using opposable semi-circular cutting blades, and the roots were carefully removed in a laboratory by hand within 48 hours of removal from the soil. Pincers were used to extract fine roots whilst minimizing root breakage and loss.

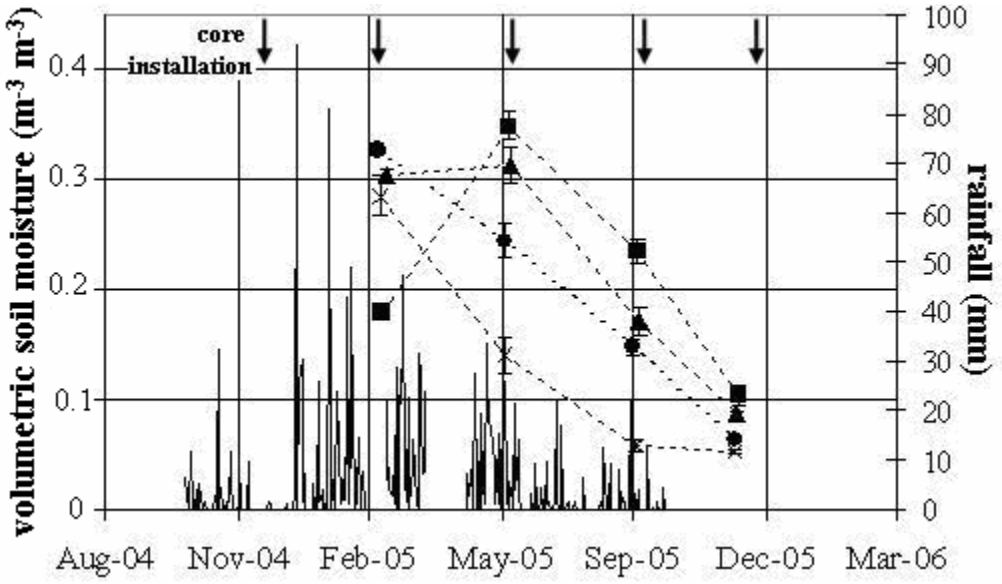

Figure 1. Daily rainfall over the study period, with mean ingrowth core volumetric soil moisture in each plot, and arrows marking ingrowth core installation and removal times. Plots: circles = OX_{sand}; crosses = OX_{dry}; squares = OX_{clay}; triangles = $OX_{fertile}$. Error bars indicate SE of the mean, *n* is 25.

Root production was estimated using the ingrowth core method (Vogt *et al*., 1998; Steingrobe *et al*., 2000; Hendricks *et al*., 2006). At the beginning of November 2004, soil cores were extracted from 16 points in each plot (using the equipment described above), the roots were carefully removed by hand in a laboratory and the remaining soil was reinserted into the holes surrounded by plastic mesh bags (mesh aperture diameter = 1 cm). This was repeated four times (every three months) between November 2004 and November 2005 (Fig. 1). The amount of root material which grew into the mesh bags was used to calculate new root production for each three-month interval. Soil samples were not washed, nor were sieves used, because this would have substantially altered the structure and texture of the soil samples. Instead, roots were retrieved from the soil in the laboratory by hand and placed into plastic bags to minimize desiccation. Root samples were then cleaned of residual soil and detritus with a soft brush and scanned at high resolution (600 dpi) within 48 hours of removal from the soil. From the scans, root length (divided into 0. 1 mm diameter

categories) and surface area was calculated using image analysis software (WinRHIZO Pro version 2003b, Regent Instruments, Canada). Roots greater than 5 mm diameter constituted a very small proportion of total length (average across all plots of 0.74 %), and so were grouped together into a single category.

Root samples from both the standing crop and ingrowth cores were dried at 70 ^{o}C to constant mass and weighed. Before core extraction, *in situ* soil moisture (CS616 probe, Campbell Scientific, Loughborough, U.K.) and soil temperature (Testo 926 probe, Testo Ltd., Hampshire, U.K.) was recorded at a depth of 30 cm, and leaf litter above each core was removed, dried at 70 ^{o}C to constant mass and weighed. Two mass measurements were made for standing crop root samples: 1) roots finer than 5 mm in diameter, and 2) all roots. Dried ingrowth core root samples from each plot were pooled and analyzed for C and N content.

3.3.3. Data analysis

From the ingrowth core data, SRL and SRA were estimated by dividing root length and surface area by root dry mass. Root turnover was calculated as annual root dry mass production divided by mean standing crop dry fine root mass (Aerts *et al*., 1992; Aber *et al*., 1985). Estimates of root standing crop and production were likely to be conservative because they only sampled roots from the surface 30 cm soil layer. To correct for this, I used data and equations derived from root profiles taken from tropical evergreen forests to estimate that 28% (intermediate to values of 31% and 24% reported by Jackson *et al.*, 1996 and Schenk & Jackson, 2002 respectively) of the total root mass present at this site occurs below the depth sampled. Thus, I derived approximate estimates of root standing crop and production in the entire soil column by multiplying initial values by 1.28. While this correction factor may compensate for underestimates of the quantity of root material present at the site, it did not account for any changes in root dynamics which may occur in deeper soil layers.

The effect of soil moisture, soil temperature and litter mass upon the root variables was assessed using a linear regression. The output from each regression was an adjusted R-squared (R_a^2) and a significance *P*-value. Plot data were pooled in the regression analysis. To assess whether plot differences confound the overall relationship between soil moisture and root variables, a general linear model (GLM) was used, and interaction terms between plot and soil moisture were included. The GLM was used to test for whether a significant interaction between soil moisture and plot might explain any observed variation in root variables. No significant interaction indicated that data from different plots may be pooled. Statistical analysis was carried out using SPSS 13.0 for Windows (SPSS Inc., Chicago, U.S.A). It was necessary to apply a natural logarithmic transformation to the root variables so that the data conformed to the assumptions of parametric analysis.

3.4. Results

	OX_{sand}	OX_{dry}	OX_{clay}	$OX_{fertile}$
Root standing crop				
total mass (t ha^{-1})	34.9 (9, 70)	25.0 (4, 85)	31.0 (12, 60)	23.4 (8, 53)
mass ≤ 5 mm (t ha^{-1})	14.3 (5, 29)	10.1 (4, 18)	15.0 (8, 26)	11.1 (5, 23)
Root production				
mass (t ha^{-1} yr^{-1})	4.1 (2, 7)	2.9 (1, 4)	3.7 (3, 5)	6.5 (4, 9)
length (km m^{-2} yr^{-1})	3.3 (2, 7)	2.2 (1, 4)	2.3 (2, 3)	3.8 (2, 5)
surface area (m^2 m^{-2} yr^{-1})	11.1 (5, 23)	7.5 (5, 13)	8.5 (6, 12)	11.7 (8, 15)
Root morphology				
SRL (km kg^{-1})	9.6 (7, 13)	10.3 (6, 18)	8.94 (7, 12)	7.7 (5, 11)
SRA (m^2 kg^{-1})	32.6 (21, 48)	33.8 (21, 51)	33.2 (26, 45)	23. 9 (18, 33)
Root turnover (%)	28.7	28.7	24.7	58.6
Root chemistry				
carbon content (g kg^{-1})	443.8	454.7	454.8	427.5
nitrogen content (g kg^{-1})	17.2	17.6	14.3	12.3
carbon : nitrogen ratio	26 : 1	26 : 1	32 :1	35 : 1

Table 2. Root standing crop, production, morphology, turnover and chemistry, measured in the surface 30 cm soil layer. Standing crop and production is quantified as the mean (5^{th} percentile, 95^{th} percentile). Root turnover and chemistry values represent single, plot-averaged estimates.

3.4.1. Root standing crop mass

To understand how drought might impact upon below-ground plant growth in the Amazon region, variation in root characteristics and soil moisture was recorded over one year in four rain forest plots with contrasting soil type and vegetation structure in the eastern Amazon. For all the plots surveyed, mean total standing crop root mass, recorded in the surface 30 cm soil layer, ranged between 25.0 and 34.9 t ha^{-1} (Table 2). A large proportion of this total mass (40-48%) was invested in roots finer than 5 mm in diameter. There was no clear difference in standing crop mass recorded during the wet and dry seasons. The majority of the measured variation in standing crop was caused by within-plot spatial heterogeneity, rather than systematic differences among plots and changes between seasons. For example, on average, 67 % of the total range

in root standing crop mass recorded across all plots and seasons was also observed within each plot and season (Table 2 & Fig. 3f). In a regression analysis, soil moisture, temperature and litter mass combined did not explain this variation in standing crop root mass ($R_a^2 = 0.02$, $P = 0.515$).

3.4.2. Root mass, length and surface area production

On all plots, root mass, length and surface area production in the surface 30 cm soil layer declined during the transition from the wet to dry seasons, though there was substantial within- and between-plot variation around this general trend (Figs. 2a – 2c). Soil temperature and leaf litter mass together did not explain the observed variation in root production. Instead, there was a significant positive relationship

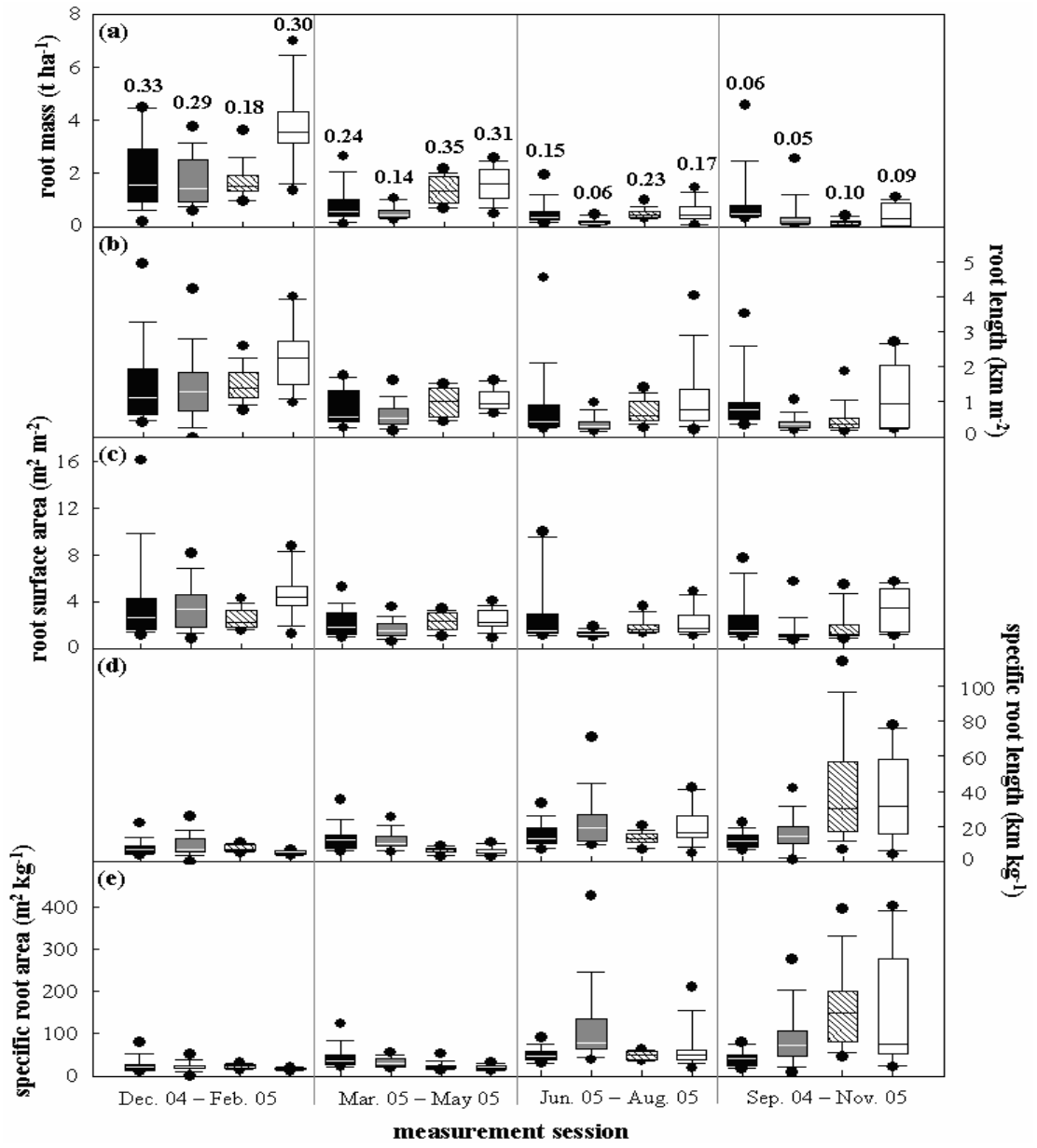

Figure 2. Seasonal pattern of **(a)** root mass production, **(b)** root length production, **(c)** root surface area production, **(d)** SRL and **(e)** SRA in the surface 30 cm soil layer. Lines within boxes denote median of 16 measurements per plot for each session, upper and lower box boundaries denote 25th and 75th percentiles, error bars denote 10th and 90th percentiles, and black circles denote outliers. Numbers above columns in Fig. 2a represent mean volumetric soil moisture (m^{-3} m^{-3}) on each plot and measurement session. Plots: black fill = OX_{sand}; grey fill = OX_{dry}; black cross hatch = OX_{clay}; white fill = $OX_{fertile}$.

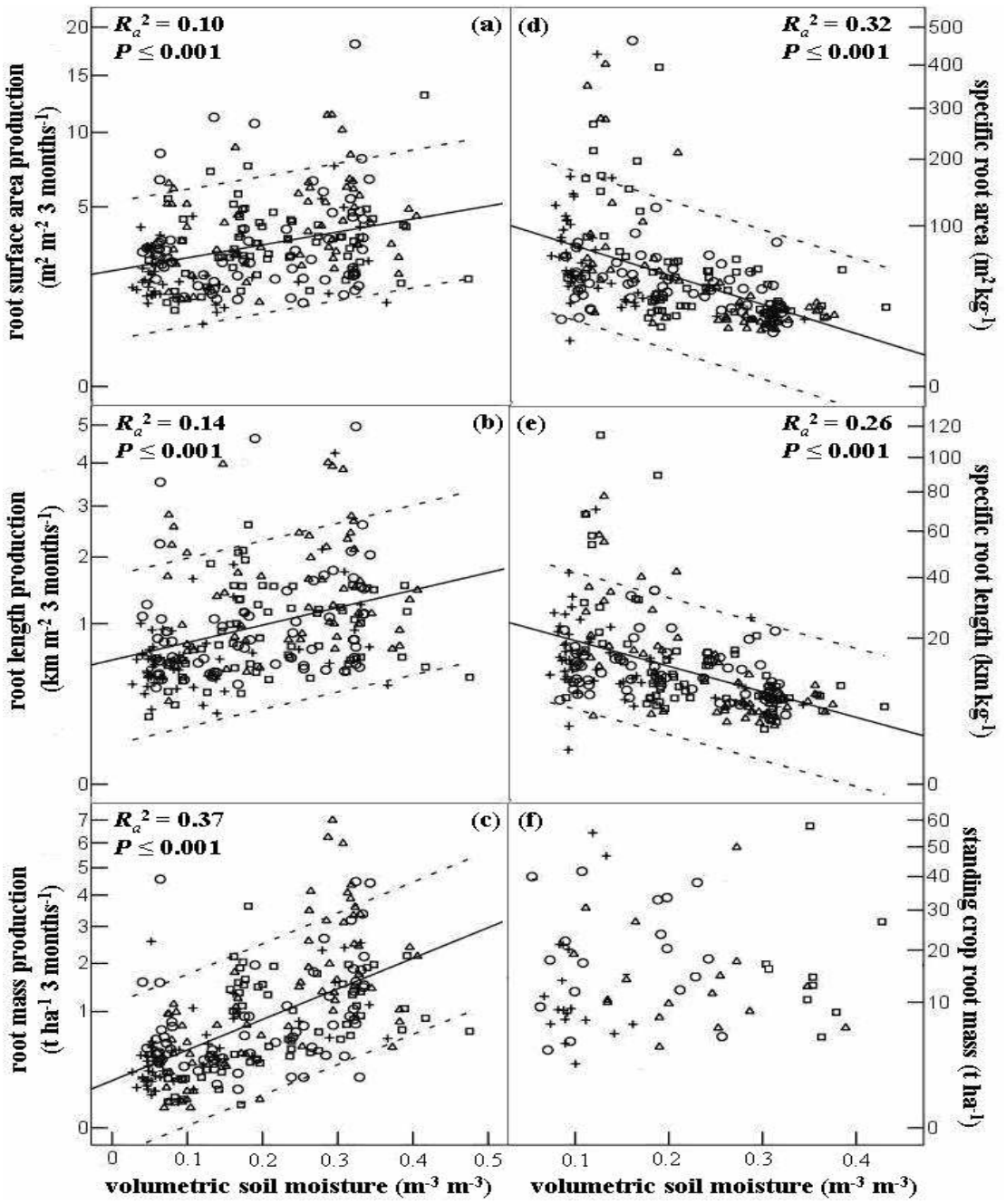

Figure 3. Volumetric soil moisture plotted against **(a)** root mass, **(b)** length, **(c)** surface area production, **(d)** SRA, **(e)** SRL, and **(f)** standing crop root mass in the surface 30 cm soil layer. Plots: circles = OX_{sand}; crosses = OX_{dry}; squares = OX_{clay}; triangles = $OX_{fertile}$. Black lines indicate mean linear trend for the entire dataset, and dashed lines denote 95% confidence intervals around the mean.

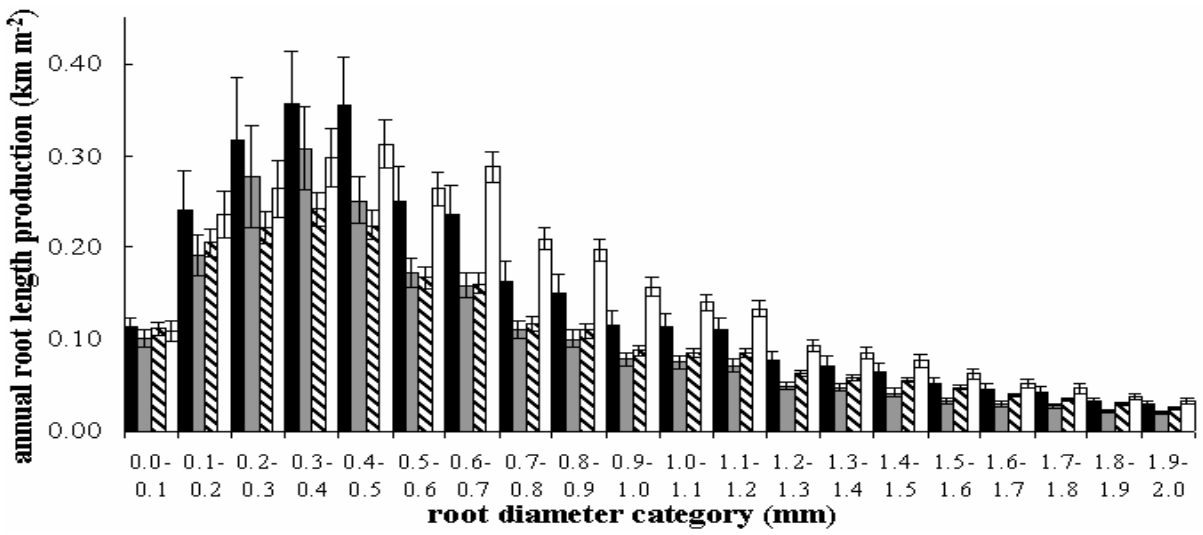

Figure 4. Total root length production, divided into 0.1 mm diameter categories, in the surface 30 cm soil layer. Plots: black fill = OX_{sand}; grey fill = OX_{dry}; black cross hatch = OX_{clay}; white fill = $OX_{fertile}$. Error bars indicate SE of the mean, *n* is 16.

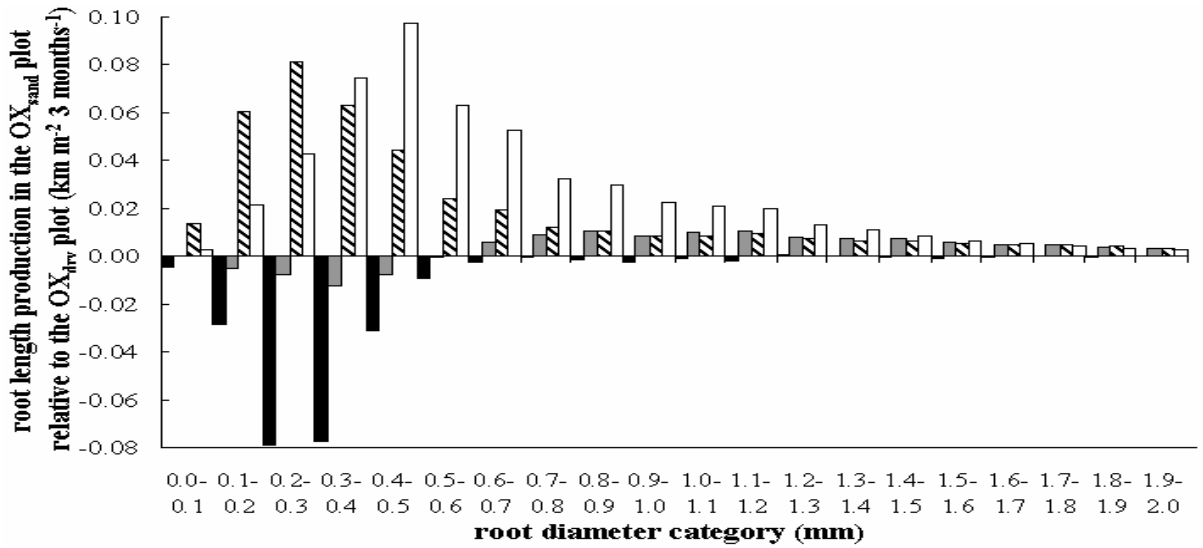

Figure 5. Seasonal root length production, divided into 0.1 mm diameter categories, on the OX_{sand} plot relative to the OX_{dry} plot. Columns indicate different measurement periods. Values indicate the difference between plot mean root length in different diameter categories (*n* is 1), so there are no error bars. Measurement sessions: black fill = December 2004 – February 2005; grey fill = March 2005 – May 2005; black cross hatch = June 2005 – August 2005; white fill = September 2005 – November 2005.

between spatial variation in soil moisture and root production every three months (Figs. 3a-3c). There was no significant interaction between plot and soil moisture to explain observed variation in any of the root variables measured (mass: $P = 0.082$; length: $P = 0.141$; surface area: $P = 0.115$).

Fine roots (≤ 2 mm in diameter) accounted for the majority (91 - 93%) of total root length grown in all of the plots. Between 75 and 79% of this fine root growth occurred in roots less than one mm in diameter (Fig. 4). Roots less than one mm in diameter also displayed the strongest responses to seasonal changes, in all plots (Fig. 5).

3.4.3. Root specific length and surface area

On all plots, SRL and SRA measured in the surface 30 cm soil layer increased during the transition from the wet to dry season (Figs. 2d & 2e). In contrast to root production, SRL and SRA were significantly lower where soil moisture was depleted (Figs. 3d & 3e). This was because the rate of increase of root production with soil moisture was greater for mass than it was for length and surface area (Figs. 3a-3c). Thus, more root length and surface area per unit mass was produced under drier conditions. There was no significant interactive influence of plot upon the relationship between soil moisture and the root morphology variables recorded (SRL: $P = 0.362$; SRA: $P = 0.337$).

3.4.4. Root turnover and chemistry

The low number of sample replicates ($n = 4$) precluded statistical analysis of plot differences in root turnover and chemistry. However, comparison of the OX_{sand} and OX_{dry} plots revealed no clear effect of the rainfall exclusion treatment upon root turnover (both 28.7 % per year) and C or N content (Table 2). Instead, the greatest

differences were between the plots on sandy (OX_{sand}, OX_{dry}) and clay-rich soils (OX_{clay}, $OX_{fertile}$). Roots on the $OX_{fertile}$ plot displayed relatively rapid turnover (58.6%), and contained smaller concentrations of C and N, compared to the other plots (Table 2). The C and N content of OX_{clay} plot roots was also low compared to the other plots, but they exhibited relatively slow turnover (24.7%).

3.5. Discussion

3.5.1. Root characteristics

A summary of root standing crop estimates for major global vegetation types reported mean root biomass of 49 t ha^{-1} for the tropical evergreen forest biome, based upon data from nine studies (Jackson *et al.,* 1996). This value is 29 - 52% higher than my mean estimates (Table 2), probably because in the current study roots were sampled only from the surface 30 cm soil layer. Once a sampling depth correction was applied (see methods, data analysis section), standing crop mass in the entire soil column was estimated to be 30 - 45 t ha^{-1}, from the four plots surveyed. The sampling depth correction did not account for changes in root dynamics with soil depth. Further work is required to improve current knowledge about root processes in deeper ($\geq$ 1 meter) soil depth. At this site, root standing crop mass shows considerable spatial variation, and often does not follow a normal distribution. Instead, mass may be right-skewed (Table 2), with a number of outliers of relatively large mass potentially biasing estimates of mean mass. This is not necessarily a problem for statistical analysis, since data can often be transformed, but does mean firstly, that care needs to be taken in how these properties are reported (it is, for example, not appropriate to apply standard deviations or standard errors to data which are not normally distributed), and secondly, that relatively more sampling effort is required to avoid excessive influence of outliers. Thus, the spatial heterogeneity and frequently skewed distribution of

standing crop mass and, to a lesser extent, other root characteristics can confound comparisons between studies and ecosystems.

Estimates of total root mass production from this study ranged between 2.9 - 6.5 t ha^{-1} yr^{-1} (Table 2) or 3.7 – 8.3 t ha^{-1} yr^{-1} when incorporating the sampling depth correction (see methods, data analysis section), which was consistent with data from other tropical forests. For example, one study used a combination of methods to calculate annual root mass production in the surface 40 cm soil layer of a western Amazon forest of 2.0 t ha^{-1} yr^{-1} (Jordan & Escalante (1980), while another estimated production (in the top 10 cm) at a central Amazon site of 2.3 and 1.5 t ha^{-1} yr^{-1}, for years one and two respectively of their study (Silver *et al.,* 2005). Higher values of root mass production have been reported: 5.1- 20.8 t ha^{-1} yr^{-1} (Roderstein *et al.,* 2005) and over 9.9 t ha^{-1} yr^{-1} (Priess *et al.,* 1999) but both at high altitude rain forests in the western Amazon.

Much less information is available regarding root length and surface area. This study provided, to my knowledge, the first estimates of root length and surface area production per unit ground area in any ecosystem. While rhizotrons also provide data on root length (e.g.: Field studies: Itoh, 1985; Sword et al., 1996; West *et al*., 2003; Davis *et al*., 2004. Reviews: Vogt *et al*., 1998; Hendricks *et al*., 2006), the unit of measurement (root length per unit area of observation screen) is not easily integrated into models of plant water and nutrient uptake. A global review of values in the literature estimated mean standing crop root length in tropical evergreen forests of 4.1 km m^{-2}, and mean forest SRL of 12.2 km kg^{-1} (Jackson *et al.,* 1997). Research at a disturbed tropical forest site in Costa Rica estimated standing crop root surface area from a of 4.1 m^2 m^{-2} (Berish 1982), while another study, at a temperate deciduous forest, reported standing crop area of 14.8 m^2 m^{-2} (Farrish 1991). Additional root length and surface area production data are required to determine how these root characteristics vary between ecosystems, and respond to environmental change.

Estimates of annual root turnover from this study ranged between 24.7 – 58.6%, from the four plots surveyed (Table 2). This equated to an estimated period for

complete fine root stock turnover of 1.7 – 4.0 years. Whilst these estimates are constrained by the lack of plot replication, and uncertainties associated with the ingrowth core method (Vogt *et al*., 1998; Steingrobe *et al*., 2000; Hendricks *et al*., 2006), they provide a preliminary insight into root dynamics at the study site. Other studies conducted in the eastern Amazon rain forest have reported similar turnover times of 1.4 – 2.6 years (Silver *et al.* 2005), and 1.0 – 3.4 years (Trumbore *et al*., 2006). There is evidence that root turnover is affected by soil texture; one study (Silver *et al.* 2005) found that turnover, estimated twice for consecutive years, was consistently higher on a clay rich soil (70%, 69%) compared to a sandy soil (57%, 39%). At the study site, there was a difference between root turnover in plots on sandy (OX_{sand}, OX_{dry}) and clay-rich soil (OX_{clay}, $OX_{fertile}$). However, roots on the OX_{clay} plot displayed relatively slow turnover (24.7%), while turnover on the $OX_{fertile}$ was rapid (58.6%), compared to turnover of 28.7% on the sandy plots (Table 2).

Root longevity and turnover should be partly determined by the cost of root tissue construction and maintenance, which is related to root C and N content (Gill & Jackson 2000). There is evidence that low root tissue N content is linked with slower turnover rates (Hendricks *et al*., 1993; Gordon & Jackson 2000). However, according to my estimates the plot with the lowest root N content ($OX_{fertile}$) had the fastest root turnover (Table 2). A global review of data in the literature estimated mean root C and N content of 480 and 11.1 g kg^{-1} respectively, and C : N ratio of 43 : 1 (Gordon & Jackson 2000). In comparison, across the plots surveyed at this site, root C contents appeared to be consistently higher (427.5 - 454.8 g kg^{-1}), while N contents (12.3 - 17.6 g kg^{-1}) and C : N ratios (26 : 1 - 35 : 1) were lower. However, other measurements of root chemistry in the eastern Amazon (Silver *et al.* 2005) reported relatively similar results to those obtained in this study (C : N ratio of 35 : 1 at a site on sandy soil). If these root chemistry results are representative of the Amazon as a whole, this could alter regional estimates of the flux of C and N into the soil via root mortality, and root decomposition rate. (Norby *et al*., 2001).

3.5.2. Root responses to soil moisture

A GLM was used to assess whether observed variation in root variables could be explained solely either by changes in soil moisture, or variation between plots, or by some interaction between the two. The results of the GLM analysis showed that landscape-scale environmental variation among plots did not alter the general relationships between soil moisture and root characteristics. Root productivity or morphology may vary among plots, but the response of these characteristics to changes in soil moisture remained consistent across plots. This finding suggests that despite substantial environmental variation both between plots at this site and across the Amazon as a whole (Williams *et al*., 2002), it may be valid to extend these localised measurements to larger spatial scales.

I found no evidence to support either H_1 or H_2 - that soil moisture deficit leads to an increase in root standing crop and/or production (Fig. 3). However, estimates of both standing crop and production were spatially variable (Table 2) and consequently more intensive sampling may be required to fully resolve the effects of soil moisture deficit on root growth. In a review of five stand-level irrigation studies (ranging in duration from 2-10 years), Joslin *et al.* (2000) found only one study which reported a significant increase in root mass production under drier conditions. The other studies reviewed found either insignificant increases or no change. In this study, production of root mass (Fig 3c), length (Fig. 3b) and surface area (Fig. 3a) were consistently lower where soil conditions were drier. This suggests that, at least at this site, root production in the surface 30 cm soil layer was not strongly affected by the changes in plant allocation predicted by the functional balance theory. Instead my results are consistent with the theory of control of root growth by local soil conditions or root turgor (Whalley *et al*., 1998; Bingham & Bengough, 2003; Bengough *et al*., 2006), and/or the amount of CO_2 assimilated through photosynthesis (Farquhar & von Caemmerer, 1982; Williams *et al*., 1998; Schwarz *et al*., 2004). To reinforce this preliminary assessment, further measurements (of above-ground biomass,

photosynthesis, and root respiration) over multiple years, at other sites, are required. It is, for example, possible that while root biomass production declined under drier conditions, root metabolic activity increased, and thus the quantity of photosynthate allocated to roots remained the same. Another alternative explanation for my observations is that root growth remained the same under drier conditions, but shifted downwards, to deeper soil layers beyond the sampling range of the equipment used in this study. Whatever the underlying causal mechanisms, observed changes in surface root production could significantly alter the pattern of C and nutrient cycling within the forest.

Comparison of root length production between the OX_{dry} and OX_{sand} plots indicated that long-term exposure to drier conditions did increase root growth responses to seasonal rises in water availability (Fig. 5). However, further replication of the rainfall exclusion treatment is necessary to reinforce this preliminary conclusion. While root length production was relatively higher on the OX_{sand} plot compared to the OX_{dry} plot during the dry season, this pattern was reversed during the wet season (Fig. 5) even though the OX_{dry} plot remained drier than the other plots throughout the year. This implies that plants on the OX_{dry} plot were compensating for lower annual production rates by increasing production during seasonal periods of relatively high soil moisture. While this interpretation is based upon only one year of measurement, it is corroborated by a range of studies which found that prior exposure to water deficit led to higher growth either in other portions of the root system where conditions were more favourable (for example, in deeper soil layers), or for the root system as a whole when the soil was rewetted (Fernandez & Caldwell 1975; Meisner & Kornok 1992; Dickman *et al*., 1996; Hendrick & Pregitzer, 1996; Hendrick & Pregitzer 1997; Torreano & Morris, 1998; Comas *et al*., 2005). For example, Joslin *et al*. (2000) artificially modified water availability on three plots over five years at a temperate deciduous forest site. Overall, they found little evidence for a net increase in fine root production on the drier plot, but conclude that 'periods of lower root

production in the dry treatment were compensated for by higher growth during favourable periods'.

Roots finer than one mm in diameter accounted for the majority (69-74%) of annual root growth (Fig. 4), and showed distinct seasonal shifts in production (Fig. 5). This is consistent with other studies which also suggest that finer roots tend to be more dynamic and responsive to external stimuli, compared to coarse roots (Eissenstat *et al*., 2000). However, my results call into question the arbitrary definition of dynamic fine roots as less than two mm in diameter, since I find that roots between one and two mm diameter account for only ~20% of the total growth of roots finer than two mm diameter (Fig. 4). Therefore, the existing categories of root morphology (fine $\leq$ 2 mm, coarse $\geq$ 2 mm) may not adequately capture the full variation in, particularly very fine, root activity. Further work is required to provide more detailed information about the links between root structure (e.g.: diameter) and function (e.g.: growth rate).

Measurements of root morphology from this study provided clear support for H_3- that plants respond to soil moisture deficit by increasing SRL (Fig. 3e) and SRA (Fig. 3d). The advantage to the plant of modifying root morphology instead of production is that it potentially increases water and nutrient uptake, without requiring extra photosynthate to construct and sustain more root material. In addition, fine roots tend to be more dynamic than coarse roots with higher growth rates and turnover (Eissenstat *et al*., 2000), which is beneficial for searching out and exploiting transient patches of high soil moisture.

Comparison of the OX_{sand} and OX_{dry} plots did not support either H_4 or H_5, since there is no clear effect of the rainfall exclusion treatment upon either root turnover, or C and N content (Table 2). However, further replication of the rainfall exclusion treatment would allow a more detailed analysis of the effects of soil moisture on root turnover and nutrient content.

3.6. Conclusion

This study tested several hypotheses regarding how plants alter root characteristics in response to soil moisture deficit. Root production was consistently lower in drier soils, while SRL and SRA displayed the opposite response. The pattern of root production observed was consistent with a decline in C assimilation and/or changes in soil properties which impede the ability of roots to penetrate the soil (either directly through altered soil impedance, or indirectly through changes in root turgor), under drier conditions. Observed changes in SRL and SRA suggested that altering root morphology may provide an important additional strategy for plants to increase water uptake. There was no clear evidence that a decline in soil moisture was linked to changes in either root turnover or root C and N content. There was substantial spatial heterogeneity in standing crop root mass, root production and morphology, but these variables responded to changes in soil moisture in a similar way across different vegetation and soil types. Whilst there was a significant relationship between root characteristics and soil moisture at this study site, none of the environmental variables measured could explain the majority of within-plot spatial variation. Therefore, a more comprehensive measurement program may be required to further elucidate the effects of other potentially important drivers (e.g.: above-ground growth, soil fertility) of root patterns and processes.

Chapter 4

4. Factors controlling spatio-temporal variation in respiration from litter, roots and soil organic matter at four contrasting rain forest sites in the eastern Amazon.

4.1. Abstract

This study partitioned monthly soil CO_2 efflux into contributions from surface litter, roots and soil organic matter over one year at four rain forest plots with contrasting vegetation structure and soil type in the eastern Amazon, Brazil. Subsequently, abiotic and biotic causes for observed differences within and between plots were explored. Across the four plots, estimated mean annual soil CO_2 efflux varied between 12.5 - 16.6 t C ha^{-1} yr^{-1}, which was partitioned into 0.1 – 1.7 t C ha^{-1} yr^{-1} from litter, 6.2 – 9.3 t C ha^{-1} yr^{-1} from roots, and 4.7 – 5.8 t C ha^{-1} yr^{-1} from soil organic matter. For the site as a whole, mean contribution of soil organic matter respiration fell from 49.1 % during the wet season to 31.5 % in the dry season, while root respiration contribution displayed the opposite trend: increasing from 42.0 % in the wet season to 60.5 % during the dry season. Litter contribution showed no clear seasonal change, though experimental precipitation exclusion over a one-hectare plot was associated with a ten-fold reduction in litter respiration relative to unmodified plots. There was substantial within- and between-plot variation in respiration from soil, litter, roots and soil organic matter, which was not explained by soil moisture or temperature. Instead, spatial variation in ground surface litter mass and root mass accounted for 44% of observed variation in soil respiration ($p < 0.001$). In particular, variation in litter respiration per unit mass and root mass accounted for much of variation the observed variation in respiration from litter and roots respectively, and hence total soil respiration. This information about patterns of, and underlying controls on, CO_2 efflux from different soil components should assist attempts to accurately model soil CO_2 fluxes over space and time.

4.2. Introduction

Soil respiration (R_s) releases 75 – 80 billion tones of C each year (Schlesinger, 1977; Raich & Potter, 1995, Raich *et al*., 2002; Davidson *et al*., 2006). This efflux is more than 11 times the recent rate of C produced from human combustion of fossil fuels (Marland & Boden, 1993). So even a slight change in global R_s could significantly alter atmospheric CO_2 levels, and hence climate. On a regional scale R_s usually accounts for a large proportion of ecosystem respiration (Lavigne *et al.*, 1997; Law *et al.*, 1999; Janssens *et al.*, 2001) and variation in R_s may determine whether an ecosystem is a net source or sink of CO_2 (Valentini *et al.*, 2000; Chambers *et al*., 2004; Davison *et al*., 2006). Yet despite its clear importance for global C cycling and climate change, understanding of the processes controlling spatial and temporal variation in R_s is limited. This is largely because soil is a complex and spatially heterogeneous mixture of different compounds (e.g.: surface organic litter, live roots, soil organic matter pools). Understanding the individual responses of these compounds to environmental change and the net effect upon R_s remains a key objective for research into ecosystem C cycling and biosphere-atmosphere interactions.

R_s is derived from autotrophic respiration by roots (R_r) and heterotrophic respiration by microorganisms that decompose ground surface organic litter (R_l) and soil organic matter or SOM (R_{som}). In this study, R_{som} also includes CO_2 derived from microbial decomposition of root tissue and exudates, and contributions from mycorrhizal fungi. These different sources of soil CO_2 may respond to environmental change in different ways, whilst estimates of the autotrophic component of R_s range between 12 and 93% depending upon the ecosystem studied and the method used to estimate R_r (Hanson *et al.*, 2000). R_l and R_{som} are directly driven by microbial activity, which, in turn, is strongly affected by temperature (Fang & Moncrieff, 2001; Melillo *et al.*, 2002; Davidson *et al*., 2006) and available moisture (Orchard & Cook,

1983; Sotta *et al.*, 2004; Davidson *et al*., 2006). This explains frequent observations, particularly in temperate and boreal regions where diurnal and seasonal fluctuations in temperature are greatest, that R_s rises as soil becomes warmer and wetter (e.g.: Davidson *et al.*, 1998; Lindroth *et al.*, 1998; Grogan, 1999; Hollinger *et al.*, 1999; Savage & Davidson, 2001; Widen & Majdi, 2001). However, both R_l and R_{som} are also partly decoupled from local soil conditions because they are affected by the supply of substrate from above-ground in the form of organic litter (Raich & Nadelhoffer, 1989; Högberg *et al*., 2001; Sulzman *et al.*, 2005, Högberg & Read, 2006). R_r is also partly a product of the level of metabolic activity within root tissue, affected by factors such as soil temperature (see review by Atkin *et al.*, 2000, and references therein), water availability (Bouma *et al.*, 1997; Burton *et al.*, 1998) and N supply (Ryan *et al*., 1996; Zogg *et al*., 1996), and the supply of photosynthate from above-ground (Hogberg *et al*., 2001; Nordgren *et al*., 2003), influenced by ecosystem GPP and plant allocation strategy. Thus, R_s and its component fluxes may display substantial spatial and temporal variability which is not readily attributable to changes in soil temperature and moisture. This variability reflects changes in both the total amount of respiring tissue (e.g.: root mass) or available substrate, (e.g.: surface litter mass) and the rate of respiration per unit mass of tissue or substrate (specific root respiration: SRR, specific litter respiration: SLR). Understanding the extent and causes of this variability represents an important step towards accurately modelling ecosystem C cycling, and up-scaling localized measurements across larger spatial scales for comparison with top-down measurement systems (e.g.: satellites, flux towers). The overall objectives of this study, therefore, were to:

(1) Partition R_s into R_l, R_r and R_{som} over one full seasonal cycle at four rain forest plots with contrasting vegetation and soil types in the eastern Amazon.

(2) Investigate potential biotic (roots, ground surface litter) and abiotic (soil moisture, soil temperature) causes for observed differences in respiration within and between plots and seasons.

(3) Quantify the relative contributions of mass and respiration per unit mass to total R_r and R_l.

I focused upon the Amazon because the region plays an important role in global biogeochemical cycles (Houghton *et al*., 2001; IPCC, 2001), and displays a high degree of spatial heterogeneity in terms of many ecosystem properties (Williams *et al.*, 2002), but may experience an increase in drought conditions over this century due to a possible increase in El Niño-Southern Oscillation events (Trenberth & Hoar, 1997; Timmermann *et al.*, 1999; Cubasch *et al*., 2001; Tudhope *et al*., 2001; Schöngart *et al*., 2005) driven by global climate change, and reductions in rainfall caused by regional deforestation (Shukla *et al.*, 1990; Nobre *et al.*, 1991; Costa & Foley, 2000; Werth & Avisar, 2002) and fire (Rosenfeld, 1999; Andreae *et al.*, 2004).

4.3. Materials and methods

4.3.1. Site and experimental design

The experimental site is located in the Caxiuanã National Forest, Pará State, north-eastern Brazil (1º43'3.5"S, 51º27'36"W). The forest is a lowland *terra firme* rain forest with a high annual rainfall (~ 2200-2500 mm) and a pronounced dry season (Fisher *et al*., 2006; Malhi *et al*., 2006). The most widespread soil type is a highly weathered yellow Oxisol (Brazilian classification: Latosol), though there is substantial spatial variation in the relative proportion of sand and clay. There are also patches of relatively fertile soil, called anthropogenic dark earths (ADE) or *Terra Preta do Indio*, which mark areas which were intensively managed by indigenous populations of pre-Columban inhabitants (da Costa & Kern 1999; Lehmann *et al*., 2003). To represent existing variation in soil type at the site, we established one-hectare plots (see Table 1 for additional plot details) on a well drained sandy Oxisol (OX_{sand} plot), a clay-rich Oxisol (OX_{clay} plot), and an ADE ($OX_{fertile}$ plot). In January

2002, a fourth plot, also on sandy Oxisol soil, was modified by the installation of plastic panels placed at two meters above the ground in order to exclude a proportion of incident rainfall (OX_{dry} plot).

Plot characteristics	OX_{sand}	OX_{dry}	OX_{clay}	$OX_{fertile}$
Vegetation				
Tree number ha^{-1}	434	421	419	544
Stem basal area (m^2 ha^{-1})	23.9	24.0	25.1	36.8
Leaf area index (m^2 m^{-2})	5.3 (4, 7)	5.3 (3, 6)	5.5 (4, 7)	
Soil				
Clay content (%)	18	13	42	20
Silt content (%)	5	4	14	22
Sand content (%)	77	83	44	57
pH	4	4	5	5
Carbon content (g kg^{-1})	9	12	22	46
Nitrogen content (g kg^{-1})	0.4	0.3	2	3
Carbon:Nitrogen ratio	23	35	9	15
P (mg kg^{-1})	3	3	4	36
Ca^{2+} (mg kg^{-1})	63	–	65	2213
Mg^{2+} (mg kg^{-1})	43	–	39	313
Carbon stocks				
Total	81.2 (68, 98)	44.8 (35, 62)	106.7 (97, 121)	199.6 (191, 215)
Ground litter (t ha^{-1})	2.1 (1, 4)	1.7 (1, 3)	1.9 (1, 3)	3.0 (1, 6)
Roots (t ha^{-1})	15.5 (4, 31)	11.4 (2, 40)	14.1 (6, 27)	10.0 (3, 23)
Soil (t ha^{-1})	63.6	31.7	90.7	186.6

Table 1. Key vegetation and soil features for each plot surveyed. Values indicate mean and, where possible, 5th percentile, 95th percentile around mean (in brackets). Tree number and basal area represents all individuals over 10 cm diameter at breast height, measured in January 2005. Leaf area index values are means of 25 replicate measurements taken each month at each plot in 2005 (25 ×12 = 300 replicates), no data are available for the $OX_{fertile}$ plot. Soil type values are collated from data in Ruivo & Cunha (2003) and Sotta (2006). Percentiles could not be calculated for soil C stocks because Ruivo & Cunha (2003) present no error estimates. Root and soil C stocks are estimated only for the surface 30 cm and 100 cm soil layers respectively.

Data from the fourth year of the rainfall exclusion on the OX_{dry} plot were combined with data from the other, unmodified, plots to examine R_s over a wider range of soil

moisture than currently exists naturally. The boundaries of the OX_{dry} plot were trenched to a depth of one meter to minimize lateral flow of water into the plot. The OX_{sand}, OX_{dry} and OX_{clay} plots are located about 15 m above river water level, the water table has occasionally been observed at a depth of 10 m during the wet season, and excavation confirms that the soil and live roots extend to at least 10 m depth. Less information is available for the $OX_{fertile}$ plot: the ADE forms a surface soil layer of approximately 40 cm, below this layer a clay-rich Oxisol extends to at least 60 cm depth (total recorded soil depth of at least 1 metre), the plot is located approximately 6-10 m above river water level, and during the wet season the water level rises near the soil surface of some parts of the plot (da Costa & Kern 1999).

4.3.2. Measurements

All measurements were made at 20 meter intervals along a regularly spaced grid, marked within each plot. R_s was measured with an Infra-Red Gas Analyzer or IRGA (EGM-4 and SRC-1 chamber, PP Systems, Hitchin, U.K.) The SRC-1 chamber was not vented to the atmosphere, had a diameter of 12 cm and approximate internal volume of 1530 cm^3, and used a fan to mix air within the chamber. To test whether measurements were an artefact of chamber design, the EGM-4 and SRC-1 system was compared to an alternative IRGA design (see design in Sotta *et al*., 2006) which utilized a vented, 30 cm diameter chamber with no fan (LI-6262, LI-Cor, Lincoln, U.S.A.). No significant differences were found between measurements made by the contrasting IRGA systems ($P = 0.21$, $n = 16$).

Monthly measurements of R_s were made at 25 replicate points in each plot using the IRGA. Plastic collars were inserted into the soil at each measurement location, to a depth of approximately 2 cm, to ensure a good seal between the IRGA chamber and soil. Collars were installed 2 months prior to the initiation of the measurement program in November 2004, to minimize any effect of soil disturbance upon

subsequent R_s measurements. Soil CO_2 efflux (R_s, g m^{-2} hr^{-1}) was calculated from the change in CO_2 concentration over time within the IRGA chamber according to:

$$R_s = \frac{\Delta C}{\Delta T} \bullet \frac{P}{1000} \bullet \frac{273}{t+273} \bullet \frac{44.01}{22.41} \bullet \frac{V_{ch}}{A} \Big/ 1000 \bullet 3600 \qquad (1)$$

Where $\Delta C / \Delta T$ represents the change in CO_2 within the chamber (ppm) per unit time (seconds), P is atmospheric pressure (Pa), t is the temperature of the air within the chamber (^oC), V_{ch} is the total internal volume of the chamber (m^3) and A is the ground area covered by the chamber (m^2). These terms were then divided by 1000 and multiplied by 3600 to convert R_s from units of kg m^{-2} s^{-1} to g m^{-2} hr^{-1}. All of my measurements showed a positive linear relationship between C and T, indicating a constant rate of CO_2 release from the ground into the atmosphere.

An additional 18 locations (9 each in November 2004 and June 2005, corresponding to the peaks of the dry and wet seasons respectively) in each plot were selected to: (1) estimate the percentage contribution of surface litter, roots and soil organic matter (SOM) to total R_s, and (2) examine factors controlling spatial and temporal variation of R_s in greater detail. At these points, R_s was measured twice with the IRGA: once with surface organic litter and once without. Using repeated IRGA measurements immediately after litter removal at three points I determined that an interval of two minutes was sufficient to allow CO_2 concentrations near the soil surface to equilibrate with the atmosphere. I defined surface litter as identifiable plant material on the ground surface which did not pass through a one millimetre mesh diameter sieve. The area of soil measured by the IRGA was then extracted as a soil core (diameter = 12 cm, depth = 30 cm) using opposable semi-circular cutting blades, and the roots were carefully removed by hand and cleaned of detritus. Fresh roots from each core were then placed into a cuvette which was connected to an IRGA that measured the rate of CO_2 accumulation within the cuvette. Root and litter samples were then dried at 70 ^oC to constant mass and weighed. Two mass measurements

were made for root samples: 1) roots less than 5 mm diameter, and 2) total. At all R_s measurement locations, soil moisture (CS616 probe, Campbell Scientific, Loughborough, U.K.) and soil temperature (Testo 926 probe, Testo Ltd., Hampshire, U.K.) was recorded at a soil depth of 30 cm.

4.3.3. Data analysis

For each core, R_l (g m^{-2} hr^{-1}) was estimated as the difference between the first (with litter) and second (without litter) IRGA measurements. At some locations, the respiration value recorded by the second IRGA measurement was greater than the first, presumably because of disturbance to the soil surface caused by retrieving surface litter. In these cases, the data were not used in the analysis. SLR (g g^{-1} hr^{-1}) was calculated by dividing R_l by sample dry litter mass. SRR (g g^{-1} hr^{-1}) was calculated by dividing the respiration rate of fresh root samples placed in the cuvette by sample dry mass of roots less than 5 mm diameter. I did not split root mass into the more conventional category of fine roots less than 2 mm diameter, because this would have led to a greater underestimate of the mass of respiring root tissue. R_r (g m^{-2} hr^{-1}) was then estimated by multiplying SRR by $1/A$. Estimates of R_r, following this method, did not include contributions from mycorrhizae and microbes dependent upon root exudates. Instead, in this analysis, these sources of CO_2 were ascribed to R_{som} (see calculation method below, and further discussion of partitioning methodologies by Subke *et al*., 2006; Hogberg & Read 2006). To identify any confounding influence of the extraction process upon root activity I recorded the time interval between core extraction and sub-sample respiration measurement, and plotted this against SRR (Fig. 1).

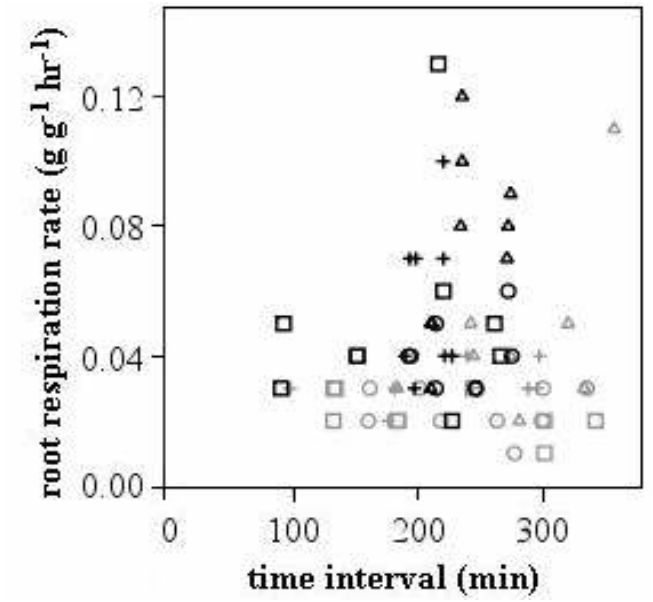

Figure 1. Relationship between respiration rate of CO_2 per unit mass of root sub-samples and time interval between sample root excision and respiration measurement within the cuvette. To convert CO_2 to C multiply by 0.27. Measurement periods: grey symbols = November 2004; black symbols = June 2005. Plots: circles = OX_{sand}; crosses = OX_{dry}; squares = OX_{clay}; triangles = $OX_{fertile}$.

While there was considerable variation in SRR between plots and season of measurement, no consistent change in SRR over time since excision was found (Fig. 1), and therefore I propose that my estimates of root respiration rate are not likely to be strongly biased by wound respiration caused by root excision (Amthor 1994). R_{som} (g m^{-2} hr^{-1}) was estimated as the residual respiration remaining after R_l and R_r were taken account of (i.e.: the difference between measured R_s and the sum of estimated R_l and R_r, for each measurement point).

The monthly measurements of R_s were used to estimate total monthly and annual soil CO_2 efflux, while the detailed core measurements (in November 2004 and June 2005) were used to partition this flux into contributions from surface litter, roots and SOM, for each plot. To do this, it was necessary to make several assumptions. Estimates of the proportional contribution of individual soil components derived from

the June 2005 measurements were applied to monthly R_s measurements during June, April and May. Estimates of contributions taken in November 2004 were applied to monthly R_s measurements during November, October and December. The intervening two three-month R_s measurement periods were assigned values of the proportional contribution of soil components intermediate to the June and November measurement periods. This approach is clearly a simplification of reality but, in the absence of more regular measurements of the proportional contribution of individual soil components to R_s, it does provide approximate estimates of seasonal and annual respiration from litter, roots and SOM. All measurements were made during the day. If there was a clear overall difference between day and night time respiration values this could adversely affect my estimates. To test for this I recorded diurnal R_s for three periods in the year but found no significant difference between overall day (07:00-19:00) and night time (19:00-07:00) respiration values ($P = 0.48$, $n = 9$).

Linear regression was used to assess whether spatial heterogeneity in soil moisture, soil temperature, litter mass and root mass could explain observed variation in R_s and its component fluxes. I assumed that CO_2 flux from any individual component of R_s (e.g. roots, surface litter) was adequately described by

$$R_c = C_m \bullet C_{rr} \bullet \frac{1}{A} + E\,, \tag{3}$$

Where R_c is component respiration (g m^{-2} hr), C_m is component mass (g), C_{rr} is component respiration rate per unit mass (g g^{-1} hr^{-1}), and E is a measurement error term. In this study, R_r was not directly measured, but was calculated as solely the product of root mass and SRR. In addition, SLR was not directly measured, but was estimated as the residual variation in R_l, once variation in litter mass was accounted for. Therefore, my estimates of R_r and SLR are likely to include some component of measurement error. I performed a stepwise regression which quantified the individual and combined contributions of estimated C_m and C_{rr} to R_c of roots and leaf litter. The

output from each regression was a test statistic (F), an adjusted R^2 (R_a^2) and a p-value. Plot and measurement period were included as factors in a general linear model (GLM) to assess whether they confounded any effects of soil moisture, soil temperature, litter mass and root mass upon R_s and its component fluxes. Potential interactions between variables were assessed by including interaction terms in the GLM analysis. Statistical analysis was carried out using SPSS 13.0 for Windows (SPSS Inc., Chicago, U.S.A). Data were transformed, where necessary, to conform to the assumptions of parametric analysis.

4.4. Results

4.4.1. Spatial and temporal variation in CO_2 efflux from soil and its components

There was substantial variation between plots in the respiration variables recorded (Table 2 & Fig. 2). Thus, estimated mean annual plot soil CO_2 efflux varied between 12.5 - 16.6 t C ha^{-1} yr^{-1}, which was partitioned into 0.1 – 1.7 t C ha^{-1} yr^{-1} from litter, 6.2 – 9.3 t C ha^{-1} yr^{-1} from roots, and 4.7 – 5.8 t C ha^{-1} yr^{-1} from soil organic matter. The estimated turnover time taken for C stocks to be completely lost via respiration also varied considerably (Table 2). In particular, estimated litter turnover on the OX_{dry} plot was slow (17.0 years) compared to the other plots surveyed (1.7 – 1.9 years) because of the low litter respiration rate, whilst soil CO_2 efflux on the $OX_{fertile}$ plot was low given the very high estimated soil C stock which led to a relatively long estimated soil C turnover time of 32.2 years (Table 2).

	OX_{sand}	OX_{dry}	OX_{clay}	$OX_{fertile}$
Annual respiration				
Total soil (t C ha^{-1} yr^{-1})	13.2 (9, 20)	12.5 (8, 18)	12.8 (10, 18)	16.5 (13, 30)
Litter (t C ha^{-1} yr^{-1})	1.1 (1, 2)	0.1 (0.0, 1)	1.1 (1, 2)	1.7 (1, 4)
Roots (t C ha^{-1} yr^{-1})	6.2 (4, 9)	7.3 (4, 9)	7.0 (6, 10)	9.3 (8, 17)
SOM (t C ha^{-1} yr^{-1})	5.8 (4, 10)	5.0 (4, 8)	4.7 (4, 6)	5.8 (4, 9)
Litter contribution				
November 2004 (%)	8.5 (0, 29)	5.7 (0, 15)	8.9 (0, 23)	12.9 (0, 42)
June 2005 (%)	10.4 (2, 19)	4.7 (0, 14)	10.0 (2, 25)	10.6 (0, 25)
Root contribution				
November 2004 (%)	48.4 (19, 81)	55.2 (30, 85)	63.6 (42, 85)	74.7 (50, 91)
June 2005 (%)	38.4 (19, 60)	41.1 (9, 69)	47.5 (32, 66)	41.0 (26, 59)
SOM contribution				
November 2004 (%)	45.8 (4, 81)	39.1 (11, 60)	27.5 (4, 54)	13.6 (6, 28)
June 2005 (%)	51.2 (31, 70)	54.2 (31, 81)	42.4 (23, 60)	48.4 (33, 67)
Specific respiration rate				
Litter (g C kg^{-1} hr^{-1})	0.08 (0, 0.16)	0.05 (0, 0.13)	0.08 (0, 0.20)	0.10 (0, 0.39)
Roots(g C kg^{-1} hr^{-1})	0.11 (0.05, 0.2)	0.14 (0.1, 0.24)	0.09 (0.05, 0.15)	0.18 (0.1, 0.34)
Carbon stock turnover				
Total soil (yr)	6.2 (3, 11)	3.6 (2, 10)	8.3 (5, 12)	11.9 (6, 17)
Litter (yr)	1.9 (0.4, 4)	17.0 (1, 31)	1.7 (0.2, 4)	1.8 (0.2, 4)
Roots (yr)	2.5 (0.5, 8)	1.6 (0.2, 10)	2.0 (0.6, 5)	1.1 (0.2, 3)
Soil organic matter (yr)	11.0 (3, 11)	6.3 (4, 9)	19.3 (14, 26)	32.2 (20, 47)

Table 2. Annual CO_2 flux from soil and its components, contribution of surface litter, roots and soil organic matter to total soil respiration, specific respiration of litter and roots, and annual C stock turnover for each plot. Values indicate mean (5^{th} percentile, 95^{th} percentile), *n* is 18, except estimates of percentage contribution from components where *n* = 9. Soil C stocks are calculated from plot soil C content depth profiles in Ruivo & Cunha (2003). Mean plot turnover is calculated as mean C stock divided by mean annual flux. Turnover 5^{th} percentile = 5^{th} percentile C stock divided by 95^{th} percentile C flux, turnover 95^{th} percentile = 95^{th} percentile C stock divided by 5^{th} percentile C flux. Variability around values of mean soil C turnover is likely to be underestimated because no error estimates are available for soil C stocks.

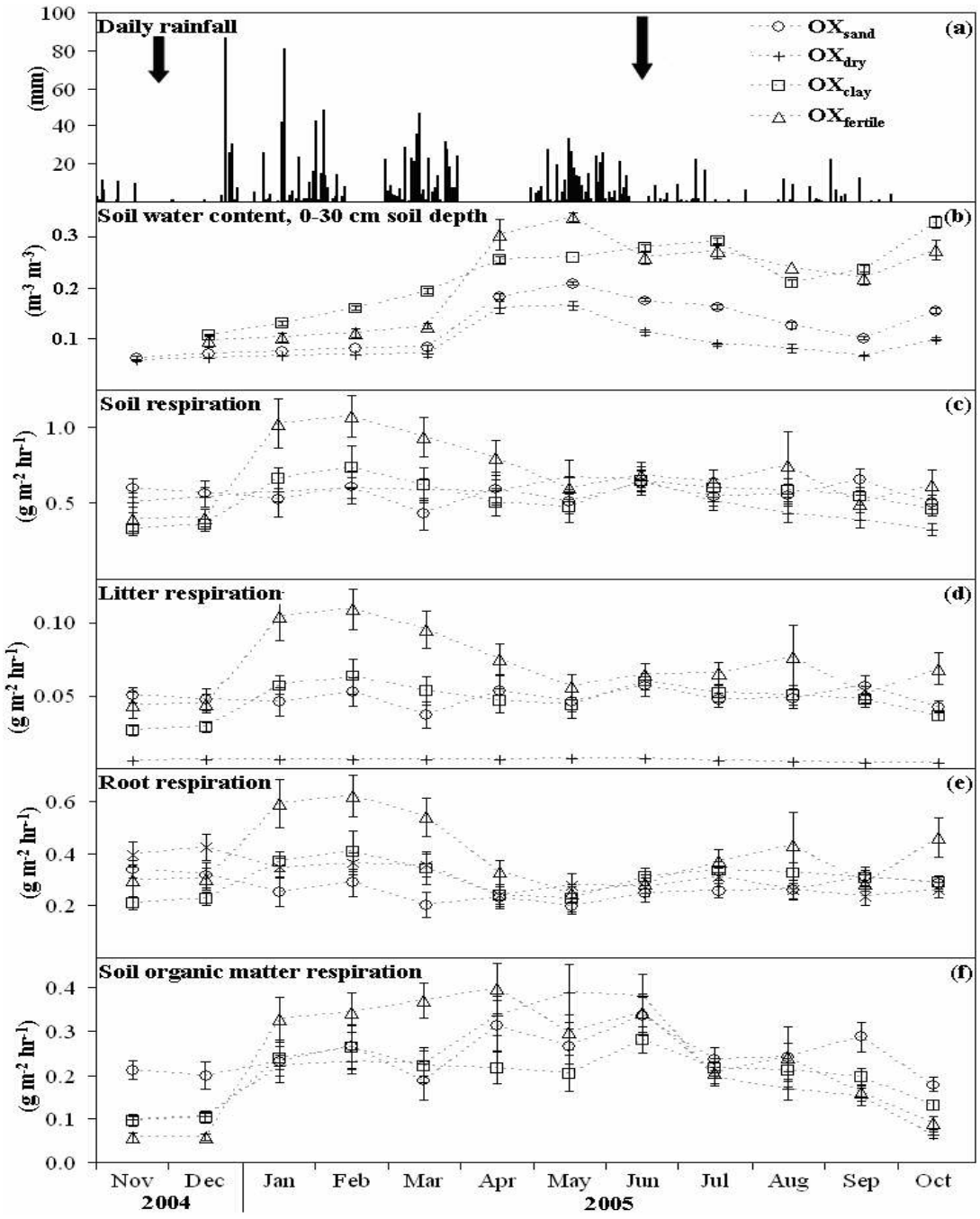

Figure 2. Temporal trends in **(a)** rainfall, **(b)** volumetric soil moisture, respiration of CO_2 from **(c)** soil, **(d)** litter, **(e)** roots and **(f)** soil organic matter on all plots. To convert CO_2 to C multiply by 0.27. Plots: circles = OX_{sand}; crosses = OX_{dry}; squares = OX_{clay}; triangles = $OX_{fertile}$. Black arrows mark soil core removal times. Error bars indicate SE of the mean, *n* is 25.

In addition, there was considerable heterogeneity in the variables measured within plots (Table 2). Thus, on average, 51% of the total range in R_s values recorded across all plots and measurement periods was also observed within each plot and period. A large proportion of the recorded variation in R_s was, therefore, caused by within-plot spatial heterogeneity, rather than systematic changes between plots and periods. Plot mean fluxes ranged between 4.7 – 12.9 %, 38.4 – 74.7 %, and 13.6 – 54.2 % of total soil respiration for litter, roots and SOM respectively (Table 2). Mean R_{som} contribution declined from 49.1 % during the wet season to 31.5 % in the dry season (Fig. 2f), while R_r contribution displayed the opposite trend: increasing from 42.0 % in the wet season to 60.5 % during the dry season (Fig. 2e). In contrast, R_l contribution showed no clear seasonality, though experimental precipitation exclusion on the OX_{dry} plot was associated with an apparent reduction in R_l of approximately 90 % relative to the unmodified plots (Fig 2d).

4.4.2. Factors affecting soil CO_2 efflux

A variety of non-linear models were applied to the monthly R_s data, but none explained above 0.07 % of the observed variation in R_s. Thus, the data were log-transformed and analyzed with a linear regression. Soil temperature did not contribute significantly to the regression model, and so was removed from subsequent analyses. There was a significant positive relationship between soil moisture and monthly R_s (Fig. 3. $F = 29.79$, d.f. = 763, $R_a^2 = 0.04$, $p < 0.001$), even though soil moisture explained very little of the observed variation in R_s. Given the low R_a^2, the significance of the relationship between R_s and soil moisture likely reflects the large sample size, rather than strong evidence of any causal link. A subset of R_s measurements, made in November 2004 and June 2005, were used to examine factors affecting R_s in more detail. Based upon these data, with a lower sample size, neither

soil temperature nor soil moisture (Fig. 4a) could explain observed variation in R_s. Instead, regression analysis revealed that ground surface litter and root mass in the

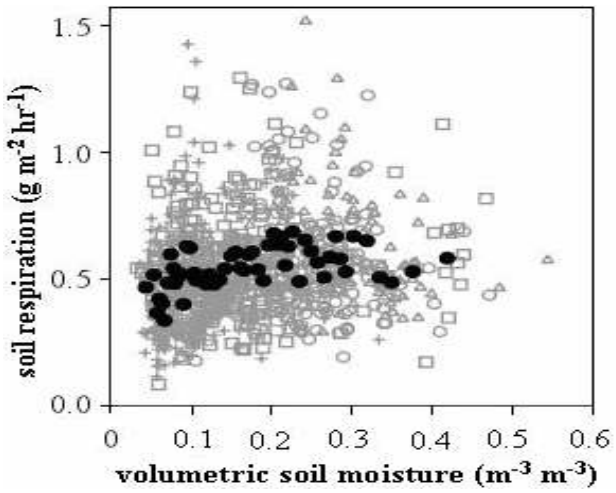

Figure 3. Relationship between monthly soil CO_2 efflux and surface soil moisture. Data from all plots and months have been pooled. To convert CO_2 to C multiply by 0.27. Data: grey symbols = individual values; black symbols = mean of 15 values. Plots: grey circles = OX_{sand}; grey crosses = OX_{dry}; grey squares = OX_{clay}; grey triangles = $OX_{fertile}$.

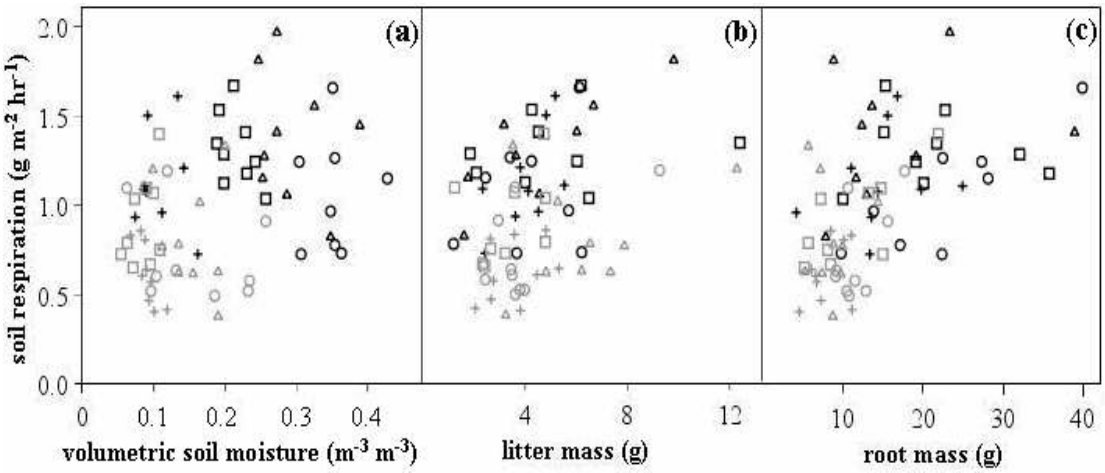

Figure 4. Relationship between soil CO_2 efflux and **(a)** soil moisture, **(b)** root mass and **(c)** litter mass. To convert CO_2 to C multiply by 0.27. Measurement periods: grey symbols = November 2004; black symbols = June 2005. Plots: circles = OX_{sand}; crosses = OX_{dry}; squares = OX_{clay}; triangles = $OX_{fertile}$.

surface 30 cm soil layer together were more useful predictors of R_s, accounting for 44% of observed variation in R_s (Fig. 4b & c. F = 17.43, d.f. = 68, R_a^2 = 0.44, p < 0.001). The majority of this variation (31%) was attributable solely to heterogeneity in soil surface root mass (Fig 4c), while litter mass accounted for the remaining 13% (Fig 4b). There was no significant interaction between plot and litter (F = 1.03, d.f. = 3, p = 0.39) or root mass (F = 0.84, d.f. = 3, p = 0.48) to derive R_s. Similarly, incorporating an interaction between measurement period and litter (F = 1.03, d.f. = 1, p = 0.32) or root mass (F = 0.09, d.f. = 1, p = 0.78) did not increase the explanatory power of the GLM model.

4.4.3. Factors affecting CO_2 efflux from litter, roots and soil organic matter

Based upon the subset of measurements made in November 2004 and June 2005, there was no significant relationship between soil moisture and R_l, R_r and R_{som} (Fig. 5), despite the fact that both R_r and R_{som} contributions to total R_s changed substantially between the wet and dry seasons and R_l was consistently lower on the OX_{dry} plot (Table 2 & Fig. 2). Heterogeneity in ground surface litter mass accounted for only 25 % of observed variation in R_l (Fig. 6b). The majority of variation in R_l was, therefore, attributed to differences in SLR and measurement error (Fig. 6a). In contrast, fine root mass explained 73% of variation in R_r, (Fig. 7b) while changes in SRR played a relatively minor role, accounting for just 16% (Fig. 7a). Together, root mass and SRR accounted for only 89% of variation in estimated R_r, the remaining 11% constituted residual measurement error. There was a significant interactive effect of plot and measurement period upon R_l (F = 3.7, d.f. = 3, p = 0.029) and R_r (F = 3.2, d.f. = 3, p = 0.039). However, neither plot nor period interacted with potential determinants of R_l and R_r (e.g.: soil moisture, root and litter mass).

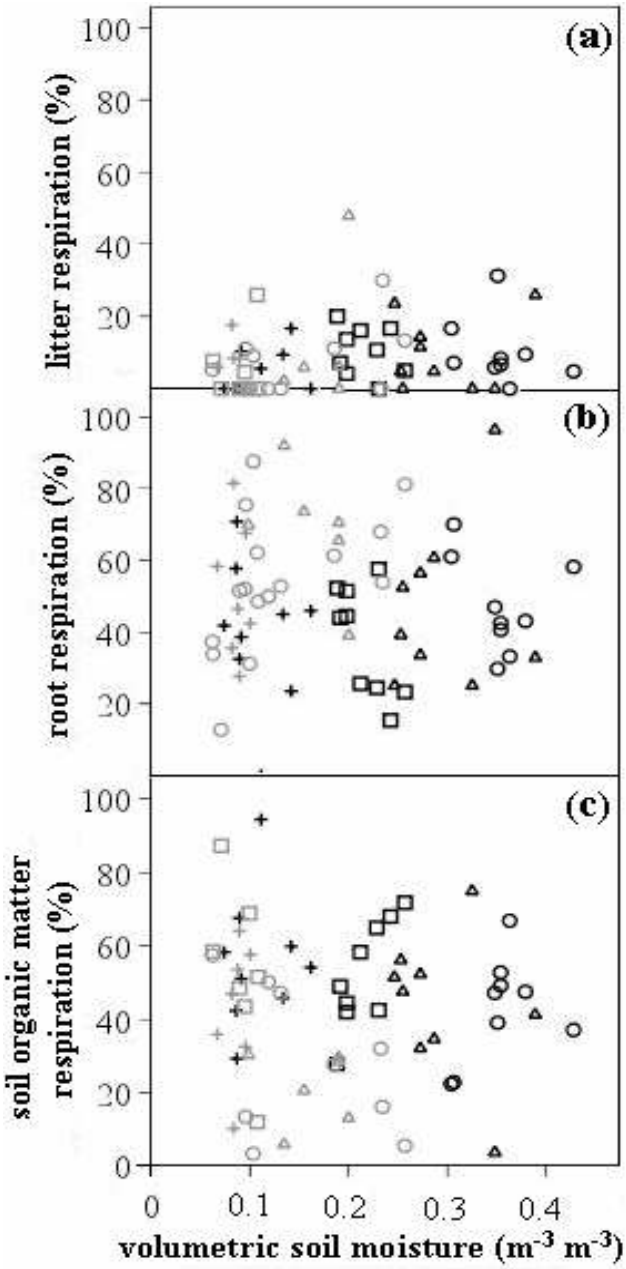

Figure 5. Relationship between soil moisture and respiration contribution from **(a)** litter, **(b)** roots and **(c)** soil organic matter. Measurement periods: grey symbols = November 2004; black symbols = June 2005. Plots: circles = OX_{sand}; crosses = OX_{dry}; squares = OX_{clay}; triangles = $OX_{fertile}$.

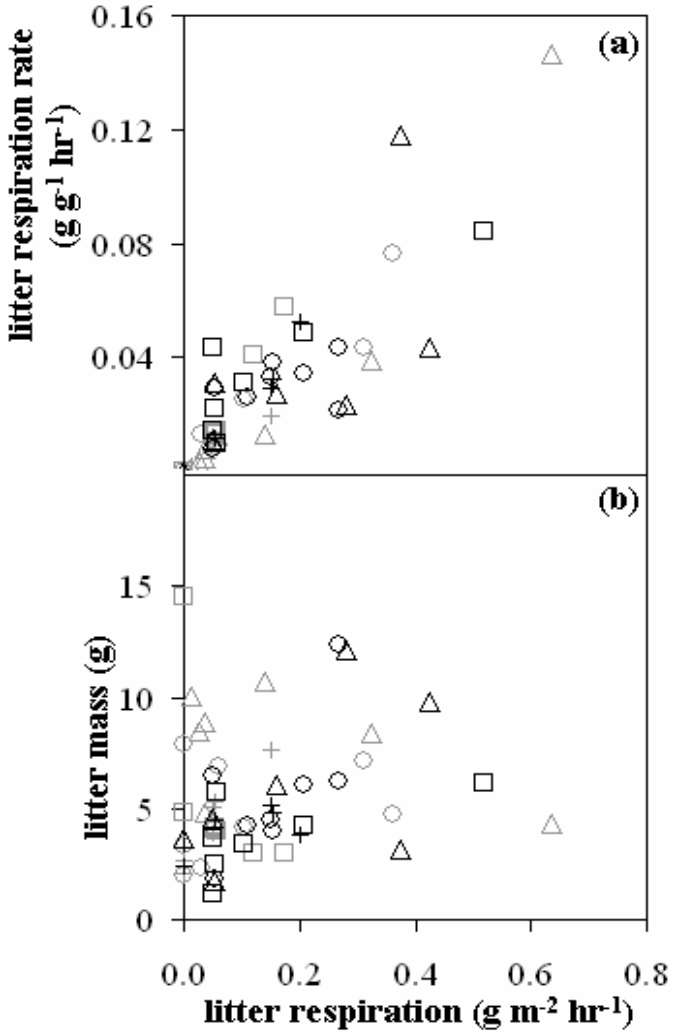

Figure 6. Relationship between litter respiration and **(a)** specific litter respiration rate of CO_2 and **(b)** litter mass. To convert CO_2 to C multiply by 0.27. Litter mass represents the quantity of organic material retrieved from the ground surface within the IRGA chamber (area = 113 cm^2). Measurement periods: grey symbols = November 2004; black symbols = June 2005. Plots: circles = OX_{sand}; crosses = OX_{dry}; squares = OX_{clay}; triangles = $OX_{fertile}$.

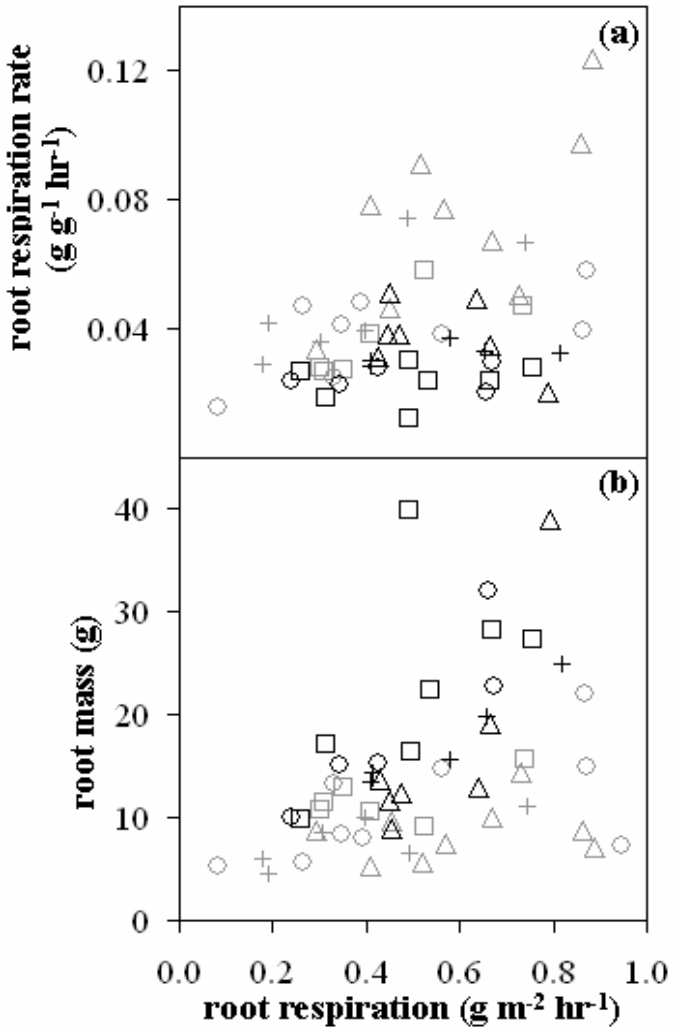

Figure 7. Relationship between root respiration and **(a)** specific root respiration rate of CO_2 and **(b)** root mass. To convert CO_2 to C multiply by 0.27. Root mass represents the quantity of root material (≤ 5mm diameter) retrieved from a 30 cm deep soil core corresponding to the area enclosed by the IRGA chamber. Measurement periods: grey symbols = November 2004; black symbols = June 2005. Plots: circles = OX_{sand}; crosses = OX_{dry}; squares = OX_{clay}; triangles = $OX_{fertile}$.

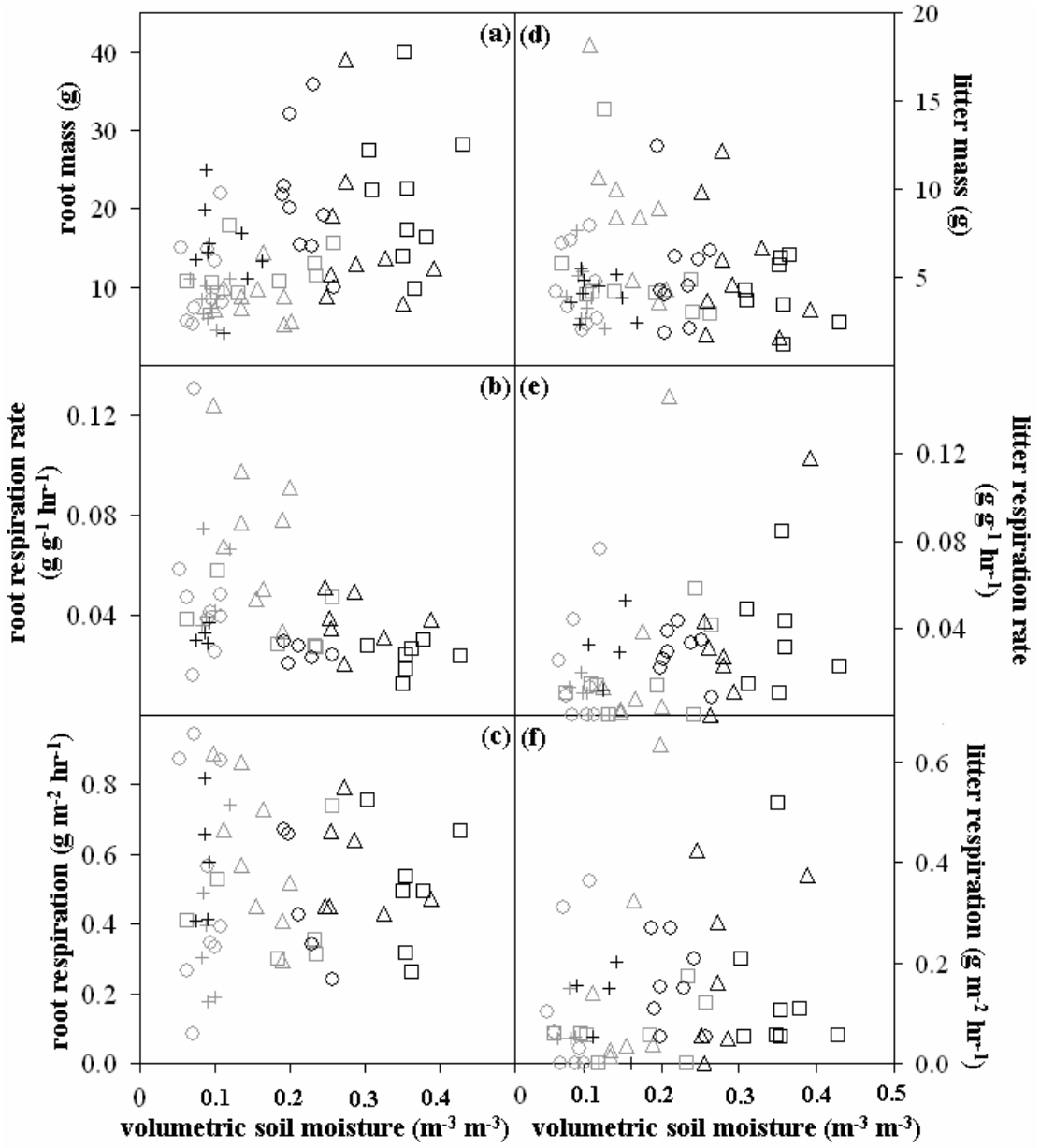

Figure 8. Relationship between soil moisture and **(a)** root mass, **(b)** specific root respiration rate of CO_2, **(c)** root CO_2 respiration, **(d)** litter mass, **(e)** specific litter respiration rate of CO_2, **(f)** litter CO_2 respiration. To convert CO_2 to C multiply by 0.27. Measurement periods: grey symbols, November 2004; black symbols, May 2005. Plots: circles = OX_{sand}; crosses = OX_{dry}; squares = OX_{clay}; triangles = $OX_{fertile}$.

Soil moisture had no clear effect upon R_l (Fig. 8f. $F = 2.02$, d.f. = 45, $R_a^2 = 0.02$, $p = 0.162$) or litter mass (Fig. 8d. $F = 0.1$, d.f. = 69, $R_a^2 = -0.01$, $p = 0.754$). Root mass, in contrast, increased significantly with soil moisture (Fig. 8a. $F = 17.43$, d.f. = 70, $R_a^2 = 0.19$, $p < 0.001$), while SRR decreased (Fig. 8b. $F = 13.01$, d.f. = 69, $R_a^2 = 0.15$, $p = 0.001$). The net outcome of these two opposing patterns was that R_r was not clearly affected by soil moisture (Fig. 8c. $F = 0.08$, d.f. = 70, $R_a^2 = -0.01$, $p = 0.785$).

4.5. Discussion

4.5.1. Annual CO_2 efflux estimates

In this study, estimates of annual R_s were broadly consistent with results from other studies. Subke *et al.* (2006) presented a global review of R_s partitioning across biomes, with ten separate studies in tropical deciduous forest ecosystems. Based upon data from this review I estimated mean CO_2 efflux in tropical deciduous forests of 14.1 t C ha^{-1} yr^{-1} (ranging from 8.4 - 24.0 t C ha^{-1} yr^{-1}) compared to values from this study of 12.5 – 16.5 t C ha^{-1} yr^{-1} (Table 2). Existing measurements of R_s at the OX_{sand} and OX_{dry} plots reported similar fluxes of 15.1 and 12.3 t C ha^{-1} yr^{-1} respectively (Meir *et al*., 2006). Additionally, I estimated mean annual heterotrophic contribution (the sum of R_l and R_{som}) to total R_s of 40.4 – 52.1%, compared to a mean of 51% (ranging from 27-76%) from other studies in the same ecosystem (Subke *et al.*, 2006). The observed relationships between R_s, root mass and litter mass (Fig. 4) offered a supplementary method for partitioning R_r and R_l (the 'root regression' method, see discussion by Subke *et al.*, 2006). The regression method relies upon establishing a positive linear relationship between R_s, root mass and/or litter mass, and then regressing the linear relationship to the intercept where root mass or litter mass equals zero. R_s at the intercept is assumed to represent R_{som}, and any values above this base level should be derived from roots or litter. Using this approach I estimated, for the

entire site, R_r and R_l contribution to R_s of 20.1 and 17.4% respectively. This led to an alternative estimate of heterotrophic contribution to respiration of 79.0%, which was almost within the range of values reported from this ecosystem, but was substantially higher than my other estimates (Table 2). The regression method is unlikely to provide an accurate picture of CO_2 flux partitioning because it assumes that R_{som} is constant, and that all the spatial variation in R_s may be attributed solely to roots or litter (Subke *et al.*, 2004). Nevertheless it provides a useful comparison with the other estimates provided by this study.

I divided estimated plot C stocks by annual fluxes to provide an approximate measure of the rate of C stock turnover at each plot. The results indicate that the rate of C cycling varied substantially between plots, though there was considerable uncertainty around these estimates. For example, estimated mean turnover time for litter stocks varied little (1.7 – 1.9 years) with the exception of the OX_{dry} plot where the low R_l meant that estimated complete turnover of stocks via respiration would take 17 years. Root turnover is more difficult to interpret, because root stocks are being compared with a metabolic flux, but my data suggest that root tissues at this site respire their own weight in C over 1.1 – 2.5 years. Variation in estimated SOM turnover provides clues about the proportion of soil C stocks at these plots which are labile. For example, the estimated soil C stock on the OX_{sand} plot was over twice as large as on the OX_{dry} plot, but R_s on the OX_{sand} plot was only 5 % greater than the OX_{dry} plot. This suggests that though the OX_{dry} plot possesses a lower soil C stock, a greater proportion of this C exists in a relatively labile form, compared to the OX_{sand} plot. Similarly, annual R_s on the $OX_{fertile}$ plot was low compared to what might be expected from its very high soil C stock (Tables 1 & 2), and it seems likely, therefore, that a relatively large proportion of the C stock is recalcitrant. This interpretation is consistent with much of the few existing data on this unusual soil type (Lehmann *et al.*, 2003). Anthropogenic soils, such as that found in the $OX_{fertile}$ plot, exist in isolated pockets throughout the Amazon, where they were created by pre-Columban inhabitants and have been successfully cultivated since. Given the sensitivity of most

Amazonian soils to many current forms of agriculture, there is substantial interest in how these soils have sustained such a high level of fertility after hundreds, sometimes thousands, of years of cultivation, and potentially how to recreate them across the Amazon again (see review by Mann 2002). Within this context, this study provides potentially important insights into how, and why, the ADE or *Terra Preta do Indio* soil on the $OX_{fertile}$ plot differs from the more widespread highly weathered Oxisol soils on the other plots.

The method used for partitioning R_s in this study may have caused disturbance to the soil system but did allow collection of a large number of sample replicates. Sample size is an important consideration because to up-scale site-specific observations across a heterogeneous environment it is crucial to capture spatial and temporal variation in CO_2 efflux from soil and its components. I propose that estimates of R_l and R_r presented here are likely to be underestimates, for the following reasons. R_l was calculated as the difference between two IRGA measurements; the first with surface litter, and the second without. Litter removal was likely to disturb to the soil surface, which may have caused elevated CO_2 efflux rates during the second IRGA measurement relative to the first (despite my attempts to minimize this, see methods section). Estimates of R_r provided by this study only consider contributions from roots in the upper 30 centimetre soil layer, and ignore the potentially significant contributions of associated mycorrhizae and microbes dependent upon root exudates (Nguyen, 2003; Jones *et al.*, 2004).

4.5.2. Factors affecting CO_2 efflux from soil, litter, roots and soil organic matter

The GLM analysis tested for interactions between potential causal variables (e.g.: soil moisture, soil temperature, litter mass, root mass, plot and measurement period) to explain observed variation in R_s and its component fluxes. Results showed that plot

and measurement period interacted together with a significant effect on the *amount* of R_l and R_r, but the *pattern of response* of R_s, R_r and R_l to changes in driver variables (soil moisture, litter and root mass) remained consistent across plots and seasons. This finding suggests that despite substantial environmental variation both between-plots at this site and across the Amazon as a whole (Williams *et al*., 2002), it may be valid to extend my localized observations of R_s responses to soil moisture, litter and root mass across larger spatial and temporal scales.

At this site there was considerable variability in R_s and its component fluxes, both within and between plots, which did not appear to be directly explained by either surface soil temperature or moisture (Figs. 3, 4a, 5, 8c & 8f). I did record an asymptotic response pattern of R_s to moisture (Fig. 3) which was consistent with reports from other studies (e.g.: Davidson, *et al*., 2000; Schwendenmann *et al*., 2003; Sotta *et al*., 2006) however, at the study site this trend was weak, and surrounded by considerable variation. Surface soil temperature was relatively invariant at the study site- variation around the annual mean across all measurement locations and dates was ~ 5 ^{o}C, whilst diurnal variation was typically 1-2 ^{o}C- and thus could not account for the considerable level of heterogeneity in R_s and its component fluxes. In comparison with temperature, variability in soil moisture was much higher and appeared to coincide with seasonal changes in both R_r and R_{som} contributions, and differences in R_l on the OX_{dry} plot relative to the other plots (Table 2 & Fig. 2). However, with regards to R_l, there may not be a simple direct relationship between litter moisture conditions and soil moisture. In addition, rainfall exclusion on the OX_{dry} plot could cause changes in the chemical composition of litter fall which could then affect litter decomposition and respiration, independent of changes in soil moisture (Gosz *et al*., 1972; Xu *et al*., 2003). Soil moisture measurements made in this study were of the surface 30 centimetre soil layer, whereas R_{som} may be more controlled by water content in deeper soil layers. Finally, R_{som} was estimated in this study as the CO_2 flux remaining after R_l and R_r have been taken into account. As such, it is likely to include CO_2 derived from mycorrhizae and microbes dependent upon

root exudates which may be controlled primarily by plant photosynthesis and allocation of assimilate, not soil moisture (Högberg *et al*., 2001, Högberg & Read, 2006). All of these confounding factors could account for the lack of any clear general relationship between surface soil moisture and respiration from soil and its components observed in this study. A large number of other studies report ed a relationship between R_s and soil temperature and/or soil moisture (Meir *et al*., 1996; Davidson *et al*., 2000; Sotta *et al*., 2004, Sotta *et al*., 2006). For example, Meir *et al.* (1996) found that soil temperature at five centimetres depth accounts for 76-88% of variation in R_s, at a rain forest site in the south-western Amazon. Sotta *et al.* (2004) reported a lower, but still significant, effect of soil temperature from a forest in the central Amazon, and also identified key roles for soil moisture both by stimulating microbial respiration in the soil, and altering conditions for transport of CO_2 to the soil surface. However, these results were based upon short-term temporal trends in R_s, whereby repeated measurements were taken from the same points over, a relatively short, time. When Sotta *et al.* (2004) attempted to correlate R_s with tree basal area distribution they found no relationship, possibly because there was only a weak relationship between tree stem location and litter and root distribution. They concluded that 'temperature and soil water content….can mostly only explain temporal variation [in R_s], especially in relatively uniform ecosystems.' I propose that, in addition to spatial patterns in R_s, longer-term temporal (seasonal and inter-annual) trends in R_s, previously attributed solely to soil moisture and soil temperature, may be confounded by changes in root and litter mass or respiration rate of these components. For example, in this study, observed increases in R_s during the wet season (Fig. 2) may have been partly caused by a rise in root mass under wetter conditions (Fig. 7a), not just soil moisture and temperature. This has important implications, particularly for the numerous studies conducted in temperate deciduous forest ecosystems, because seasonal changes in temperature and moisture often coincide with major shifts in leaf litter and root activity (Gosz *et al.*, 1972; Burke &

Raynal, 1994; Vose *et al.*, 2002). It is important, therefore, to incorporate litter and root dynamics into spatial and temporal models of soil and ecosystem C cycling.

Results from this study indicate that the combined effects of spatial variation in litter and particularly root mass (in the surface 30 centimetres of soil) are more useful predictors of R_s (Fig. 4); together accounting for 44% of the observed spatial variation in total soil CO_2 efflux. In particular, variation in SLR (since litter mass was only weakly linked to R_l) and root mass accounted for much of variation in R_l and R_r respectively (Figs. 6 & 7), and hence R_s. It is important to distinguish between the two determinants (mass and respiration rate per unit mass) of component respiration because they represent different potential C flux pathways which are likely to respond to environmental variation in different ways. For example, increased drought-like conditions in the Amazon may cause increased leaf litter fall (Neilson & Drapek, 1998; Nepstad *et al.*, 2002) and thus surface litter mass, but an associated drop in litter moisture could drive a decline in SLR (Couteaux *et al.*, 1995), until rewetting occurs. Results from this study suggest that if this happened, a drought-induced decline in respiration rate would have a much greater impact on the contribution of litter to R_s. Similarly, changes in plant C assimilation or allocation caused by drought (Thornley, 1972; Cannell & Dewar, 1994; Meir *et al.*, 2006; Fisher *et al.*, 2006), which affect root mass could have considerable effects upon R_r, and hence R_s. These preliminary findings could be improved with additional, direct measurements of component respiration, component mass and component respiration per unit mass, to isolate any confounding effect of measurement error.

4.6. Conclusion

This study examined spatial and temporal variation in CO_2 efflux from soil and its components- litter, roots and SOM. There was substantial variation in respiration, both within and between plots and seasons. Neither soil moisture nor soil temperature

could explain this heterogeneity. Instead, surface litter and root mass accounted for much of the observed spatial variability in soil CO_2 efflux. Soil moisture was not clearly linked to respiration from litter, roots or SOM, despite the fact that both R_r and R_{som} contributions to total R_s changed substantially between the wet and dry seasons and R_l was consistently lower on the OX_{dry} plot. This information about the underlying controls upon CO_2 efflux from different soil components has important implications for modelling soil CO_2 fluxes over space and time.

Chapter 5

5. Carbon cycling and allocation in an eastern Amazon rain forest after four years of an experimental drought.

5.1. Abstract

The Amazon rain forest plays an important role in global biogeochemical cycling, but the region may undergo an increase in the frequency and severity of drought conditions. The effects of drought on Amazon vegetation are potentially large but remain poorly understood. This study examined the impacts of drought upon C allocation and cycling at a primary rain forest in the eastern Amazon. Extended drought conditions have been simulated since 2002 by excluding rainfall from a one hectare (100 × 100 metre) plot, with plastic panels placed above the ground. Data from the fourth year of this drought treatment (OX_{dry} plot) were compared with data from a floristically and structurally similar control plot (OX_{sand} plot). Over the year of measurement, the drought treatment on the OX_{dry} plot was associated with a decrease in wet season surface soil moisture of approximately 35 %. During this period, estimated NEP on the OX_{sand} plot forest was -0.8 (5^{th} percentile = -6.7, 95^{th} percentile = 4.3) t C ha^{-1} yr^{-1}, whereas NEP on the OX_{dry} plot forest was 0.5 (5^{th} percentile = -3.7, 95^{th} percentile = 6.3) t C ha^{-1} yr^{-1}. The forest canopy appeared to be relatively resilient to extended drought with no clear plot difference in LAI, a small reduction in the rate of leaf litter fall, and slight changes in litter chemistry. The OX_{dry} plot produced less reproductive litter fall (7 % of total litter fall) than the OX_{sand} plot (13 % of total). If these reproductive differences persist, they indicate that future drought conditions could alter seedling recruitment, tree population age structure and forest C storage capacity. Estimated GPP was relatively similar on the two forests: 28.4 and 29.0 t C ha^{-1} yr^{-1} on the OX_{sand} and OX_{dry} plots respectively. Of this total assimilated C, 28.5 % (8.1 t C ha^{-1} yr^{-1}) was invested in NPP on the OX_{sand} plot, compared to 26.2 % (7.6 t C ha^{-1} yr^{-1}) on the OX_{dry} plot. Roots accounted for a greater proportion of NPP on the OX_{dry} plot (36 %) compared to the OX_{sand} (30 %). On both plots, estimated stem wood production accounted for 16 % of NPP. Overall, NPP constituted Soil respiration constituted an estimated flux of 13.4 and 12.5 t C ha^{-1} yr^{-1}

on the OX_{sand} and OX_{dry} plots respectively. On the OX_{sand} plot, this flux was divided almost equally between autotrophic and heterotrophic sources, whereas heterotrophic respiration appeared to be inhibited on the OX_{dry} plot and accounted for 41 % of total respiration. These results provide clues about Amazon forest responses to drought, which may help to refine model predictions of future climate and vegetation change in the region.

5.2. Introduction

Tropical forests play an important role in regional and global biogeochemical cycles and climate. The Amazon rain forest alone contains 70 – 80 billion tonnes of C in vegetation- an amount of C equivalent to over a decade of global anthropogenic emissions (Houghton *et al*., 2000). So even a slight change in Amazonian C cycling could significantly alter atmospheric CO_2 levels, and hence climate. However, the frequency and severity of drought may increase in the Amazon, both due to a possible increase in the frequency of El Niño-Southern Oscillation events driven by global climate changes (Trenberth & Hoar, 1997; Timmermann *et al.*, 1999, Cubasch *et al*., 2001; Tudhope *et al*., 2001; Schöngart *et al*., 2005), and reductions in rainfall caused by regional deforestation (Shukla *et al.*, 1990; Nobre *et al.*, 1991; Costa & Foley, 2000; Werth & Avissar, 2002) and fire (Rosenfeld, 1999; Andreae *et al.*, 2004). The effects of drought upon ecosystem structure and function in the Amazon are potentially large, but remain poorly defined. For example, El Niño related drought events appear to coincide with large CO_2 effluxes from the Amazon (Tian *et al*., 1998, Tian *et al*., 2000), which model analyses estimate to be as much as 0.6 Pg C year-1 (1 Pg = 1 Petagram = 1×10^9 tonnes) from 1980 to 1994 (Tian *et al*., 1998; Prentice and Lloyd 1998; Foley *et al*., 2002). However, relatively little information from field studies is available to test whether the modelled representation of drought effects in the region (decreased forest photosynthesis and increased soil respiration) is realistic. In addition, climate models predict that the Amazon may switch from a net sink of C to a source around the middle of the century, due to progressive changes in temperature and rainfall (e.g. Cox *et al*., 2000; Dufresne *et al*., 2002; Cramer *et al*., 2001; Cox *et al*; 2004). However, the accuracy of these projections is limited particularly by a lack of detailed knowledge about the physical controls upon ecosystem C allocation and soil respiration. Recent research has yielded valuable insights into drought-induced changes in above-ground C cycling and soil respiration

(e.g.: Carswell *et al*., 2002; Nepstad *et al*., 2002; Davidson *et al*., 2004; Nepstad *et al*., 2004; Sotta *et al*., 2004; Fisher *et al*., 2006; Meir *et al*., 2006) in the Amazon. However, without additional information about below-ground plant growth it remains difficult to interpret observed patterns. The overall purpose of this study, therefore, was to examine the impacts of seasonal and medium-term (~ 5 years) drought upon ecosystem C cycling and NEP, over a full seasonal cycle at two one-hectare (100 × 100 metre) rain forest plots in the eastern Amazon. The impacts of medium-term (~ 4 years) soil drought have been simulated by restricting the amount of rainfall received by one of the plots (OX_{dry} plot) since 2002, using plastic panels placed at two meters above the ground. I present data from the fourth year of the drought treatment on the OX_{dry} plot, and compare them to data from an unmodified, control plot located nearby (OX_{sand} plot). Prior to the imposition of the drought treatment, a detailed inter-comparison of the OX_{dry} and OX_{sand} plots was conducted, to ensure that the plots were structurally and floristically similar (Meir *et al*., 2006). The following results from existing research were used to develop hypotheses about the potential effects of drought upon Amazon forest foliage, woody tissue, roots and soil respiration.

The leaf canopy regulates the flow of water into, and out of, the forest by modifying transpiration from leaf stomata. When water lost through transpiration exceeds moisture supply from rainfall, plants may experience a reduction in leaf water potential and photosynthesis (Williams *et al*., 1998; Sperry *et al*., 2002; Schwarz *et al*., 2004), and an increase in xylem cavitation (Jackson et al., 1995; Sparks & Black 1999; Sperry *et al*., 2002). Plant responses to these negative impacts may include a reduction of leaf area index (Nepstad *et al*., 2002; Nepstad *et al*., 2004), with a concomitant increase in leaf litter fall, and production of new leaves with lower concentrations of N (e.g. Niinemets *et al*., 1999).

Plant reproduction is also likely to be severely inhibited by water deficit, as resources are diverted away from production of flowers and fruits, to organs responsible for water uptake and transport. A link between water deficit and tree reproduction has been demonstrated for several tropical species (Alvim 1960; Reich

& Borchert 1982), and a recent analysis of an 18 year record of reproduction in a tropical forest suggests that while mild drought events may enhance flower and seed production, severe water deficit appears to inhibit reproduction (Wright and Calderón 2006). In addition, another through-fall exclusion experiment in the Amazon reports an apparent reduction in reproductive activity in their experimentally droughted plot (Nepstad *et al*., 2002). These changes may be relatively trivial in terms of short-term impacts upon the ecosystem C budget, but could become increasingly significant over time if C lost via tree mortality and decomposition is not offset by seedling recruitment and growth.

As water becomes limiting, plants should preferentially allocate C to roots where photosynthate can be used to increase water uptake (the 'functional balance theory'; Thornley, 1972; Cannell & Dewar, 1994). The product of this shift in allocation should be an increase in the production of root tissue relative to foliage and stem wood. Relatively little information is available for seasonal stem growth in tropical rain forests since the trees do not reliably produce annual growth rings (Bormann & Berlyn, 1981). However, some studies have recorded reductions in stem diameter growth of tropical trees linked with seasonal or experimental drought (Breitsprecher & Bethel, 1990; Nepstad *et al*., 2002). In addition, evidence exists for elevated rates of tree mortality in response to periods of drought (Condit *et al*., 1995; Williamson *et al*., 2000; Laurance *et al*., 2001; Condit *el al*., 2004). These results suggest that, if the frequency and severity of drought events increase in the region (Shukla *et al*., 1990; Nobre *et al*., 1991; Rosenfeld, 1999; Costa & Foley, 2000; Cubasch *et al*., 2001; Tudhope *et al*., 2001; Schöngart *et al*., 2005; Werth & Avissar, 2002; Andreae *et al*., 2004), associated shifts in tree dynamics could fundamentally alter the structure and function of the Amazon rain forest.

In contrast, there is little consistent evidence for increases in plant root production under dry conditions (see review by Joslin *et al*., 2000, and references therein), possibly because any changes in allocation predicted by the function balance theory may be offset by drought induced reductions in GPP (Williams *et al*., 1998; Schwarz

et al., 2004) or localised changes in the structure of drying soil which impede root growth (Whalley *et al*., 1998; Bingham & Bengough, 2003; Bengough *et al*., 2006). Root mortality and decomposition constitute a major transfer pathway for C and nutrients into the soil, yet there exists relatively little information about physical controls upon root longevity. Some studies indicate that root mortality is likely to accelerate in response to drought (Klepper *et al*., 1973; Hayes & Seastedt, 1987; Huck *et al*., 1987). However, decomposition of dead root tissue may be inhibited by dry conditions. It remains unclear what the net effect of these two processes, responding independently to drought, means for the efflux of C into the soil via roots.

The response of soil respiration to soil moisture deficit is also complicated by several, potentially opposing, processes. Dry conditions inhibit microbial decomposition of labile C in organic litter and soil organic matter, with an associated decline in CO_2 production (Davidson *et al*., 1998), while waterlogged soil is not only a sub-optimal environment for aerobic respiration, but also blocks the transport of CO_2 produced within the soil matrix to the surface (Sotta *et al*., 2004). In addition, as outlined above, drought potentially affects root and leaf litter dynamics, with consequences for soil CO_2 efflux.

In this study, therefore, the following hypothetical responses to seasonal and medium term (~ 4 years) drought on the plots were examined:

H_1) reduced LAI and leaf litter N content with a rise in the rate of leaf litter fall

H_2) a reduction in the amount of reproductive structures present in litter fall

H_3) an increase in tree mortality rate

H_4) increased root production and mortality

H_5) a decline in soil respiration and surface litter decomposition rate

H_6) decreased NPP, but increased allocation to root growth relative to foliage and stem wood growth.

H_7) an increase in the net flux of CO_2 into the atmosphere from the forest.

The drought treatment on the OX_{dry} plot could not be replicated because of logistical and financial constraints. This experimental design precludes most conventional

statistical analyses of observed plot differences (Hurlbert 1984; Hurlbert, 2004), but does permit evaluation of forest processes which would have been difficult to capture in a, more easily replicated, but smaller-scale field experiment (Carpenter 1996; Sullivan 1997; Osmond *et al*., 2004). Results have been compared with earlier measurements made in the first two years of the drought treatment on the OX_{dry} plot (Fisher *et al*., 2006; Meir *et al*., 2006; Sotta *et al*., 2006), and with other studies in the region, to provide a more robust assessment of drought effects upon forest C cycling at the study site.

5.3. Materials and methods

5.3.1. Field site

The study site is located in the Caxiuanã National Forest, Pará State, north-eastern Brazil (1º43'3.5"S, 51º27'36"W). The forest is a lowland *terra firme* rain forest with a high annual rainfall (~ 2272 ± 193 mm) and a pronounced dry season between July and December, when on average only 555 mm is recorded (Fisher *et al.*, 2005). The soil type is a highly weathered yellow Oxisol (Brazilian classification: Latosol) consisting of 75-83% sand, 12-19% clay and 6-10% silt. A 0.3 - 0.4 m thick laterite layer is present at 3 - 4 m soil depth, which restricts plant root growth. The water table has been observed at a depth of 10 m during the wet season. In January 2002, a one-hectare plot was modified by the installation of plastic panels placed at two meters above the ground in order to exclude a proportion of incident rainfall (OX_{dry} plot; Figure 1). This study compares data from the fourth year of the drought treatment on the OX_{dry} plot with data from a floristically and structurally similar, but unmodified, one-hectare control plot located nearby (OX_{sand} plot), to examine ecosystem properties over a wider range of soil moisture than currently exists naturally (see Table 1 for additional plot details). The OX_{sand} and OX_{dry} plots are

located about 15 m above river water level, the water table has occasionally been observed at a depth of 10 m during the wet season, and excavation confirms that the soil and live roots extend to at least 10 m depth. A detailed plot inter-comparison, before the imposition of the drought treatment on the OX_{dry} plot, indicates that there was close environmental, structural and functional similarity between the OX_{sand} and OX_{dry} plots (Meir *et al*., 2006). The boundaries of both plots were trenched to a depth of one meter to minimize lateral flow of water from the OX_{sand} plot, and elsewhere, into the OX_{dry} plot. All subsequent measurements were made along a regular grid in each plot.

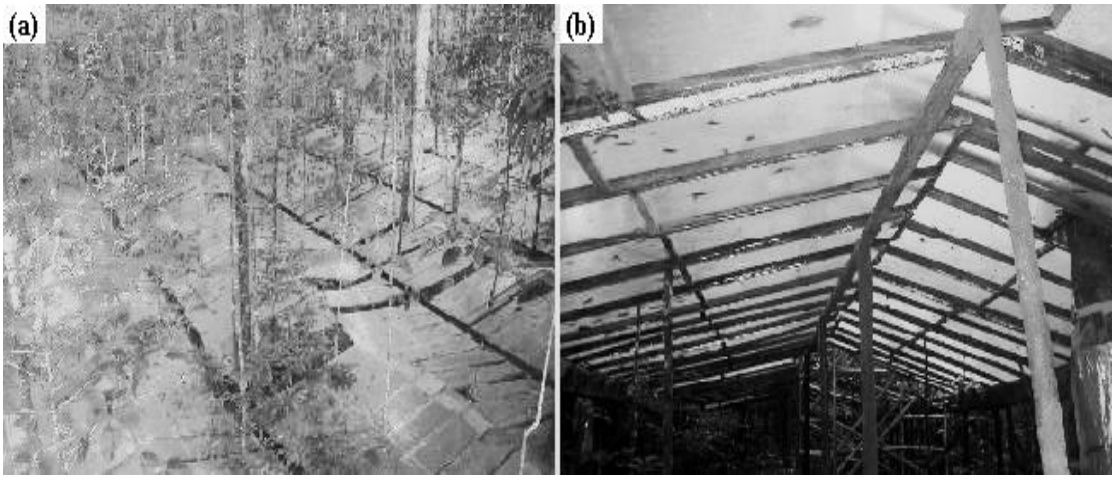

Figure 1. View **(a)** above and **(b)** below the through-fall exclusion plot.

Plot characteristics	OX_{sand}	OX_{dry}
Vegetation		
Tree number ha^{-1}	434	421
Stem basal area (m^2 ha^{-1})	23.9	24.0
Leaf area index (m^2 m^{-2})	5.3 (4, 7)	5.3 (3, 6)
Soil		
Clay content (%)	18	13
Silt content (%)	5	4
Sand content (%)	77	83
pH	4	4
Carbon content (g kg^{-1})	9	12
Nitrogen content (g kg^{-1})	0.4	0.3
Carbon:Nitrogen ratio	23	35
P (mg kg^{-1})	3	3
Ca^{2+} (mg kg^{-1})	63	–
Mg^{2+} (mg kg^{-1})	43	–

Table 1. Key vegetation and soil features for each plot surveyed. Values indicate mean and, where possible, 5th percentile, 95th percentile around mean (in brackets). Tree number and basal area represents all individuals over 10 cm diameter at breast height, measured in January 2005. Leaf area index values are means of 25 replicate measurements taken each month at each plot in 2005 (25 ×12 = 300 replicates). Soil type values are collated from data in Ruivo & Cunha (2003) and Sotta (2006). Percentiles could not be calculated for soil C stocks because Ruivo & Cunha (2003) and Sotta (2006) present no error estimates.

5.3.2. Soil respiration

Soil CO_2 efflux was measured with an Infra-Red Gas Analyzer or IRGA (EGM-4 and SRC-1 chamber, PP Systems, Hitchin, U.K.). Respiration rate was calculated from the change in CO_2 concentration over time within the IRGA chamber according to:

$$R_s = \frac{\Delta C}{\Delta T} \bullet \frac{P}{1000} \bullet \frac{273}{t + 273} \bullet \frac{44.01}{22.41} \bullet \frac{V_{ch}}{A} \Big/ 1000 \bullet 3600 \qquad (1)$$

Where R_s is soil respiration (g m^{-2} hr^{-1}), $\Delta C / \Delta T$ represents the change in CO_2 within the chamber (ppm) per unit time (seconds), P is atmospheric pressure (Pa), t is the temperature of the air within the chamber (^oC), V_{ch} is the total internal volume of the chamber (m^3) and A is the ground area covered by the chamber (m^2). These terms are then divided by 1000 and multiplied by 3600 to convert R_s from units of kg m^{-2} s^{-1} to g m^{-2} hr^{-1}. All of my measurements showed a positive linear relationship between C and T, indicating a constant rate of CO_2 release from the ground into the atmosphere. Monthly measurements of soil respiration were made at 25 replicate points in each plot using the IRGA. Plastic collars were inserted into the soil at each measurement location, to a depth of approximately 2 cm, to ensure a good seal between the IRGA chamber and soil. Collars were installed 2 months prior to the initiation of the measurement program, to minimize any effect of soil disturbance upon subsequent measurements. The collars increased the effective volume of the chamber; this was corrected for with:

$$R_{sc} = R_{suc} \bullet \frac{A}{V_{ch}} \bullet \frac{V_{co} + V_{ch}}{A}, \qquad (2)$$

Where R_{sc} and R_{suc} are corrected and uncorrected soil respiration respectively and V_{co} is the volume of the collar (m^3). This correction does not include air-filled spaces in the soil as part of the effective chamber volume (Rayment 2000). Though this bias, if it does exist at the site, is unlikely to account for the majority of variation in soil CO_2 fluxes observed at the site. All measurements were made during the day. If there was a clear overall difference between mean day (07:00-19:00) and night time (19:00-07:00) respiration values this could have adversely affected my estimates of daily, monthly and annual soil respiration. To test for this, hourly soil respiration over 24 hours was recorded at three individual measurement points, over three periods evenly spaced through the year. No significant difference was found between mean day and

night time respiration values at any of the points (P = 0.48, n = 9). Diurnal temperature variation was typically very small (~ 1.5 ^{o}C)at the site.

An additional 18 locations (9 each in November 2004 and June 2005) in each plot were selected to partition soil respiration into autotrophic and heterotrophic sources. At these points, respiration was measured with the IRGA following the protocol described above, but subsequently the area of soil measured by the IRGA was extracted as a soil core (diameter = 12 cm, depth = 30 cm) using opposable semi-circular cutting blades, and the roots were carefully removed by hand. Sub-samples of fresh roots from each core were carefully cleaned of organic detritus, and then placed into a cuvette which was connected to an IRGA that measured the rate of CO_2 accumulation within the cuvette. Root samples were then dried at 70 ^{o}C to constant mass and weighed. Two mass measurements were made for root samples: 1) roots less than 5 mm diameter, and 2) total. Root respiration rate per unit mass was calculated by dividing the respiration rate of root sub-samples placed in the cuvette by sub-sample dry mass of roots less than 5 mm diameter. I did not split root mass into the more conventional category of fine roots less than 2 mm diameter, because this would have led to a greater underestimate of the mass of respiring root tissue. Autotrophic respiration was then estimated as the product of root sub-sample respiration rate and total dry mass of roots less than 5 mm diameter extracted from each core, and then chamber measurements were up-scaled to a square meter. Estimates of autotrophic respiration, following this method, do not include contributions from mycorrhizae and microbes dependent upon root exudates. Instead, these sources of CO_2 form part of heterotrophic respiration (see calculation method below, and further discussion of partitioning methodologies by Subke *et al*., 2006; Hogberg & Read 2006). To identify any confounding influence of the extraction process upon root activity the time interval between core extraction and root sub-sample respiration measurement was recorded, and plotted against root respiration rate (data not shown). No clear change in root respiration over time was found (D. B. Metcalfe, unpublished data), and therefore I propose that my estimates of root

respiration rate are not likely to be strongly biased by wound respiration caused by root excision (Amthor 1994). Heterotrophic respiration was estimated as the residual respiration remaining after autotrophic respiration was accounted for (i.e.: the difference between total measured soil respiration and estimated autotrophic respiration, for each measurement point).

The SRC-1 IRGA chamber is not vented to the atmosphere, is relatively small (diameter = 12 cm), and uses an internal fan to mix air. To ensure measurements were not an artefact of chamber design, the EGM-4 and SRC-1 system was compared to an alternative IRGA design (D. B. Metcalfe, unpublished data) which utilizes a vented, 30 cm diameter chamber with no fan (LI-6262, LI-Cor, Lincoln, U.S.A.). No significant differences were found between measurements made by the contrasting IRGA systems ($P = 0.21$, $n = 16$).

5.3.3. Above-ground plant dynamics

Images of the canopy were recorded with a digital camera and hemispherical lens (Nikon Coolpix 900, Nikon Corporation, Japan) each month at 25 locations within each plot (see Chason *et al*., 1991, Breda 2003, for a comparison of available direct and indirect methodologies for quantifying LAI). Measurements on all plots were taken in the late afternoon when direct sunlight was at a minimum. The images were then analyzed with image analysis software (Hemiview 2.1 SR1, Delta-T Devices Ltd, U.K.) to calculate LAI (m^2 m^{-2}). Diameter growth increment of tree stems over 10 cm diameter was recorded every six months for three years (2003 – 2005) with dendrometers installed at breast height. Tree diameter was converted to above-ground stem mass using allometric equations from Malhi *et al*., (2004), and corrected for species-specific variation in wood density (density values were derived from the RAINFOR dataset, Baker *et al*., 2004). Wood C content was assumed to be 48 % of dry biomass. Trees were identified as dead if they had no live foliage, and no live phloem at breast height.

5.3.4. Below-ground plant dynamics

Soil cores (diameter = 15 cm, depth = 30 cm) were extracted using opposable semi-circular cutting blades, at nine locations in each plot at the end of November 2004 and June 2005. Conventional cylindrical soil corers were not used because they could not sever coarse roots encountered, and caused considerable soil compaction. The opposable semi-circular cutting blades were retracted, to remove discrete portions of the core at a time (thus minimizing compaction), and a knife was used to sever coarse roots encountered within the core hole. Roots were carefully removed by hand from the soil cores, cleaned of inorganic detritus, dried at 70 ^{o}C to constant mass and weighed to estimate standing crop root mass (t ha^{-1}). To convert root standing crop and production values into quantities of C, root samples from each plot were analysed for C content.

Root production was estimated using the rhizotron method (Itoh, 1985; Sword et al., 1996; West *et al*., 2003; Davis *et al*., 2004). Rhizotrons were constructed from frames supporting vertically orientated transparent plastic sheets (width = 21 cm, length = 30 cm). Nine rhizotrons were installed in each plot, in August 2004. Incremental root length extension was recorded every 15 days by tracing over roots visible at the transparent plastic face with a permanent marker. Traced roots were annotated with numbers to denote date of root appearance and disappearance, and root diameter. Tracings were scanned and root length in each diameter category was recorded for each measurement session using image analysis software (WinRHIZO Tron 2003**,** Regent Instruments, Canada). Root length was converted to root mass per unit ground area using the approach detailed by Bernier & Robitaille (2004). The number of root contacts recorded at each rhizotron observation face together with root diameter, were used to calculate the total cross-sectional surface area of intersecting roots (R_{xs}), using the following equation:

$$\sum R_{xs} = \frac{\pi^2 \bullet \sum r^2}{\sqrt{2}}, \quad (3)$$

Where r is root radius. Using the product of equation 3, root production (P_r, g m^{-2}) for each rhizotron measurement session was calculated as:

$$P_r = 2 \times 10^6 \bullet D_r \bullet (1 - F_c) \bullet R_{xs} \bullet \frac{\sin\alpha \bullet \cos\gamma}{W} \quad (4)$$

Where D_r is root tissue density (g mm^{-3}), F_c is the soil coarse fraction, α is the angle of the rhizotron observation face relative to the ground, γ is the ground angle relative to the horizontal, and W is the width of the rhizotron observation face. The 10^6 value converts mm^2 ground area into m^2. The additional multiplication factor of 2 is used because roots can only intersect with the rhizotron face from the front. It was assumed that if the rhizotron did not form a solid barrier an equal amount of roots would intersect from behind as well as from the front.

Estimating root production with this conversion method used the most reliable sources of information from the rhizotrons- the date of root appearance, and root diameter (Bernier & Robitaille, 2004). Root mortality was more difficult to quantify because there may be a substantial lag period between root death and complete disappearance from the rhizotron via decomposition. To assess the extent of this lag period, and the reliability of rhizotron root disappearance observations, the following experiment was devised. Two rhizotrons were installed adjacent to the OX_{sand} plot, in January 2005. After 3 months, root length was recorded at each rhizotron following the protocol described above, and all of the roots observed were severed *in situ* by trenching. The trenching procedure involved digging a narrow trench (width = 20 cm) around, and under, the rhizotron face where roots were recorded. The section of soil (width = 30 cm, length = 40 cm, depth = 40 cm) adjacent to the face remained undisturbed, but was covered with a plastic sheet, to prevent regrowth of roots in the

bulk soil towards the rhizotron. Subsequently, the trench was refilled with soil, to stabilize the soil section containing the severed roots observed by the rhizotron. Root disappearance after rhizotron trenching was recorded, following the tracing protocol described above, every 5 days for 70 days (Figure 2). Results show that visible roots severed by the trenching procedure clearly showed 70 % and 98 % root disappearance after 70 days (Fig 2).

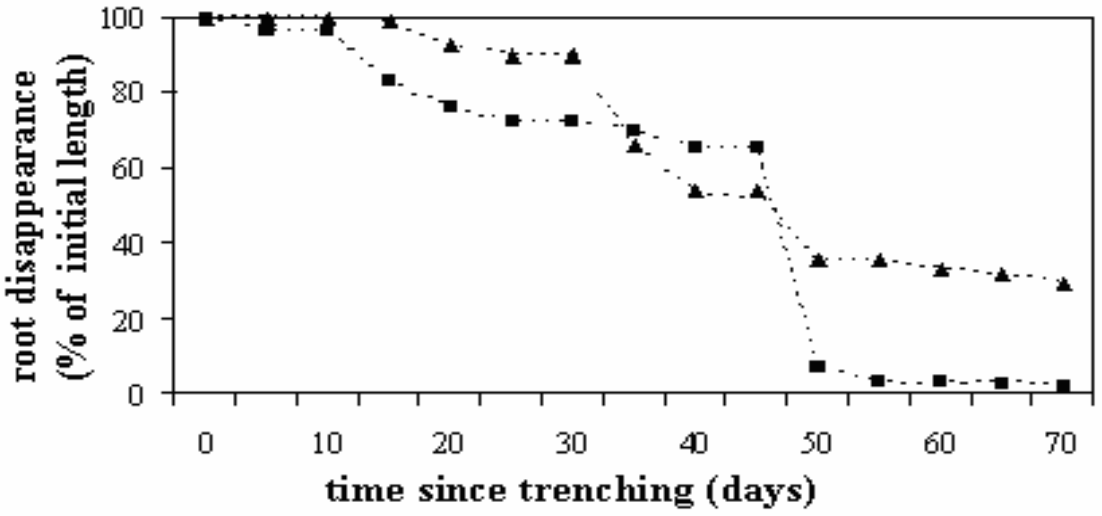

Figure 2. Root disappearance from two rhizotron observation screens, after trenching of rhizotrons to sever roots. The total population size of roots observed at both rhizotrons was 212 (98 and 114).

Estimates of root standing crop and production were likely to be underestimates because they only sampled roots from the surface 30 cm soil layer. To correct for this, data and equations derived from root profiles taken from tropical evergreen forests were used to estimate that 28% (intermediate to values of 31% and 24% reported by Jackson *et al.*, 1996 and Schenk & Jackson, 2002 respectively) of the total root mass present at this site occurred below the depth sampled. Thus, approximate estimates of root standing crop and production in the entire soil column were derived by multiplying initial values by 1.28.

5.3.5. Litter fall and decomposition

Litter fall was recorded by measuring monthly accumulation of litter in 20 mesh traps (area = 1 m^2). Traps were placed at 1 m above the ground surface on the OX_{sand} plot, and above the plastic panels on the OX_{dry} plot (height ~ 2.5 m). Litter retrieved from the traps was separated into leaves, woody tissue, reproductive structures (flowers, fruit) and unidentified material. To estimate stocks of ground surface organic litter, samples of litter were collected from the ground surface at nine 115 cm^2 areas along a regular grid in each plot at the end of November 2004 and May 2005. Ground surface litter samples were cleaned of inorganic detritus, dried at 70 ^oC to constant mass and weighed. Litter decomposition rate for each plot was estimated as mean plot ground surface litter mass divided by annual plot litter fall mass. To convert litter fall mass into estimates of C and N flux, litter fall collected in November 2004 and April 2005 on each plot was analyzed for C and N content.

5.3.6. Soil moisture and temperature

Soil moisture (CS616 probe, Campbell Scientific, Loughborough, U.K.) and soil temperature (Testo 926 probe, Testo Ltd., Hampshire, U.K.) were recorded at a soil depth of 30 cm adjacent to all soil respiration measurements (see details above).

5.3.7. Data analysis and presentation

Net ecosystem production of C (NEP, t C ha^{-1} yr^{-1}) may be calculated as:

$$NEP = GPP - R_a - R_h \quad (5)$$

Where GPP represents total ecosystem C uptake (t C ha^{-1} yr^{-1}), while R_a and R_h represent the two key ecosystem C loss terms- autotrophic and heterotrophic respiration respectively. However, GPP minus R_a is equal to NPP (t C ha^{-1} yr^{-1}), since assimilated C which is not respired is used to construct plant tissue. Thus, equation 5 may be reformulated as:

$$NEP = NPP - R_h \tag{6}$$

In this study, NPP was directly measured as the sum of canopy litter fall (including an additional estimate of coarse wood litter production from Chambers *et al*., 2001), growth of stem wood and roots. R_h was estimated as the sum of soil heterotrophic respiration (directly measured) and coarse woody debris (CWD) respiration (derived from a published estimate for a similar Amazon rain forest, Chambers *et al*., 2004a). Estimates of GPP for the study site have been derived using both an ecophysiological modelling approach (Fisher *et al*., 2006) and eddy-flux measurements (Carswell *et al*., 2002). For comparison with these contrasting methods, I calculated GPP at the site with:

$$GPP = NPP + R_a \tag{7}$$

Where R_a was estimated as the sum of soil autotrophic respiration (directly measured), and respiration from stem wood and foliage (derived from published estimates for a similar Amazon rain forest, Chambers *et al*., 2004b). Finally, forest carbon use efficiency (CUE) was estimated for both plots as the percentage of GPP invested in NPP.

The drought treatment on the OX_{dry} plot could not be replicated because of logistical and financial constraints (Hurlbert 1984). This experimental design precludes statistical analysis of observed differences, but does permit evaluation of forest processes which would have been difficult to capture in a, more easily

replicated, but smaller-scale field experiment (Carpenter 1996; Sullivan 1997; Osmond *et al*., 2004). To provide an assessment of plot differences over the period of measurement, 95 % confidence intervals were fitted around time series of canopy, root and soil characteristics on both plots (Fig. 3). Several measured C stocks and fluxes were not normally distributed, and so standard deviation error estimates were not appropriate. The approach taken in this study is to report mean values for C stocks and fluxes, to facilitate comparison with other studies, with 5th and 95th percentiles (5th and 95th Pc, in brackets when in text) around mean values.

5.4. Results

The plastic panels achieved approximately 80 % coverage of the OX_{dry} plot. This coverage reduced surface soil water content ~ 35 % in the OX_{dry} plot relative to the OX_{sand} plot during the wet season (Fig. 3b). During the dry season, volumetric soil moisture fell to similar levels (~ 0.05 m^{-3} m^{-3}) in both the OX_{dry} and OX_{sand} plots (Fig. 3b).

Carbon stocks (t ha^{-1})	**OX_{sand} plot**		**OX_{dry} plot**	
	mean	5th, 95th percentiles	mean	5th, 95th percentiles
Tree foliage	2.5	2.2, 3.0	2.5	2.3, 2.9
Tree stems	145.3	–	141.1	–
Tree roots	44.7	11.5, 89.6	32.0	5.1, 108.8
Ground litter	1.8	0.8, 3.1	1.6	1.0, 2.3
Soil	63.6	–	31.7	–

Table 2. Key C stocks on both plots. Foliage mass was calculated from plot mean LAI, assuming specific leaf area of 100 g m^{-2} (Meir *et al*., 2002; Chaves *et al*., unpublished data for this site), and converted to C stocks with litter fall C content in Table 4. Tree stem C stock estimates exclude any individuals less than 10 cm diameter at breast height at the beginning of the study. Soil C stocks are calculated from soil C content and bulk density depth profiles presented by Ruivo *et al*., (2002).

Carbon fluxes ($t\ ha^{-1}\ yr^{-1}$)	**OX_{sand} plot** mean	5^{th}, 95^{th} percentiles	**OX_{dry} plot** mean	5^{th}, 95^{th} percentiles
Litter fall				
Total	4.5	3.1, 6.2	3.6	2.6, 4.9
Leaves	2.5	1.8, 3.1	2.0	1.5, 2.6
Reproductive	0.6	0.1, 1.3	0.2	0.02, 0.4
Coarse wood *	0.9	–	0.9	–
Fine wood	0.4	0.2, 0.6	0.4	0.2, 0.9
Indeterminate	0.1	0.03, 0.2	0.1	0.02, 0.2
Tree stems				
Growth	1.3	–	1.3	–
Mortality	1.9	–	2.1	–
Roots				
Growth	2.4	1.4, 3.6	2.7	1.7, 5.1
Mortality	0.2	0.0, 0.5	0.1	0.0, 0.4
Respiration				
Soil total	13.4	9.1, 20.1	12.5	7.5, 17.7
Soil autotrophic	6.3	4.3, 9.5	7.4	4.4, 10.4
Soil heterotrophic	7.1	4.8, 10.6	5.2	3.1, 7.3
CWD #	2.0	–	2.0	–
Foliage †	9.8	–	9.8	–
Stem wood †	4.2	–	4.2	–
NPP	8.1	5.8, 11.0	7.6	5.5, 11.3
GPP	28.4	24.1, 34.5	29.0	23.9, 35.6
NEP	-0.8	-6.7, 4.3	0.5	-3.7, 6.3
CUE (NPP/GPP, %)	28.5	24.0, 32.0	26.2	23.2, 31.6

Table 3. Key C fluxes and CUE on both plots. Litter fall estimates were converted to C fluxes with measurements of litter fall C content in Table 4. Tree stem C flux estimates exclude any individuals less than 10 cm diameter at breast height at the beginning of the study. Some fluxes were not directly measured in this study, and are derived from the following published estimates: * Chambers *et al*., (2000), # Chambers *et al*., (2004), † Chambers *et al*., (2004). Root C flux estimates are derived from root mass changes measured by Rhizotrons and corrected for the depth underestimate (see methods section), then converted to C fluxes assuming root C content of 48 % (D. B. Metcalfe, unpublished data). NPP = litter fall + stem wood growth + root growth. GPP = NPP + soil autotrophic respiration + foliage respiration + stem wood respiration. NEP = NPP – soil heterotrophic respiration – CWD respiration. CUE = (NPP / GPP) × 100.

5.4.1. Canopy dynamics

During the year of measurement, estimated mean LAI was 5.3 m^2 m^{-2} on both plots (Table 1 & Fig. 3c). There was no consistent seasonal trend in LAI on either plot (Fig. 3c). Though, an abrupt decline in LAI in July 2005, particularly on the OX_{sand} plot, was closely correlated with an increase in leaf litter fall and a period of particularly low rainfall (Figs. 3a, 3c & 3d). Recorded leaf litter fall on the OX_{dry} plot was 2.0 (5^{th} Pc = 1.5, 95^{th} Pc = 2.6) t C ha^{-1} yr^{-1} compared to 2.5 (5^{th} Pc = 1.8, 95^{th} Pc = 3.1) t C ha^{-1} yr^{-1} on the OX_{sand} plot (Table 3). On both plots, leaf litter fall rose substantially at the onset of the dry season when monthly rainfall decreased, though surface soil moisture remained relatively high (Fig. 3d). C and N content was measured for litter samples taken from both plots, at two periods in the year which coincided with the peaks of the dry (November 2004) and wet seasons (April 2005). There were small but consistent differences in litter chemistry between plots and seasons (Table 4). For example, litter samples from the OX_{sand} plot had a greater N content of 15.7 g kg^{-1}, compared to 14.0 and 14.2 g kg^{-1} on the OX_{dry} plot (Table 4). On both plots, the C content of litter produced during the wet season month was higher (482.3 and 4.86.5 g kg^{-1}) than that of litter collected in the dry season (472.9 and 474.1 g kg^{-1}). Further replication of both plots and seasons is required to assess these differences statistically

5.4.2. Tree reproduction

Over the entire year of the study, the mass of reproductive structures (fruits, flowers, seeds) which fell from the canopy constituted an estimated flux of 0.6 (5^{th} Pc = 0.13, 95^{th} Pc = 1.34) t C ha^{-1} yr^{-1} on the OX_{sand} plot compared to 0.2 (5^{th} Pc = 0.02, 95^{th} Pc = 0.4) t C ha^{-1} yr^{-1} on the OX_{dry} plot (Table 3). This difference remained even after

accounting for the greater total amount of litter fall on the OX_{sand} plot: reproductive litter constituted 13 % and 6 % of total on the OX_{sand} and OX_{dry} plots respectively. Reproductive litter fall on the OX_{dry} plot showed no distinct seasonal trend, whereas the amount of reproductive structures falling from the canopy in the OX_{sand} plot increased during the two dry seasons encompassed by this study (Fig. 3e).

5.4.3. Tree mortality

Over three years (2003 – 2005), 19 trees over 10 cm diameter at breast height died on the OX_{dry} plot compared to 31 on the OX_{sand} plot. This equates to 1.5 and 2.4 % annual mortality of the tree populations on the OX_{dry} and OX_{sand} plots respectively. However, more large trees died on the OX_{dry} plot, such that mortality quantified in mass terms was slightly greater in the OX_{dry} plot (Table 3; 2.1 t C ha^{-1} yr^{-1}, 1.49 % of plot tree mass) compared to the OX_{sand} plot (Table 3; 1.9 t C ha^{-1} yr^{-1}, 1.29 % of plot tree mass).

5.4.4. Root dynamics

Estimated root growth was higher on the OX_{dry} plot- 2.7 (5^{th} Pc = 1.7, 95^{th} Pc = 5.1) t C ha^{-1} yr^{1}- compared to 2.4 (5^{th} Pc = 1.4, 95^{th} Pc = 3.6) t C ha^{-1} yr^{-1} on the OX_{sand} plot (Table 3). On both plots, growth appeared to peak around the middle of the wet season, though roots on the OX_{dry} plot displayed an additional surge in production coinciding with the large rain events which mark the beginning of the wet season (Fig. 3f). Estimated root mortality was higher on the OX_{sand} plot (Table 3), and on both plots occurred only during short periods in the wet season (Fig. 3g), through further measurement replication is required to reduce uncertainty around observations.

5.4.5. Soil respiration and surface litter turnover

Soil respiration constituted a flux of 13.4 (5^{th} Pc = 9.1, 95^{th} Pc = 20.1) and 12.5 (5^{th} Pc = 7.5, 95^{th} Pc = 17.7) t C ha^{-1} yr^{-1} into the atmosphere, from the OX_{sand} and OX_{dry} plots respectively (Table 3). The relative contribution of autotrophic and heterotrophic sources to total soil respiration differed between plots (Table 3). Thus, on the OX_{sand} plot, measured soil CO_2 efflux was divided almost equally between heterotrophic (53 %, 7.1 t C ha^{-1} yr^{-1}) and autotrophic (47 %, 6.3 t C ha^{-1} yr^{-1}) contributions, whereas soil respiration on the OX_{dry} plot was more dominated by autotrophic sources (59 %, 7.4 t C ha^{-1} yr^{-1}) while heterotrophic respiration (41 %, 5.2 t C ha^{-1} yr^{-1}) contributed relatively less.

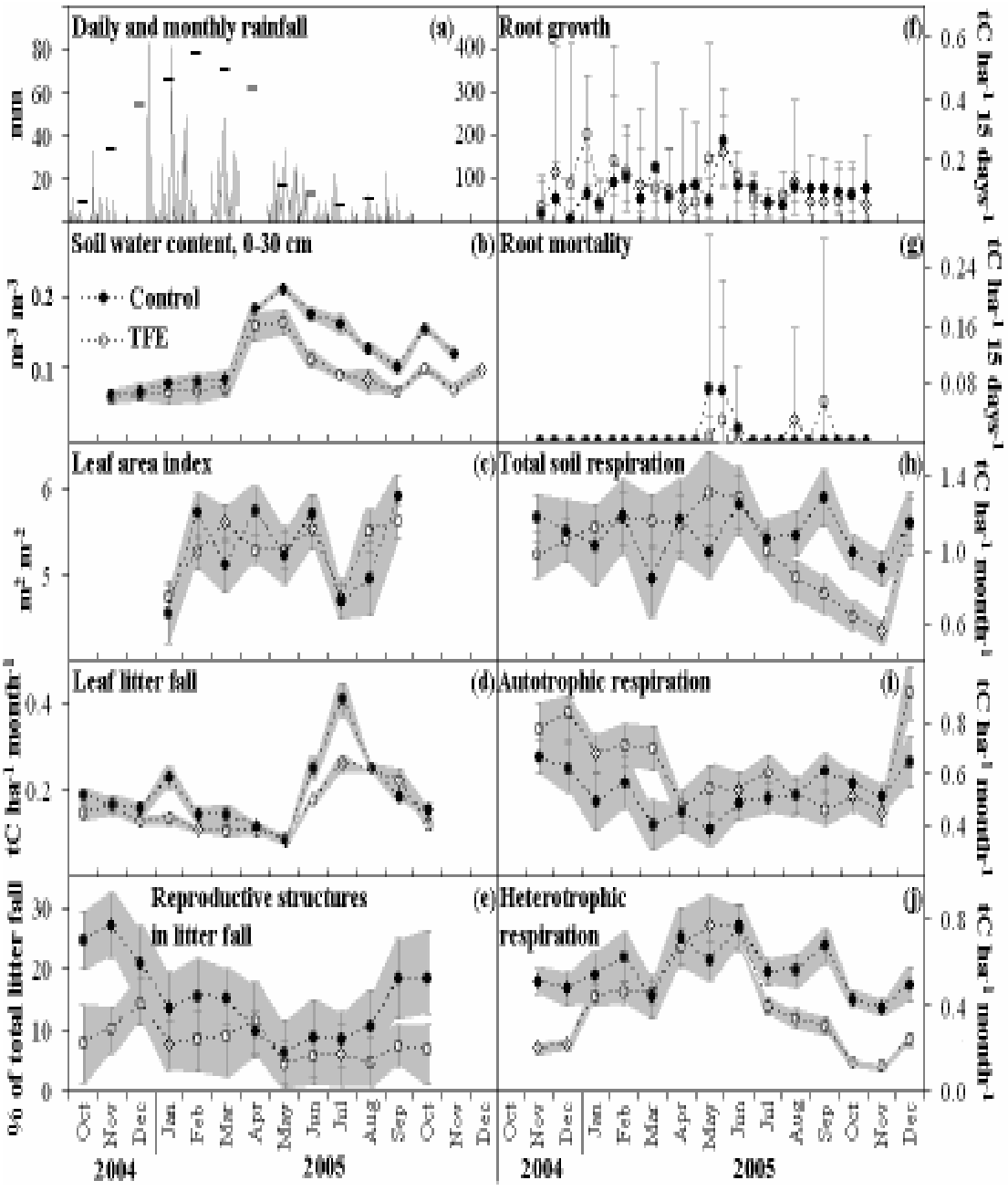

Figure 3. Temporal trends in water, above- and below-ground plant dynamics, and soil respiration on both plots. The grey regions around mean values denote 95th confidence intervals, with the exception of mean root growth and mortality where error bars denote 5th and 95th percentiles. Daily rainfall records are missing for the following periods: 14 – 28 February, 1 – 30 April, 1 October onwards. Monthly rainfall is generated for the missing period by linearly interpolating between 10 day rainfall periods before and after the gaps.

5.4.6. Tree growth and allocation

Estimated total NPP (the sum of canopy litter fall, tree stem growth and root growth) was 8.1 (5^{th} Pc = 5.8, 95^{th} Pc = 11.0) t C ha^{-1} yr^{-1} on the OX_{sand} plot as compared with 7.6 (5^{th} Pc = 5.5, 95^{th} Pc = 11.3) t C ha^{-1} yr^{-1} on the OX_{dry} plot (Table 3). The greatest uncertainties in these estimates arose from quantifying root production. Of this total NPP, a greater proportion was invested in litter fall (56 %, 4.5 t C ha^{-1} yr^{-1}) than root production (30 %, 2.4 t C ha^{-1} yr^{-1}), on the OX_{sand} plot (Table 3). Whereas, on the OX_{dry} plot, the pattern of allocation appears to have shifted such that root production accounted for a relatively greater proportion of total growth (36 %, 2.7 t C ha^{-1} yr^{-1}) at the expense of litter fall production (47 %, 3.6 t C ha^{-1} yr^{-1}). Stem wood production only differed slightly between plots (1.28 and 1.26 t C ha^{-1} yr^{-1} on the OX_{sand} and OX_{dry} plots respectively), and on both plots constituted 16 % of annual NPP (Table 3).

5.4.7. Net ecosystem production of C

On the OX_{sand} plot, the estimated amount of C assimilated as NPP was less than the estimated quantity of C released as heterotrophic respiration from soil and CWD, such that over the period of this study estimated NEP in the OX_{sand} forest was -0.8 (5^{th} Pc = -6.7 , 95^{th} Pc =4.3) t C ha^{-1} yr^{-1} (Table 3). On the OX_{dry} plot, NPP was reduced, but soil heterotrophic respiration declined even more, such that estimated NEP on the forest subjected to the OX_{dry} treatment was 0.5 (5^{th} Pc = -3.7 , 95^{th} Pc = 6.3) t C ha^{-1} yr^{-1} (Table 3).

Estimated GPP was 28.4 (5^{th} Pc = 24.1, 95^{th} Pc = 34.5) and 29.0 t C ha^{-1} yr^{-1} (5^{th} Pc = 23.9, 95^{th} Pc = 35.6) on the OX_{sand} and OX_{dry} plots respectively (Table 3), and a

relatively small proportion of this assimilated C was invested in NPP (Table 3; 28.5 % on the OX_{sand} plot, and 26.2 % on the OX_{dry} plot).

5.5. Discussion

5.5.1. Canopy dynamics

Results from this study provide only limited support for H_1- that soil drought causes a decline in LAI, foliage N content, and a rise in leaf litter fall. The amount of LAI recorded at this site (Table 1; 5.3 m^2 m^{-2}) agrees well both with existing reports from other locations in the Amazon rain forest (6.2 – 6.8 m^2 m^{-2}, Nepstad *et al*., 2002; 5.10 m^2 m^{-2}, Aragao *et al*., 2005), and from previous measurements made at this site (~ 5.5 m^2 m^{-2}, Meir *et al*., 2006). My measurements, in the fourth year of the OX_{dry} treatment, showed no clear difference in LAI between the OX_{dry} and OX_{sand} plots (Fig. 3c). This result contrasts with earlier measurements (Meir *et al*., 2006), made through the first and second years of the drought treatment on the OX_{dry} plot, that show a distinct decline in LAI on the OX_{dry} plot relative to the OX_{sand} plot of 0.5 m^2 m^{-2} in the first year and 1.2 m^2 m^{-2} by the end of the second year. My follow-up measurements suggest, therefore, that the forest in the OX_{dry} plot may have recovered from the initial impacts of the OX_{dry} treatment ($\leq$ 2 years), at least in terms of LAI. A comprehensive inter-comparison of methodologies, and additional measurements over a longer time period, are required to reinforce this preliminary finding. Though, other studies in the region corroborate my general conclusion that the rain forest canopy appears to be relatively resilient to the effects of drought. For example, Nepstad *et al*., (2002) conducted a similar through-fall exclusion in the Amazon and concluded that after several years of soil moisture deficit "the forest leaf canopy…exhibited a rather small response to the through-fall exclusion treatment", whilst a study of seasonal rain forest canopy dynamics in Barro Colorado island,

Panama, found no clear canopy response to seasonal drought (Wright and Cornejo, 1990).

Contrary to the predictions of H_1 (that drought would cause an increase in leaf litter fall), total annual leaf litter fall was lower on the OX_{dry} plot (2.0 t C ha^{-1} yr^{-1}) compared to the OX_{sand} plot (Table 3; 2.5 t C ha^{-1} yr-1) in the year of measurement. This annual difference in litter fall was entirely attributable to two transient surges in leaf litter fall on the OX_{sand} plot around January and July 2005 (Fig. 3d). In addition, measured leaf litter fall did not peak during the dry season as hypothesized (H_1). Instead, leaf litter fall rate began to increase on both plots around the annual soil moisture maximum and reached a peak several months thereafter (Fig. 3d). Both the plot differences and the seasonal trends of leaf litter fall apparent in this dataset are replicated by observations made by Meir *et al*., (2006) at this site in the first 2 years of the drought treatment on the OX_{dry} treatment. This suggests that, for the forest at this site, soil moisture deficit may not be the most important seasonal cue for leaf fall. While numerous studies in tropical forests have documented increases in leaf fall during the dry season, attempts to rigorously test the role of soil moisture in determining the magnitude and timing of leaf fall indicate that tree and forest responses are not uniform (see Wright & Cornejo 1990, and references therein), possibly because of species-specific differences in drought susceptibility and the existence of other physical cues (e.g.: radiation, air humidity). One potential explanation for the unusual leaf litter fall pattern observed in this study is that the site has a relatively high level of plant available moisture compared to other areas of the eastern Amazon (Meir *et al*., 2006), which could diminish the severity of water stress experienced by the forest during the dry season. In addition, my data suggest that the forest canopy may be responding to drought in other ways. For example, the relatively invariant LAI despite substantial changes in leaf litter fall (Figs. 3a & 3b) indicates that there may have been shifts in the rate of new leaf production seasonally and between plots over the period of measurement. The C and N content of leaf litter fall varies slightly between plots and seasons (Table 4), which points towards the

existence of subtle changes in leaf physiology. Clearly, though, more detailed measurements of leaf dynamics and physiology at this site are necessary to provide a better understanding of the factors controlling canopy structure and leaf dynamics.

5.5.2. Tree reproduction

In this study, the proportional mass of reproductive structures (flowers, fruits, seeds) in litter fall was used as a proxy for reproductive activity at the tree stand level. My observations provided only partial support for H_2- that reproduction declines with soil water availability. On an annual basis, the OX_{dry} plot did produce less reproductive litter (0.2 t C ha^{-1} yr^{-1}, 6 % of total) than the OX_{sand} plot (Table 3; 0.6 t C ha^{-1} yr^{-1}, 13 % of total). In particular, OX_{dry} plot reproductive litter production was diminished relative to the OX_{sand} plot during the dry seasons at the beginning and end of the measurement period (Fig. 3). The seasonal pattern of reproductive litter fall on the OX_{sand} plot indicated that tree reproduction was enhanced during the dry season (Fig. 3). These results should be interpreted cautiously because individual trees with particularly abundant or heavy reproductive structures may have a disproportionately large effect upon plot estimates of reproduction. However, this seasonal pattern is corroborated both by a direct visual assessment of tree reproductive phenology in another Amazon rain forest (Nepstad *et al*., 2002), and earlier measurements of reproductive litter mass production made at this site during the first and second years of the drought treatment on the OX_{dry} plot (Meir *et al*., 2006). Thus, it appears that forest reproduction displays opposing responses to seasonal drought and longer-term soil moisture deficit caused by the drought treatment on the OX_{dry} plot. Results from a recently developed ecophysiological model may resolve this apparent paradox (Fisher *et al*., 2006): under normal conditions (in a non-El Niño year, when not subjected to the drought treatment), GPP at this site may be slightly higher during the dry season than the wet season because during the dry season forest GPP is still not moisture limited but is enhanced by higher levels of radiation because of the larger

number of cloudless days (Huete *et al*., 2006). Under extended soil drought imposed by the drought treatment, however, forest GPP is reduced by 13% (Fisher *et al*., 2006). Thus, at this site, drought events of short duration (i.e.: during the dry season of a non-El Niño year) appear to increase forest C assimilation, which is reflected in a rise in reproduction during the dry season (Fig. 3e), but after longer or more severe periods of drought (i.e.: on the OX_{dry} plot) soil moisture deficit may limit GPP such that reserves of C usually available to support seasonal reproduction are not replenished and become exhausted. This preliminary conclusion calls for further detailed research into the mechanisms regulating reproduction in tropical forests. Whatever the underlying processes, results from this study suggest that projected increases in drought conditions in the Amazon over this century could potentially have immediate impacts on ecosystem nutrient cycling via reproductive litter, and longer-term implications for seedling recruitment, tree population age structure and forest C storage capacity.

5.5.3. Tree mortality

Tree mortality was recorded every six months for three years (2003 -2005), and results provide partial support for H_4- that drought causes elevated tree mortality rates. When quantified in terms of the percentage of the total population of trees surveyed which died over the measurement period, the OX_{sand} plot exhibited greater mortality (2.4 %) than the OX_{dry} plot (1.5 %). In contrast, over the first two years of the drought treatment on the OX_{dry} plot, Meir *et al*., (2006) reported an increased population mortality rate of 1.5 – 2.0 % from a pre-drought baseline population mortality rate of 1 %. However, between 2003 and 2005, more large trees died on the OX_{dry} plot, with the consequence that tree mortality expressed in mass terms was slightly higher on the OX_{dry} plot (1.49 %, 2.1 t C ha^{-1} yr^{-1}) compared to the OX_{sand} plot (Table3; 1.29 %, 1.9 t C ha^{-1} yr^{-1}). Caution should be applied when interpreting these results since the measurement period is relatively short, and mortality is likely

to show considerable spatial and temporal variation. Several studies have documented elevated tree population mortality during El Niño related drought events (Condit et al., 1995; Williamson *et al*., 2000; Laurance *et al*., 2001; Condit *el al*., 2004), but most also highlight the complexity of responses amongst species and regions, and the potential for forest drought resilience. For example, Condit *et al*., (2004) recorded responses of three rain forest plots along a rainfall gradient to the 1997 - 1998 El Niño drought, and found that forest on all plots experienced increased growth, whilst only the driest plot on the gradient displayed elevated tree mortality. For the same El Niño year, Williamson *et al*., (2000) did observe an increase in population mortality rate- 1.91 % compared to 1.12 % prior to the El Niño drought- but the forest appeared to recover by the following year. In this study, tree growth and mortality was recorded only for stems over 10 cm in diameter. It is possible that a stronger drought effect would have been observed if smaller plants had been included, since they are likely to have shallower root systems which cannot access deep water reserves.

5.5.4. Root dynamics

Rates of root production and mortality, recorded by rhizotrons at this site, displayed a high degree of spatio-temporal heterogeneity which limits the degree of confidence which may be placed in any patterns observed. Nevertheless, the rhizotrons provided useful preliminary information about a component of plant growth which is rarely quantified but could have important impacts upon Amazon ecosystem biogeochemical cycling. My results provided only partial support for H_5- that soil moisture deficit will lead to an increase in root production and mortality. Annual production of root mass was higher on the OX_{dry} plot (2.7 t C ha^{-1} yr^{-1}, 36 % of NPP) relative to the OX_{sand} plot (2.4 t C ha^{-1} yr^{-1}, 30 % of NPP), both in absolute terms and as a proportion of above-ground growth (Table 3). However, root mass production appears to have peaked on both plots as soil moisture reached its annual maximum, though roots in the OX_{dry} plot displayed an additional surge in production at the onset

of the wet season (Figure 3f). This additional surge on the OX_{dry} plot accounts for most of the estimated annual difference between plots. This brief period of elevated root production in the OX_{dry} plot implies that the trees on the plot may have been compensating for lower annual production rates by increasing production during seasonal periods of relatively high soil moisture. This interpretation is corroborated by a range of studies which found that prior exposure to water deficit led to higher growth either in other portions of the root system where conditions were more favourable, or for the root system as a whole when the soil was rewetted (Dickman *et al*., 1996; Hendrick & Pregitzer, 1996; Torreano & Morris, 1998). For example, Joslin *et al*. (2000) artificially modified water availability on three plots over five years at a temperate deciduous forest site. While they found little evidence for a net increase in fine root production on the drier plot, they do conclude that 'periods of lower root production in the dry treatment were compensated for by higher growth during favourable periods'.

Records of root disappearance (mortality and complete decay) from the rhizotrons installed in both plots do not support the hypothesis (H_5) that soil moisture deficit drives an increase in root mortality, since annual root disappearance was higher on the OX_{sand} plot (0.2 t C ha^{-1} yr^{-1}) than the OX_{dry} plot (0.1 t C ha^{-1} yr^{-1}), and through the year all root disappearance on both plots occurred during a few periods in the wet season (Figure 3g). This may be because root disappearance at the rhizotrons was partly determined by rates of root decomposition, not only mortality rate. Root mortality and decomposition could have differing responses to soil moisture which could confound attempts to derive a simple relationship between soil moisture and rhizotron root disappearance. Disapearance events were extremely variable in time and space. Two rhizotrons in the OX_{sand} plot and 5 in the OX_{dry} plot exhibited no root mortality at all over one year, whilst others experienced annual disappearance of up to 19 % of existing roots. Overall, recorded root diappearance was extremely low compared to typical estimates of root longevity derived from minirhizotron measurements (usually not more than a year: Hendrick & Pregitzer, 1992; Black *et*

al., 1998; Anderson *et al*., 2003; Majdi & Öhrvik, 2004, but see review by Trumbore & Gaudinski, 2003). In this study, of the roots produced over one year only 6.7 % and 4.8 % disappeared on the OX_{sand} and OX_{dry} plots respectively. There are several possible explanations for the disparity between values of root disappearance from this study, and other published estimates. Firstly, the apparently low root mortality at this site may have been an artefact of equipment or observers. I propose that this is unlikely to be the case because two rhizotrons, installed adjacent to the OX_{sand} plot, which were trenched to sever all visible roots clearly showed 70 % and 98 % root disappearance after 70 days (Fig 2). Secondly, it is possible that most minirhizotrons sample a relatively greater proportion of very fine, dynamic roots compared to alternative methodologies (i.e.: the rhizotron design used in this study, or isotopic tracers- see review by Trumbore & Gaudinski, 2003). Further testing of the rhizotron design used in this study could provide more information about dynamics of relatively coarse roots, which constitute an important pathway for C and nutrients allocated below-ground, but may not be fully captured by current minirhizotron methodologies.

5.5.5. Soil respiration and surface litter dynamics

Results from this study do support H_6- that soil respiration and surface litter decomposition rate decline under drier conditions. The estimated total amount of C released from soil during the year of measurement was slightly lower on the OX_{dry} plot (12.5 t C ha^{-1} yr^{-1}) compared to the OX_{sand} plot (13.4 t C ha^{-1} yr^{-1}). These fluxes appear typical for primary forest in the Amazon (see Sotta *et al*., 2004, for a review of soil respiration values reported by studies in the region). Davidson *et al*., (2004), in another drought experiment in central Amazon, did not detect any clear drought effect upon soil CO_2 efflux, though other trace gas fluxes were affected which indicates that the experimental drought treatment was altering soil biogeochemical cycling. In this study, soil respiration remained similar on both plots for much of the year, except for

a four month period (August – November 2005) during the dry season when soil CO_2 efflux on the OX_{dry} plot was consistently lower than the OX_{sand} plot (Fig. 3). Both the annual magnitude and temporal pattern of soil respiration, with maximum plot differences towards the end of the wet season, appears to be a consistent feature of the site since it was also noticeable in the first two years of the drought treatment on the OX_{dry} plot (Meir *et al*., 2006). My data builds upon these observations, by partitioning seasonal soil CO_2 flux into heterotrophic and autotrophic sources. Results suggest that the relative contributions of heterotrophic and autotrophic respiration vary seasonally, and this seasonal pattern differs between plots (Table 3 & Fig. 3). On the OX_{sand} plot, soil respiration was divided almost equally between autotrophic (6.3 t C ha^{-1} yr^{-1}, 47 %) and heterotrophic (7.1 t C ha^{-1} yr^{-1}, 53 %) sources, whereas on the OX_{dry} plot heterotrophs contributed less (5.2 t C ha^{-1} yr^{-1}, 41 %) to total soil respiration (Table 3). Autotrophic and heterotrophic respiration on the OX_{sand} plot did not change consistently through the year (Fig. 3i & 3j, with the net consequence that total soil respiration on the OX_{sand} plot was not clearly different between wet and dry seasons (Figures 3h). In contrast, heterotrophic respiration on the OX_{dry} plot rose considerably during the wet season and fell again as conditions became drier (Figure 3j), while autotrophic respiration showed a weaker, but opposite trend (Figure 3i). During the wet season the minor increase in autotrophic respiration on the OX_{dry} plot was offset by the larger decrease in heterotrophic respiration. The net effect upon soil respiration in the OX_{dry} plot was that there was little consistent change in CO_2 efflux until after the peak of the wet season, when soil respiration consistently fell over 4 consecutive months (Figure 3h). This period during the wet season accounted for the majority of the difference in annual soil CO_2 efflux between the OX_{sand} and OX_{dry} plots (Table 3).

In this study, estimates of ground surface litter turnover were derived by dividing litter mass (Table 2) by annual litter fall rate (Table 3). This approach assumes steady state conditions for stocks of ground surface litter over the year of measurement. Results indicate that the time taken for complete surface litter turnover was 7.6

months on the OX_{sand} plot, and 8.1 months on the OX_{dry} plot. This apparent difference in turnover between plots supports H_5, though additional work (e.g.: using litter bags) is required to explore litter decomposition and turnover in greater detail, to reinforce this preliminary conclusion.

5.5.6. Tree growth and allocation

According to the functional balance theory (Thornley, 1972; Cannell & Dewar, 1994), trees on the OX_{dry} plot should have responded to soil moisture deficit by increasing allocation of resources to root production relative to above-ground production of woody tissue and foliage (H_6). Comparison of production between plots is consistent with this hypothesis though observed differences are small. While NPP (the sum of canopy litter fall, stem wood growth and root growth) was lower on the OX_{dry} plot (7.6 t C ha^{-1} yr^{-1}) than the OX_{sand} plot (8.1 t C ha^{-1} yr^{-1}), on the OX_{dry} plot a greater proportion of the total was invested in root growth (36 %, 2.7 t C ha^{-1} yr^{-1}), apparently at the expense of litter fall (47 %, 3.6 t C ha^{-1} yr^{-1}). Trees on the OX_{dry} plot greater than 10 cm in diameter showed a small reduction in radial growth over the year of measurement compared to the OX_{sand} plot which translated into an estimated reduction in stem wood production of just 0.02 t C ha^{-1} yr^{-1} (Table 2). On both plots, stem wood production constituted 16 % of estimated total annual production (1.28 and 1.26 t C ha^{-1} yr^{-1} on the OX_{sand} and OX_{dry} plots respectively).

5.5.7. Net ecosystem production of C

Over the year of measurement, I estimate that NEP on the OX_{dry} plot forest was 0.5 (5^{th} Pc = -3.7, 95^{th} Pc = 6.3) t C ha^{-1} yr^{-1}. In comparison, over the same period estimated NEP on the OX_{sand} plot was -0.8 (5^{th} Pc = -6.7, 95^{th} Pc = 4.3) t C ha^{-1} yr^{-1}. The main reason for the relatively large amount of C uptake on the OX_{dry} plot is the

reduced rate of heterotrophic respiration which more than offsets a plot decline in NPP. This is potentially important because current models, which predict a large efflux of C from the forest under future drought conditions, simulate almost no drought induced change in soil respiration (Tian *et al*. 1998, Zeng *et al*. 2005). Instead, modelled respiration is usually stimulated by rising temperature. A different representation of below-ground processes in these models (i.e.: simulating a decline in soil respiration under drier conditions) might fundamentally alter model forecasts of forest NEP. While there is a considerable degree of uncertainty surrounding my estimates, they are consistent with current understanding of the links between heterotrophic respiration, soil moisture and plant photosynthesis. If photosynthesis is reduced by the drought on the OX_{dry} plot (Fisher *et al*., 2006), and if supply of photosynthate controls much of soil CO_2 efflux (Högberg *et al*., 2001; Högberg & Read 2006) then it is plausible that soil respiration will decline in response to drought, not increase as current models predict.

In this study, GPP was estimated by directly measuring growth and respiration of most major tree components. This approach is relatively rare, compared to alternatives such as eddy-flux measurements and ecophysiological modelling, because of the considerable time and effort necessary to make measurements. Using this 'bottom-up' approach, I estimate GPP of 28.4 t C ha^{-1} yr^{-1} on the OX_{sand} plot and 29.0 t C ha^{-1} yr^{-1} on the OX_{dry} plot over the year of measurement. There is substantial uncertainty surrounding these estimates, but the remarkable degree of similarity with top-down estimates from the region strengthens confidence in the validity of the estimates. For example, Fisher *et al*., (2006) developed an ecophysiological model to simulate forest C assimilation at the study site, and estimated GPP of 31.2 and 27.0 t C ha^{-1} yr^{-1} on the OX_{sand} and OX_{dry} plots respectively. In other locations in the Amazon, the eddy flux method has been used to estimate forest GPP of 20.4 – 36.3 t C ha^{-1} yr^{-1} (Grace *et al*., 2000; Malhi & Grace, 2000; Carswell *et al*., 2002; Loescher *et al*., 2003). The eddy flux approach has been used to infer a substantial C sink in Amazon forests (Grace *et al*., 1995; Grace *et al*., 1996; Malhi *et al*., 1998), however

the method may often underestimate night-time respiration (see review by Ometto *et al.*, 2005), and thus overestimate NEP. The method used in this study is not susceptible to this bias, though there are other sources of uncertainty from measuring and up-scaling C components, and suggests that not all Amazon forest sites may be such strong C sinks as previously claimed. Further research using different methodologies to calculate NEP at different forest types across the Amazon is required to clarify this issue.

This study contributes to the growing body of research which indicates that the CUE of tropical forest is low (mean of 25 % from 4 separate studies, see Amthor, 2000, and Chambers *et al*., 2004) compared to temperate forest sites (mean of 54 % from 20 separate studies, see Amthor, 2000). The low CUE of tropical forests may reflect increased respiratory demands per unit photosynthate, perhaps linked to increased temperature (Woodwell 1983; Ryan 1996). An alternative hypothesis is that tropical forests are nutrient rather than CO_2 limited, such that more C is assimilated than can be used for tissue construction. If this is true, then the surplus assimilated C may be respired through some other, unmeasured, pathway as 'wastage respiration' (Lambers, 1982; Lambers, 1997). Understanding the underlying cause for the apparently low CUE in tropical forests could be critical for predicting future forest responses to climate change. For example, if the supply of C already exceeds demand in tropical forests then it is unlikely that increases in atmospheric CO_2 levels would cause increased NPP. Whereas, if high respiration does reflect respiratory demands, then increased photosynthesis caused by elevated CO_2 levels, would enhance NPP (Lloyd & Farquhar, 2000). Quantifying the flux of C through different plant respiratory pathways could resolve why tropical forests appear to have a low CUE, and how this may affect their response to future climate change.

5.6. Conclusion

Four years of artificial soil drought on the OX_{dry} plot elicited several important responses in terms of forest growth dynamics and soil respiration. The apparent net consequence of these changes is that estimated NEP on the OX_{dry} plot forest was 0.5 (5^{th} Pc = -3.7, 95^{th} Pc = 6.3) t C ha^{-1} yr^{-1} over the period of measurement, whereas on the OX_{sand} plot forest, estimated NEP was -0.8 (5^{th} Pc = -6.7, 95^{th} Pc = 4.3) t C ha^{-1} yr^{-1}. Estimated GPP was ~ 29 t C ha^{-1} yr^{-1}, which is consistent with modelling studies and eddy flux measurements in the region. Most of this GPP appeared to be expended through respiration, and thus estimated carbon use efficiency at this site was low (~ 28 %) compared with many temperate forest sites. The forest canopy appeared to be relatively resilient to drought with little change in either leaf area index of leaf litter N content. Unexpectedly, leaf litter fall on both plots peaked during the wet season, not when conditions were dry as hypothesized. Tree reproduction appeared to be inhibited by the drought treatment on the OX_{dry} plot, but seasonal reproduction on the OX_{sand} plot was highest during the dry season. If projected increases in the frequency and severity of drought in the Amazon do cause a decline in tree reproduction in the region this could have serious implications for the age-structure and C storage capacity of the forest. The strong response of reproduction to drought on the OX_{dry} plot is consistent with the hypothesis that, under soil water deficit, plants divert resources away from non-essential tissues (i.e.: fruits, flowers, seeds), and towards organs responsible for water uptake and transport (i.e.: roots). Root production was higher on the OX_{dry} plot relative to the OX_{sand} plot, but production on both plots coincided with the annual maximum of soil moisture (with an additional peak in the OX_{dry} plot at the initiation of the wet season). Tree mortality, quantified in mass terms, was highest in the OX_{dry} plot, while root mortality was lower and peaked on both plots during the wet season. It is likely that observed patterns of root mortality reflected changes in not only root longevity, but also rates of decomposition. Annual soil CO_2 efflux was lower on the OX_{dry} plot compared to the OX_{sand} plot. There was no clear seasonal pattern in soil respiration on either plot. In the OX_{dry} plot, this lack of seasonality disguised an increase in heterotrophic respiration during the wet

season, with a rise in autotrophic respiration when conditions became drier. Autotrophic and heterotrophic respiration showed no clear seasonality on the OX_{sand} plot. Additional years of measurement at the OX_{dry} plot may reveal longer term impacts of drought such as decreases in leaf area index, and greater tree mortality. Of particular interest are what changes will mean for the net exchange of CO_2 between the forest and atmosphere, and how much spatial heterogeneity there is within the Amazon basin, in terms of the sensitivity of trees to drought.

Chapter 6

6. Discussion

6.1. Key findings and their implications

In the introduction, I described how the lack of understanding about Amazon forest responses to future drought is mainly constrained by the scarcity of data on below-ground plant activity and soil respiration. This scarcity is caused principally by the considerable time and effort required to collect and process soil and plant root samples, together with the difficulties associated with research in a remote environment. The main contributions of the research contained within this thesis have, therefore, been to: (1) develop techniques which are capable of quantifying root activity with an accuracy and temporal frequency comparable to above-ground measurements, (2) integrate above- and below-ground measurements to provide a more holistic picture of potential Amazon ecosystem C cycling responses to drought, and (3) examine how these responses differ between forest plots with contrasting soil type and vegetation structure. This data synthesis is a significant advance in understanding of C cycling in rain forests, and provides information which should allow more accurate modelling of the response of the Amazon region to future drought.

Over the course of the four data Chapters (Chapters 2 – 5) a series of scientific questions were addressed. Here, I review the answers to these questions which were provided by each Chapter, and explore some of the implications of the findings. Subsequently, the limitations of the data and future research directions are discussed.

6.1.1. Methodological considerations

How many samples are required to quantify important ecosystem carbon stocks and fluxes with high precision?

Before initiating data collection, sample size analysis was used to guide the sampling strategy at the study site. Measurements of variables, particularly of root characteristics, often displayed a high degree of spatial heterogeneity. For example, standing crop root mass, and root production required 143 – 236 and 29 – 154 samples respectively to estimate mean values within 10 % confidence intervals with 95 % probability. Other characteristics, such as soil temperature, moisture, C and N content, were more homogenous and, therefore, required fewer samples (<8) to achieve the same degree of precision. Thus, in this thesis, most sampling effort was invested in quantifying below-ground processes such as root biomass and production, and respiration from soil.

How is it possible to adequately sample roots, given considerable spatial heterogeneity in root mass, and the substantial amount of time and effort required to process samples?

Root material is usually retrieved from soil cores by hand or using sieves (e.g.: Prathapar *et al.*, 1989; Chotte *et al*., 1995; Benjamin & Nielsen, 2004). In this thesis, roots were manually removed from soil cores *but* the period of root extraction was split into time-steps, to reveal the pattern of extraction over time. This pattern, unique to each sample, was used to predict the amount of roots remaining uncollected in the soil sample after manual processing had ended. This method corrects for the underestimates of root mass, which usually result from most root sampling methods, whilst allowing for a relatively rapid rate of sample processing. For example, at the study site, the prediction method added 21 – 32 % to initial estimates of standing crop root mass (derived from 40 minutes of manual root removal). Complete manual collection of roots from the 18 soil samples would have taken approximately 239 hours for one person, compared to just 12 hours using the combined manual collection and prediction approach. While the prediction method does introduce uncertainty into estimates, this uncertainty is minor compared to uncertainty caused

by not taking enough samples to adequately capture spatial heterogeneity of root mass.

What is the effect of rhizotron root length – biomass conversion method upon estimates of root mass production per unit mass? Which is the least biased conversion method?

There exist several reviews of different methodologies for quantifying root properties (Vogt *et al*., 1998, Hendricks *et al*., 2006). However, there has been no systematic review of the various rhizotron length – mass conversion methods used in the literature (Taylor *et al*., 1970; Itoh, 1985; Tingey *et al*., 2000; Bernier & Robitaille 2004; Hendricks *et al*., 2006). To this end, four different conversion methods were applied to the same rhizotron dataset collected from the study site, resulting in root production estimates ranging from 4.1 to 18.9 t ha^{-1} yr^{-1}. In addition to the annual magnitude of root production, the monthly pattern of production also varied between methods. There is currently no 'gold standard' against which to compare these estimates, to objectively evaluate which conversion method produces the most accurate results. Instead, potential sources of bias and error inherent in each conversion method were assessed, to produce an informed judgment of which method is likely to produce the most reliable estimate of root production. I conclude that, of the four methods reviewed, the method proposed by Bernier & Robitaille (2004) is subject to the fewest biases and errors, for the following reasons: (1) it is not, as are the other methods, inter – calibrated with data from ingrowth cores or soil cores. It is, therefore, an independent estimate of root production, which does not rely upon the, potentially biased, ingrowth core and sequential soil core methodologies (Vogt *et al*., 1998, Steingrobe *et al*., 2000); (2) it calculates production based upon the number of roots which intersect the observation screen at each interval. Whereas all other methods calculate production from changes in root length visible at the rhizotron observation screen, which are likely to be biased by the presence of the screen

(Withington *et al*., 2003) and, therefore, may not be representative of production in the surrounding soil environment.

6.1.2. Root responses to environmental changes

How do recorded root characteristics and responses compare to observations from other studies?

A wide variety of studies have documented that plants in dry ecosystems tend to allocate a greater proportion of their resources below-ground, compared to vegetation in wetter climates (see Joslin *et al*., 2000, and references therein). These observations of general plant community characteristics shaped over an evolutionary time-scale have contributed to the development of the concept that plants may respond to short-term drought conditions by increasing growth of below-ground biomass relative to above-ground components. However, attempts to test this hypothesis, either by surveying vegetation along a rainfall gradient or using large-scale irrigation experiments, have yielded conflicting results (Joslin *et al*., 2000, and references therein). For example, in a review of five stand-level irrigation studies (ranging in duration from 2-10 years), Joslin *et al.* (2000) found only one study which reported a significant increase in root mass production under drier conditions. The other studies reviewed found either insignificant increases or no change (see Joslin *et al*., 2000). This thesis, therefore, provides another instance of root production apparently being inhibited by drought. However, additional evidence from this thesis (see Fig. 3f and discussion in Chapter 5), and other studies, indicate that under soil water deficit plants may compensate for lower average root production by drastically increasing production during seasonal periods of relatively high soil moisture (Dickman *et al*., 1996; Hendrick & Pregitzer, 1996; Torreano & Morris, 1998; Joslin *et al*., 2000). Root standing crop and mass production data recorded in this study are consistent with values reported in the literature. For example, a meta-analysis of root

characteristics across major global vegetation types, reports a mean dry root biomass in the tropical evergreen forest ecosystem of 49 t ha^{-1}, based upon data from nine studies (Jackson *et al.,* 1996), compared to 30 - 45 t ha^{-1} within the entire soil column, from the four plots surveyed at this study site. Estimates of total dry root biomass production, from this study, range between 3.7 – 8.3 t ha^{-1} yr^{-1} within the entire soil column, which is consistent with reports from other studies in the region. For example, Jordan & Escalante (1980) calculated annual root mass production in a western Amazon forest of 2.0 t ha^{-1} yr^{-1}, while Silver *et al.* (2005) estimated production at a central Amazon site of 2.3 and 1.5 t ha^{-1} yr^{-1}, for years one and two respectively of their study. These studies calculated root production only in the surface soil layer (down to 40 cm and 10 cm depth for Jordan & Escalante 1980 and Silver *et al*., 2005, respectively), and are therefore likely to be underestimates. Much higher values have been reported in the region (5.1- 20.8 t ha^{-1} yr^{-1}, Roderstein *et al.* 2005; 9.9 t ha^{-1} yr^{-1}, Priess *et al.* 1999), but at montane forest sites in the western Amazon.

This study provides, to my knowledge, the first information about production of root length and surface area *per unit ground area* in any ecosystem. Numerous studies using rhizotrons have made earlier measurements of root length and surface area (e.g.: Field studies: Itoh, 1985; Sword et al., 1996; West *et al*., 2003; Davis *et al*., 2004. Reviews: Vogt *et al*., 1998; Hendricks *et al*., 2006), but the rhizotron unit of measurement (root length/surface area per unit area of observation screen) is difficult to integrate into models of plant nutrient and water uptake.

The advantage to the plant of modifying root morphology instead of production is that it potentially increases water and nutrient uptake, without requiring extra photosynthate to construct more root material. In addition, fine roots tend to be more dynamic than coarse roots with higher growth rates and turnover (Eissenstat *et al*., 2000; but see Trumbore & Gaudinski, 2003), which is beneficial for searching out and exploiting transient patches of high soil moisture.

How do observed root characteristics and responses vary between plots?

The magnitude of root characteristics varies substantially between plots. For example, mean annual standing crop root mass ranges between 30 - 45 t ha^{-1} on all four plots surveyed. The $OX_{fertile}$ plot is, in particular, an outlier in terms of root properties, with the lowest total standing crop, highest production rate of mass, length and surface area, lowest specific root length and surface area, highest estimated annual turnover rate, and quite distinct root chemical content. However, in general, variation between plots was minor compared to the degree of variation in root properties observed within plots. For example, 67 % of the total range in root standing crop mass recorded across all plots and seasons was also observed within each individual plot and season. A general linear model was used tot test for any interactive effect of plot upon the observed relationships between soil moisture and root variables: the results indicate that landscape-scale environmental variation among plots does not alter the general relationships between soil moisture and root characteristics. This finding suggests that despite substantial environmental variation both between plots at this site and across the Amazon as a whole (Williams *et al*., 2002), it may be valid to extend these localized measurements of responses to larger spatial scales.

How are root characteristics affected by soil water content?

There is relatively little information about root characteristics in tropical forests, and how they might respond to climate change. Given projections of increasing frequency and severity of drought in the Amazon region, there is particular interest in understanding root responses to drought in the Amazon. Thus, at the study site, I recorded root standing crop mass, root morphology, root production of mass, length and surface area, root turnover, root C and N content, and soil water content. Conclusions about root responses were based upon the following three distinct sources of evidence: (1) the correlation between spatial variation of root

characteristics and soil water content; (2) the seasonal change in root characteristics (i.e.: changes between the dry and wet seasons); and (3) comparison of root characteristics between the OX_{dry}, and OX_{sand} plots. All lines of evidence point towards the same trends. Spatial heterogeneity is not clearly linked to spatial variation in soil water content, though this may be partly due to uncertainty surrounding estimates of standing crop. Production of root mass, length and surface area is lower where surface soil is drier ($P < 0.001$, $n = 256$), while root length and surface area per unit mass show the opposite pattern ($P < 0.001$, $n = 256$). Neither root turnover nor nutrient content are clearly associated with soil moisture.

Are observed root responses consistent with a change in any or all of the following: plant allocation, plant photosynthesis, and soil structure?

There are three mechanisms whereby soil water availability could affect root growth: (1) changes in the quantity of C captured through plant photosynthesis (Williams *et al*., 1998; Schwarz *et al*., 2004), (2) changes in the allocation of photosynthate to different plant organs (Thornley, 1972; Cannell & Dewar, 1994), and (3) changes in the ability of roots to penetrate soil caused by altered root turgor or soil structure (Whalley *et al*., 1998; Bingham & Bengough, 2003; Bengough *et al*., 2006). It is possible that all, or some, of these processes are operating simultaneously at the site. With only below-ground data it is not possible to definitively test which mechanism is dominant (for this, above – ground data is required, see section 6.1.4 below). It is possible, however, to conclude that the data *is not consistent* with an increase in below-ground allocation in response to drought (as is predicted by the functional balance theory, Thornley, 1972; Cannell & Dewar, 1994). Evidence which supports this preliminary conclusion include observed decreases in root mass production (1) where soil is dry, (2) from the wet to dry season and (3) on the OX_{dry} plot compared to the OX_{sand} plot. Instead, changes in GPP and/or soil structure or root turgor may play a more important role in determining root production, at this study site. Fisher *et*

al., (2006), for example, estimated that the OX_{dry} plot experiences an annual decrease in GPP of 13% relative to the OXsand plot. It should also be noted that changes in the total amount of biomass (i.e.: amount of leaves or roots) are not the only possible responses to soil water deficit. Instead, as already discussed, plants may alter the morphology of their tissues, to maximize resource uptake without requiring additional photosynthetic assimilate to construct and sustain more tissue. To explore the possibility that changes in allocation are not observed because they are offset by opposing changes in total GPP and soil structure/root turgor below-ground data was integrated with above-ground production data (see section 6.1.4 below).

6.1.3. Soil respiration responses to environmental changes

How much do ground surface organic litter, roots and soil organic matter contribute to total soil respiration? How do these values compare to observations from other studies?

Across all plots and seasons, organic litter, roots and soil organic matter contribute 7.1 %, 55.1 %, and 38.1 % to total soil respiration respectively. This constitutes a mean CO_2 efflux of 3.9 t ha^{-1} yr^{-1} from litter, 29.2 t ha^{-1} yr^{-1} from roots, and 20 t ha^{-1} yr^{-1} from soil organic matter. Thus, the mean heterotrophic contribution (the sum of respiration from organic litter and soil organic matter) to total soil respiration is 45.2 %. This balance between heterotrophic and autotrophic respiration is broadly consistent with results from other studies. For example, based upon a review of data from soil respiration partitioning studies in tropical deciduous forest ecosystems (see references in Subke *et al.* 2006), I estimate a mean contribution of heterotrophic respiration to total of 51 % (ranging from 27-76%, $n = 10$). In addition, the mean total efflux of CO_2 from soil recorded at this study site (52.9 t ha^{-1} yr^{-1}) is with the range of

with previously published estimates for the tropical forest ecosystem (30.6 – 88.0 t ha^{-1} yr^{-1}, Subke *et al.*, 2006).

How does respiration from soil and its components vary seasonally, and between plots?

The different plots examined in this study exhibit markedly different rates of soil CO_2 efflux, and relative contribution of litter, roots and soil organic matter to this efflux. Thus, mean annual plot soil respiration varied from 47.7 – 63.4 t ha^{-1} yr^{-1}, and this efflux was partitioned into 4.7 – 12.9 %, 38.4 – 74.7 %, and 13.6 – 54.2 % from litter, roots and soil organic matter respectively. However, much of the variation across alls plots and seasons was derived from within-plot heterogeneity. For example, 51% of the total range in soil respiration values recorded across all plots and measurement periods were also observed within each plot and period.

There also appears to be considerable seasonal variation in CO_2 effluxes from soil and its components: the mean contribution of soil organic matter to total soil respiration fell from 49.1 % during the wet season to 31.5 % in the dry season, while root contribution increased from 42.0 % in the wet season to 60.5 % during the dry season. In contrast, organic litter contribution showed no clear seasonality, though the OX_{dry} plot exhibited a ten-fold reduction in annual litter respiration relative to the unmodified plots. All plots appeared to show the same general seasonal trends in CO_2 effluxes (though respiration on the $OX_{fertile}$ plot showed markedly stronger seasonality compared to the other plots). Thus, though the magnitude of fluxes varied among plots, the *pattern of response* of CO_2 efflux from soil and its components to changes in soil moisture remained consistent across plots and seasons. This uniformity of response suggests that despite substantial environmental variation both between plots at this site and across the Amazon as a whole (Williams *et al*., 2002), it may be valid to extend these localized observations of soil respiration responses soil moisture across larger spatial scales.

Is variation in litter and root respiration caused by changes in mass, or respiration per unit mass, or some combination of the two?

In this study, root respiration was not directly measured, but was calculated as solely the product of root mass and root respiration per unit mass. In addition, litter respiration per unit mass was not directly measured, but was estimated as the residual variation in litter respiration, once variation in litter mass was accounted for. Therefore, my estimates of root respiration and litter respiration per unit mass are likely to include some component of measurement error.

Heterogeneity in fine root mass explained 73% of variation in root respiration, while changes in root respiration rate per unit mass played a relatively minor role, accounting for just 16%. In contrast, ground surface litter mass accounted for only 25 % of observed variation in litter respiration, and therefore it is likely that litter respiration per unit mass is the main determinant of litter respiration.

This is, to my knowledge, the first attempt to isolate the effects of changes in tissue/substrate mass and respiration rate per unit mass upon respiration from soil components. It is important to distinguish between these two determinants of component respiration because they represent different C flux pathways which are likely to respond to environmental variation in different ways. For example, increased drought-like conditions in the Amazon may cause increased leaf litter fall (Neilson & Drapek, 1998; Nepstad *et al*., 2002) and thus surface litter mass, but an associated drop in litter moisture could drive a decline in litter respiration per unit mass (Couteaux *et al*., 1995). Results from this study suggest that if this happened, a drought-induced decline in litter respiration per unit mass have a much greater impact on the contribution of litter to total soil respiration. Similarly, changes in plant C assimilation or allocation, caused by drought, which affect root mass could have considerable effect upon root respiration, and hence total soil respiration.

Additionally, long-term (seasonal and inter-annual) trends in soil respiration, previously attributed solely to soil moisture and soil temperature, may be confounded by changes in root and litter mass or respiration per unit mass of these components. This has important implications, particularly for the numerous studies conducted in temperate deciduous forest ecosystems, because seasonal changes in temperature often coincide with major shifts in leaf litter and root activity (Gosz *et al.*, 1972; Burke & Raynal, 1994; Vose *et al.*, 2002).

6.1.4. Above- and below-ground ecosystem responses to environmental changes

How are the principal tissues responsible for plant resource capture (i.e.: leaves and roots) affected by drought?

Overall, results from this site indicate that the forest canopy was relatively resilient to the effects of drought. This may be because the forest was able to access deep reserves of soil water, and thus remained unaffected by seasonal drought or the OX_{dry} treatment. Additionally, the site has a relatively high level of plant available moisture compared to other areas of the eastern Amazon (Meir *et al*., 2006), which could diminish the severity of water stress experienced by the forest during the dry season. In the fourth year of drought on the OX_{dry} plot, I detected no clear decline in leaf area index, relative to the OX_{sand} plot. This result contrasts with earlier measurements (Meir *et al*., 2006), made through the first and second years of drought treatment on the OX_{dry} plot, that show a distinct decline in LAI on the Ox_{dry} plot relative to the OX_{sand} plot of 0.5 m^2 m^{-2} in the first year and 1.2 m^2 m^{-2} by the end of the second year. My follow-up measurements suggest, therefore, that the forest in the OX_{dry} plot may have recovered from the initial impacts of the artificial drought ($\leq$ 2 years), at least in terms of LAI. Other studies in the region corroborate my general conclusion

that the Amazon forest canopy may be relatively resilient to the effects of drought. For example, For example, Nepstad *et al*., (2002) conducted a similar through-fall exclusion in the Amazon and concluded that after several years of soil moisture deficit "the forest leaf canopy…exhibited a rather small response to the through-fall exclusion treatment", whilst a study of seasonal rain forest canopy dynamics in Barro Colorado island, Panama, found no clear canopy response to seasonal drought (Wright and Cornejo, 1990).

Annual leaf litter production was lower on the OX_{dry} plot compared to the OX_{sand} plot, and on both plots began to increase around the annual soil moisture maximum and reached a peak several months thereafter. These observations have been replicated by measurements during the first two years of the artificial drought on the OX_{dry} plot (Meir *et al*., 2006), and suggest that soil moisture deficit may not be the most important seasonal cue for leaf fall at this forest site.

There are, however, some indications that the forest canopy may be responding to drought in other ways For example, the relatively invariant LAI despite substantial changes in leaf litter fall indicates that there may have been shifts in the rate of new leaf production seasonally and between plots. The C and N content of leaf litter fall varied slightly between plots and seasons, which points towards the existence of subtle changes in leaf physiology.

Rates of root production and mortality, recorded by rhizotrons at this site, displayed a high degree of spatio-temporal heterogeneity which limits the degree of confidence which may be placed in any patterns observed. Annual root mass production was slightly higher on the OX_{dry} plot, this difference was almost entirely attributable to a rise in root production on the OX_{dry} plot at the onset of the wet season. This elevated production on the OX_{dry} plot provides further support for measurements made with ingrowth cores in this study and other studies (Dickman *et al*., 1996; Hendrick & Pregitzer, 1996; Torreano & Morris, 1998; Joslin *et al*., 2000) which imply that plants subjected to dry conditions at this and other sites, may

compensate for lower annual production rates by increasing production during seasonal periods of relatively high soil moisture.

How is plant reproduction affected by drought?

In this study, the amount of reproductive structures (fruits, flowers, seeds) in litter fall, expressed as a percentage of total mass, was used as a proxy for tree reproductive activity. Trees on the OX_{dry} plot produced consistently less reproductive litter (0.2 t C ha^{-1} yr^{-1}, 6 % of total) compared to the nearby OX_{sand} plot (0.6 t C ha^{-1} yr^{-1}, 13 % of total). Reproductive activity on the OX_{dry} plot operated at a constant, low level throughout the year, whereas activity on the OX_{sand} plot displayed strong seasonal increases during the dry season. Thus, most of the annual difference in reproductive litter production between the plots was accounted for by this disparity during the dry season. These results should be interpreted cautiously because individual trees may have a disproportionately large effect upon plot estimates of reproduction. However, this seasonal pattern is corroborated by a direct visual assessment of tree reproductive phenology in an Amazon rain forest (Nepstad *et al*., 2002) and earlier measurements of reproductive litter mass production made at this site during the first and second years of the artificial drought on the OX_{dry} plot (Meir *et al*., 2006). These results indicate that increases in drought conditions in the Amazon over this century could have immediate impacts on ecosystem nutrient cycling via reproductive litter and longer-term implications for seedling recruitment, tree age structure and, thus, forest C storage capacity.

While the OX_{sand} plot exhibited seasonal increases in reproduction during the dry seasons, longer-term drought (on the OX_{dry} plot) appeared to strongly inhibit production of reproductive litter. Reproduction at this site, therefore, appeared to show opposite responses to seasonal and longer-term soil drought. This may be because, under normal conditions at this site (in a non-El Niño year, when not subjected to an artificial drought), GPP is enhanced by the higher solar radiation

levels during the dry season, but under extended drought conditions on the OX_{dry} plot GPP is reduced by 13 % (Fisher *et al*., 2006). More detailed research into the mechanisms regulating reproduction in tropical forests, together with frequent measurements of tree non-structural carbohydrate reserves could test these hypotheses. Whatever the underlying reasons, these results caution against extrapolating long-term responses from short-term observations.

How is net primary production, and above- and below-ground allocation affected by drought?

Estimated total annual plant growth (the sum of litter fall, stem wood growth and root growth) was lower on the OX_{dry} plot (7.6 t C ha^{-1} yr^{-1}) than the OX_{sand} plot (8.1 t C ha^{-1} yr^{-1}). On the OX_{dry} plot a greater proportion of total annual production was invested in root growth compared to the OX_{sand} plot, apparently at the expense of litter fall production. On both plots, stem wood production constituted only 16 % of estimated total annual production. These observations are consistent with the functional balance theory (Thornley, 1972; Cannell & Dewar, 1994), which suggests that as water becomes a limiting resource plants should preferentially allocate photosynthate away from leaves, where it is used for light and CO_2 capture, and towards roots where it can be used to increase water and nutrient uptake. There were pre-existing differences between plots in terms of total stem mass, and standing crop root mass, but these did not account for observed differences in annual production. Thus, annual root production on the OX_{dry} plot was 18.7 % of total standing crop, compared to 11.8 % on the OX_{sand} plot.

What are the likely consequences of these drought – induced changes for the net ecosystem production of carbon dioxide between the forest and atmosphere?

In this study, NEP was calculated as the difference between forest NPP and heterotrophic respiration from soil and CWD. Using this approach, net C uptake in the forest on the OX_{sand} plot was estimated to be -0.8 t C ha^{-1} yr^{-1}, because heterotrophic respiration fluxes were greater than NPP. In contrast, in the forest on the OX_{dry} plot NPP was reduced but heterotrophic respiration declined even more, such that estimated net C uptake was 0.5 t C ha^{-1} yr^{-1}. In addition, estimated GPP remained similar between plots: 28.4 and 29.0 t C ha^{-1} yr^{-1} on the OX_{sand} and OX_{dry} plots respectively.

These are important results, because models which have predicted a fundamental change in the Amazon C balance over the next century have simulated large changes in GPP but relatively small changes in soil respiration (Tian *et al*., 1998; Prentice & Lloyd 1998). A different representation of below-ground processes in these models (i.e.: simulating a decline in soil respiration under drier conditions) might fundamentally alter model predictions of forest NEP over time. While there is a considerable degree of uncertainty surrounding my estimates, they are consistent with current understanding of the links between heterotrophic respiration, soil moisture and plant photosynthesis. If photosynthesis is reduced by the drought on the OX_{dry} plot (Fisher *et al*., 2006), and if supply of photosynthate controls much of soil CO_2 efflux (Högberg *et al*., 2001; Högberg & Read 2006) then it is plausible that soil respiration will decline in response to drought, not increase as current models predict. Clearly, though, more research is required, in a wide variety of areas, to reinforce conclusions drawn from this study (see section 6.2, below).

6.2. Possible future studies

6.2.1. Measurement of additional ecosystem carbon stocks and fluxes

In this study, some ecosystem C stocks and fluxes were not recorded, because of constraints imposed by available time and resources. These include respiration from CWD, stem wood and foliage, and C lost via soil leaching. Stem and leaf respiration are a particularly high priority because they could potentially impact upon observed differences between the OX_{dry} and OX_{sand} plots in terms of ecosystem exchange of CO_2. Stem respiration could be recorded with a modified chamber, designed to fit closely to tree stems (e.g.: Xu *et al*., 2000; Meir & Grace 2002), attached to an infra-red gas analyzer. Stem respiration would then be up-scaled to the entire plot with values of total plot tree stem surface area. Leaf dark respiration could be recorded *in situ* with a specialized cuvette (e.g.: Meir *et al*., 2001), and scaled up with leaf area index values. An important complication is how to up-scale respiration from these components given the wide diversity of plant species at the site, and across the Amazon generally.

Samples of soil water could be collected with lysimeters, and the C content of the water analyzed, to calculate the amount of water leached out of surface soil. It is, however, difficult to decide whether or not the soil water is truly leaving the soil system, or is actually still accessible to trees with deep roots, and thus still part of the short-term ecosystem C cycle. An alternative approach could be to regularly record flow rate and C content of nearby rivers, to estimate the amount of C leaving the system, and how this varies seasonally, and between watersheds with different vegetation types (Richey *et al*., 2002; Moreira-Turcq *et al.*, 2003).

6.2.2. Spatial and temporal extrapolation

One limitation of this study is that the measurements and, thus, conclusions are, to an extent, specific to the location and time-period of measurement. Plot replication is difficult because of the very large amount of time and effort required to construct an experimental through-fall exclusion treatment in a remote environment. However, without replication, most conventional statistical methods may not be applied to

assign any statistical confidence to the observed difference between plots (within-plot measurements may not be independent, and therefore cannot be counted as individual replicate samples. See Hurlbert, 1984; and Legendre, 1993 for a more detailed discussion of experimental design and pseudoreplication). One method to tackle this issue would be to make large numbers of measurements (≥ 100) of C stocks and fluxes at a range of spatial scales, to observe how autocorrelation between measurements changes as inter-measurement distance increases. The threshold distance beyond which measurements of a certain ecosystem property cease to be spatially autocorrelated could then be used to guide collection of independent samples within plots, which would permit rigorous statistical comparison of plot characteristics.

To derive reliable conclusions about Amazon C cycling it is necessary to extend the period of measurement over several years and, if possible, decades. These measurements should also be expanded over a larger area, to include sites with distinct soil and vegetation types across the Amazon. Such networks do exist, where relatively long-term measurements of ecosystem structure and function have been made at a variety of plots across the Amazon basin (Malhi *et al*., 2002). But below-ground measurements tend to be scarcer, and where they do exist they have usually been initiated more recently than above-ground measurements. There is, clearly, a trade-off between the number of plots surveyed, and the amount of measurements which can be taken at each individual plot. Other issues are logistical constraints upon where plots can be established, such that personnel and equipment can travel to the site without too much difficulty, and the limited number of plots for which historical data is available (which is necessary to trace changes over long time periods). However, results from this thesis indicate that it is feasible to quantify below-ground C cycling, and that this extra information may substantially alter conclusions about forest-climate interactions which are based solely upon above-ground measurements.

6.2.3. Effects of other climate changes

Drought is an important component of projected climate change in the Amazon, but it is not the only one. Other current changes which could potentially affect Amazon C cycling are increases in air temperature (Malhi & Wright, 2004) and atmospheric CO_2 concentration (Lloyd.1999). Temperature plays a key role in regulating the speed of chemical reactions, and therefore could have numerous influences on C cycling, from leaf photosynthesis to organic matter decomposition. There is already strong evidence that elevated atmospheric CO_2 concentrations are causing fundamental changes in the structure and function of the Amazon ecosystem (Phillips *et al*., 1998; Phillips *et al*., 2002; Lewis *et al*., 2004). What is required, therefore, is an assessment of the separate, and combined, effects of each of these factors upon forest C cycling. This would, however, require an experimental design with multiple plots each subject to different combinations of soil water availability, temperature and CO_2 concentration. It would be extremely challenging to construct and maintain this experiment if each plot was one hectare in size, but it may be possible, at least for some measurements (e.g.: soil respiration), to have much smaller plots (e.g.: 10 m^2). A variety of ecosystem chambers have been constructed to record gas exchange within individual trees, or small stands, whilst controlling for various climatic factors (e.g.: Lloyd *et al*., 1995; Medhurst *et al*., 2006). Applying this chamber methodology to a tropical forest would present special difficulties because of the large size of the trees and large species diversity per unit area, but would yield novel insights into climate impacts upon the ecosystem. An important additional effect of climate changes on the Amazon may be an increase in the frequency and severity of fires in the region (Laurance & Williamson, 2001; Nepstad *et al*., 2004). Fire releases a large quantity of C, previously stored in vegetation and soil, into the atmosphere as CO_2 and particulate matter. It potentially has important consequences, therefore, not only for global atmospheric CO_2 levels, but also for regional patterns of rainfall (since the particulates inhibit rain-bearing cloud formation, see Rosenfeld, 1999; Andreae *et al.*, 2004). Further work needs to be done to examine the factors which cause outbreaks

of fire in the region, and to quantify the contribution of fire to annual and decadal patterns of CO_2 exchange between the forest and atmosphere.

6.2.4. Effects of human activity

While climate change is important, perhaps the most immediate threat to the Amazon forest is deforestation and habitat degradation by humans. These anthropogenic changes take a wide variety of forms; from selective and clear-fell logging for commercial timber extraction, to conversion into cattle pasture or soy and palm-oil plantations, to road building to connect up disparate urban centres across the continent. Several studies document profound changes in ecosystem C cycling caused by changes in land-use within the region (selective logging: Asner *et al*., 2004; Keller *et al*., 2004. pasture conversion: Moraes *et al*., 1996; Neill *et al*., 1997. crop conversion: Sakai *et al*., 2004; road building: Nepstad *et al*., 2001, Soares-Filho *et al*., 2004). The main difficulty arises from extending localized observations across space, and predicting changes in the future, because economic, political and social factors need to be incorporated. Some researchers have made concerted efforts to integrate ecology, politics and economics into projections of the impacts of land-use on the Amazon (e.g.: Nepstad *et al*., 2002; Soares-Filho *et al*., 2004; Lopez & Galinato, 2005). Such an inter-disciplinary approach is, however, still rare. There is a real need, then, to build upon existing knowledge of C cycling in the Amazon under different land-uses, and to incorporate the influence of government policies and economics into existing coupled atmosphere-biosphere models. Obviously, including a realistic description of these complex phenomena into, already complicated, ecological models will be extremely challenging. A first step towards this goal would be increased collaboration and consultation with government strategists and professional economists, who already have considerable experience in describing and predicting consequences of political and economic actions. The end product would be extremely

powerful because it could provide insights into the impacts of different 'policy scenarios' upon the extent and integrity of the Amazon ecosystem.

6.2.5. Impacts upon plant community structure

In this thesis, I have focused primarily upon the seasonal and medium-term (~ 4 years) impacts of drought upon plant allocation and growth. Over this century, however, the principal climate-induced changes in ecosystem C cycling in the Amazon will be driven not by changes in plant allocation, but by changes in the species composition and structure of the forest. In other words, if the region switches from a C sink to a source in the future (Cox *et al*., 2000; Dufresne *et al*., 2002; Cramer *et al*., 2001; Cox *et al*; 2004) this will likely be because the forest is gradually transformed into savannah. There is already evidence for significant changes in the abundance of some plant functional types across the Amazon, possibly favoured by the increase in atmospheric CO_2 levels (Phillips *et al*., 2002; Lewis *et al*., 2004, and references therein). Measurements of reproductive structures in litter fall, within this thesis, point towards strong changes in tree reproduction under drier conditions. Inhibition of mature tree reproduction is exactly the kind of event which could trigger a gradual shift in the ecosystem; from a primary forest, to a more open canopy forest with much greater abundance of pioneer species, to savannah with dispersed scrub and trees. If drought accelerates mature tree mortality (Condit *et al*., 1995; Williamson *et al*., 2000; Laurance *et al*., 2001; Condit *el al*., 2004) this process could occur even faster. There is, thus, an urgent need to investigate how climate is likely to impact upon plant diversity and community structure in the Amazon, and what any changes will mean for the ecosystem C balance. One potentially interesting line of investigation would be to measure and model how climate-induced changes in tree seed production affect seedling recruitment, forest age-structure and C storage in biomass over time (i.e.: after 10, 20, 50 and 100 years). It would be relatively simple to record seed fall at the OX_{sand} and OX_{dry} plots, and to predict the gradual

accumulation of biomass as the seedlings grow (using allometric models of tree growth). The principal difficulty is calculating the proportion of seeds which fall that successfully germinate, and the rate of seedling mortality (Hans ter Steege, personal communication). Another line of inquiry would be to record changes in C storage across forest-savannah transition zones. This would provide some insight into what conversion of the Amazon rain forest into grassland would mean in terms of the amount of C retained in the plants and soil, and the amount released into the atmosphere.

6.2.6. Data – model integration

One way to significantly advance upon the information reported in this thesis would be to incorporate the data into an ecosystem model, to provide a more dynamic view of the multiple interactions occurring, and the net consequences of these interactions for ecosystem exchange of CO_2. A process-based physiological model has already been used at the field site (Fisher *et al*., 2006) to simulate ecosystem GPP and water balance. Inclusion of below-ground processes as parameters in the model would enhance the reliability of the model (Fisher *et al*., 2006), and provide a useful mechanism for extrapolating results across time and space (though the lack of basic data on soil and vegetation properties across the Amazon is still a limiting factor), and linking observations to current global climate models. A data assimilation approach could be used to combine the model with observations in a way which minimizes uncertainty associated with predictions and makes fullest use of the available data (see Williams *et al*., 2005 for a more detailed explanation of the data assimilation approach). This would then allow predictions of C cycling and allocation at the study site, and at other locations if data is available to parameterize the model, under different drought 'scenarios'.

6.3. Concluding remarks

The importance of the Amazon rain forest, in terms of global climate, biodiversity, and cultural wealth, is truly epic in scale. The region is, however, threatened by climate change and human activity. Effective management of the area urgently requires information about the potential effects of both of these processes. This thesis addresses one potentially important aspect of climate change in the region: drought. I find that, despite a high degree of natural spatial heterogeneity, different forest sites tend to respond similarly to seasonal drought, spatial variation in soil water content, and artificial rainfall exclusion. The apparent net consequence of these responses is that, over the period of measurement, the amount of CO_2 moving out of the forest and into the atmosphere is diminished. There are, however, two sets of caveats to this conclusion. Firstly, greater spatial and temporal replication is required to assess whether this pattern is consistently observed over multiple years, and across different vegetation and soil types. Secondly, the effects of other factors such as temperature, atmospheric CO_2, land-use, and community species composition, need to be taken into account. These factors are likely to directly, and indirectly through interactions with other factors, affect forest structure and function. To incorporate the complexity of the multiple factors, and their interactions, it is necessary to develop a model of ecosystem C cycling. This thesis is intended to inform such models by providing much needed data about above- and below-ground C allocation and cycling at an Amazon forest site. The priority now must be to extend measurements and model outputs across larger spatial scales, and incorporate the, difficult to quantify but crucial, impacts of government social and economic policies.

Chapter 7

7. Appendix: detailed field protocol

7.1. Rhizotrons

7.1.1. Construction

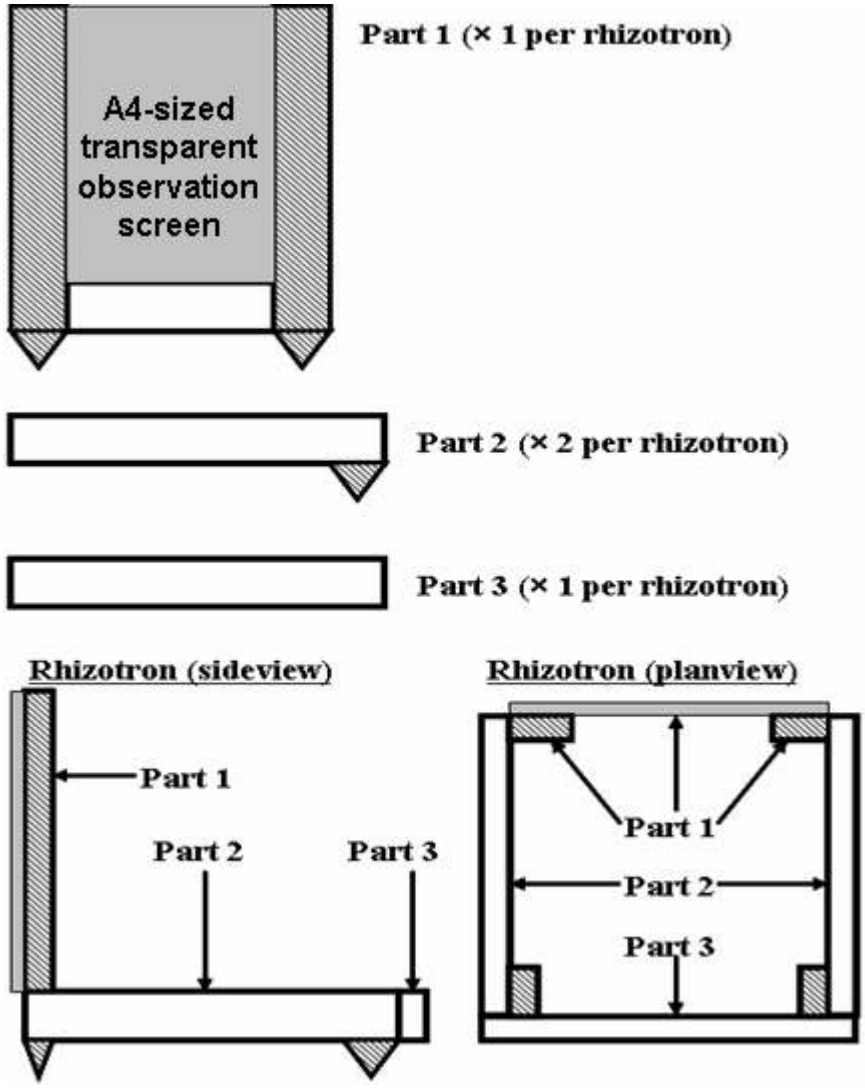

Figure 1. Construction plan for rhizotron. Material and equipment required: wooden planks (width ~ 4cm, thickness ~ 2cm), anti-termite wood varnish, transparent Perspex sheets (length = 27cm, width=36cm, thickness = 3 mm), wood screws (length ~ 4cm), Saw, electric drill with screwdriver attachments.

7.1.2. Installation

A square hole in the soil (width ~ 0.5m, length ~ 0.5m, depth ~ 0.5) was excavated. Some of the excavated soil was saved in a labelled plastic bag, in cases where there were distinct soil horizons present, soil from each horizon was placed in separate plastic bags.

Figure 2. An installed rhizotron. Note insulation foam in place covering the observation screen, a plastic cover (folded over) which usually protects the screen from light and rainfall. The larger plastic rain cover is set behind the rhizotron.

The chamber was then roughly inserted to test that the hole was approximately the right size. One soil face was cut so that it was as flat as possible. Then the rhizotron was inserted, ensuring that the transparent observation screen was as close to the flattened soil face as possible. A hammer was used to secure the base of the rhizotron in the soil at the bottom of the hole, whilst ensuring that the top edge of the observation screen remained level with the soil surface. Using the soil in the plastic bags, the space between the transparent rhizotron observation screen and soil face

was filled. If there was soil from separate bags representing different horizons, the soil was then inserted to replicate the level of horizons present in the undisturbed soil profile. A rod was used to compact the soil to replicate density of undisturbed soil. Foam insulation was placed next to the inside face of the rhizotron, and the plastic cover over the chamber, to protect the transparent observation screen from variation in temperature and light and exposure to rainfall (see figure 2). The plastic rhizotron cover was orientated such that water was not diverted onto the interface between the observation screen and soil. Finally, the perimeter of the rhizotron was encircled with marker tape to discourage disturbance, and organic litter was placed over the fresh soil surfaces at the observation screen-soil interface to replicate natural conditions.

7.1.3. Data collection

Root length was recorded by placing a transparent A4 sheet over the rhizotron observation screen and tracing visible roots using a fine permanent marker pen (see Figure 3). To avoid apparent changes in root growth, changes between personnel were avoided as much as possible. A method was developed to quantify and correct for systematic differences between different data recorders (see section 7.1.5.). Each A4 sheet was marked with an identity code denoting plot and rhizotron number, and bars along the long edge to mark 10 cm and 20 cm from the soil surface (Figure 3). Each root was divided into segments marked by crossbars. The segments corresponded to the incremental increases in root length observed each recording session. Beside each traced root segment was noted the number of the recording session that the segment

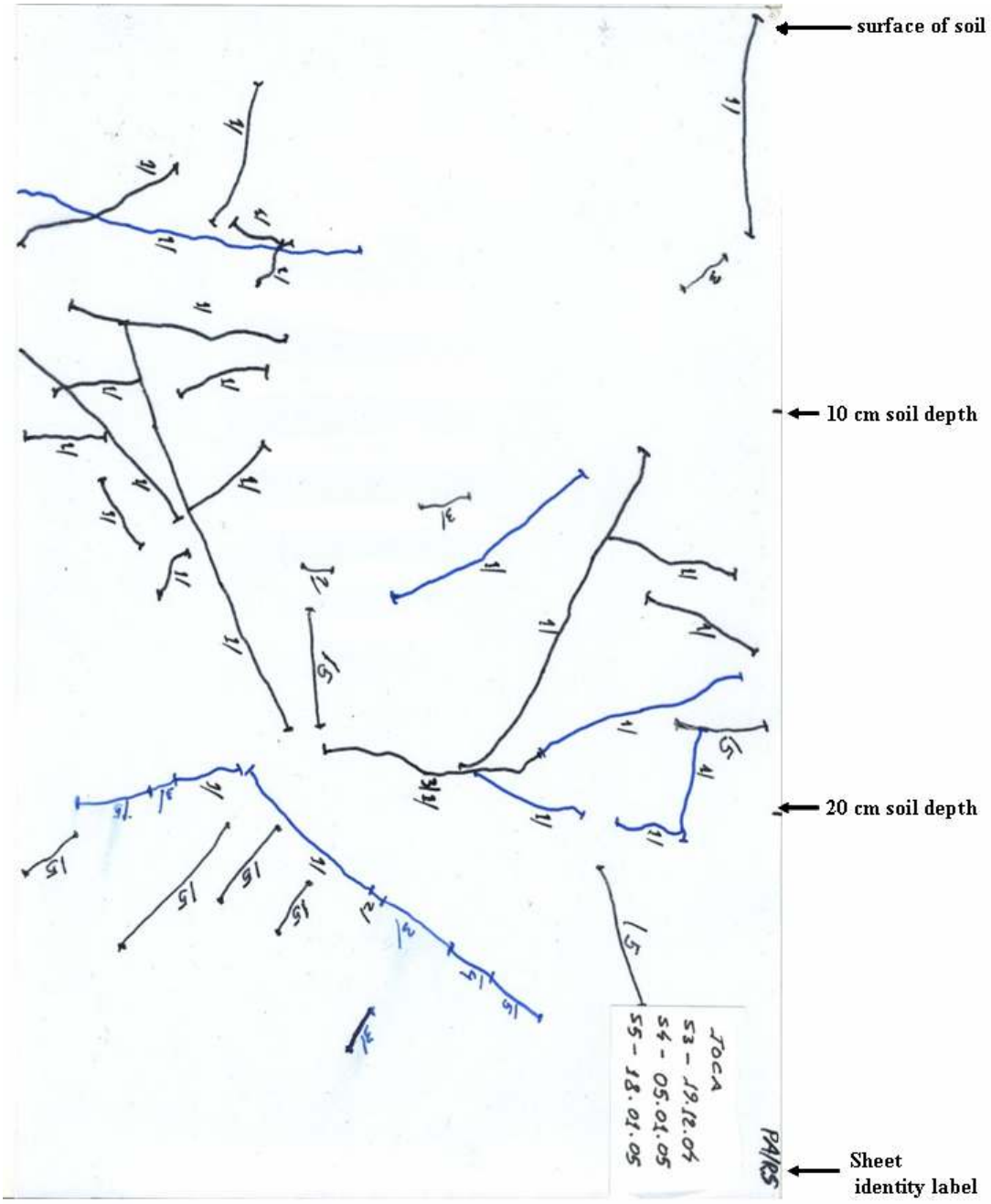

Figure 3. Example of a tracing on a rhizotron transparent sheet. Note different diameter classes, indicated by line colour, and segments indicating root growth over one session, separated by crossbars. No roots have yet disappeared so the all the segments are marked just by the session number when they appeared followed by a slash. Example of completed notation = 1/5 = appeared by session 2 and disappeared by session 5.

appeared, and the number of the session that the segment disappeared (each measurement session number equates to a certain date). Root diameter category was indicated using different colour marker pens (≤ 1 mm = black, 1-2 mm = blue, 2-3 mm = red, ≥ 4 mm = green). The majority of tracing occurred on session 1; after this only appearance of new roots, and growth of existing roots needed to be traced. Soil moisture (CS616 probe, Campbell Scientific, Loughborough, U.K.) and temperature (Testo 926 probe, Testo Ltd., Hampshire, U.K.) was recorded every session at the same point within 0.5 m of the rhizotron, but not near the interface between the observation screen and soil. The soil moisture probe output was converted to volumetric soil moisture (*VMC*) with:

$$VMC = -0.0663 - 0.0063P + 0.0007P^2$$

Where *P* is the probe output (microseconds), recorded with a digital multimeter.

7.1.4. Data processing

The transparent A4 sheet from each rhizotron was scanned (colour scan, j.peg image file, 150 dpi). It was not necessary to scan the sheets every session since the history of growth from all sessions was recorded in the sheets themselves. The scanned images were then analyzed with commercially available software (WinRHIZO Tron, Regent Instruments, Canada). The software allowed length measurement of traced roots, and attachment of relevant root and segment information (session appearance and disappearance, and root diameter). However, to convert these length measurements into units of root biomass per unit ground area (see review in section 2.2) the following methodology was used. The number of roots contacting the rhizotron observation screen each session, together with root diameter, was used to calculate

the total cross-sectional surface area of intersecting roots (*XSr*), using the following equation:

$$\sum XSr = \frac{\pi^2 \sum r^2}{\sqrt{2}}$$

Where *r* is root radius. Roots which have branched after contact with the rhizotron observation screen were not counted. Using *XSr*, root production (g m^{-2}) for each rhizotron measurement session was calculated as:

$$\mathrm{Pr} = 2 \times 10^6 Dr(1 - Fc) XSr \frac{\sin\alpha \cos\gamma}{W}$$

Where *Dr* is root tissue density (g mm^{-3}), *Fc* is the soil coarse fraction, α is the angle of the rhizotron observation screen relative to the ground, γ is the ground angle relative to the horizontal, and W is the width of the rhizotron observation screen. Root density was calculated by dividing ingrowth core sample root mass by volume (see section 7.2.3.). The 10^6 value converted mm^2 ground area into m^2. The additional multiplication factor of 2 was used because roots can only intersect with the rhizotron screen from the front. It was assumed that if the rhizotron did not form a solid barrier an equal amount of roots would intersect from behind as well as from the front.

7.1.5. Data calibration

To test the reliability of the tracing method, it was necessary to record: 1) the error of length estimates from the same data collector, 2) the error of length estimates between different trained collectors. To do this, the principal rhizotron data collector traced root length 5 times each from 4 rhizotrons (a total of 4 × 5 = 20 transparencies). For the same 4 rhizotrons, 4 other assistants made tracings ((4 + 1) × 4 = 20). The

assistants had been properly instructed by the principal root tracer about the method and the level of detail which was required. The 5 measurements per rhizotron from the same collector were used to calculate within-collector average variance and standard deviation. The 5 measurements per rhizotron from the 5 different collectors were used to calculate between-collector average variance and standard deviation.

7.1.6. Key references

For a general review of methodologies for quantifying root dynamics, including rhizotrons, see Vogt *et al*., (1998) and Hendricks *et al*., (2006). The following are field studies using the rhizotron methodology: Itoh, (1985), Sword et al., (1996), West *et al*., (2003), Davis *et al*., (2004). The following articles outline methods for converting rhizotron length measurements into units of biomass per unit ground area: Tingey *et al*., (2000), Bernier & Robitaille, (2004), Hendricks *et al*., (2006). The conversion method described in detail in this Chapter is that of Bernier & Robitaille, (2004).

7.2. Ingrowth cores

7.2.1. Core installation and removal

A cylindrical metal corer was used to remove sample cores of soil (diameter ~ 14 cm, depth ~ 30 cm). Each core was then placed into a labelled plastic bag, and roots were removed from the soil with a coarse sieve (mesh aperture diameter ~ 0.5 cm) and by hand. The roots collected were dried, weighed and used to estimate standing crop root mass (see section 7.3.). Cylindrical mesh bags were inserted into the holes, and the root-free soil was re-inserted back into the holes from which they came. After an interval of approximately 3 months, the mesh bags were extracted, and the soil cores

were placed into labelled plastic bags. Before core extraction organic litter above the core was removed, and placed into labelled plastic bags, and soil moisture (CS616 probe, Campbell Scientific, Loughborough, U.K.) and soil temperature (Testo 926 probe, Testo Ltd., Hampshire, U.K.) was recorded at a soil depth of 30 cm. The soil moisture probe output was converted to volumetric soil moisture (*VMC*) with:

$$VMC = -0.0663 - 0.0063P + 0.0007P^2$$

Where P is the probe output (microseconds), recorded with a digital multimeter. Surface organic litter was defined as identifiable plant material on the ground surface which did not pass through a fine sieve (mesh aperture diameter = 0.1 cm). Each time after soil core installation, some organic litter was replaced onto the core surface, to mimic field conditions. Small sub-samples of soil from each core, for each 3 month measurement session, were stored in labelled plastic bags. Chemical analyses of these samples were used to identify any confounding influence of changes in soil structure and chemistry within each core over time upon root dynamics (see section 7.2.4.).

7.2.2. Extracting roots from soil

Roots were removed by hand for a period of 40 minutes per ingrowth core sample, but the sampling period was split into 10 minute time-steps. Whilst processing each sample, variation in sampling effort was minimized. Subsequently, all root sub-samples collected each time step were placed into placed plastic bags to minimize desiccation. The purpose of sampling by hand instead of using sieves was to avoid excessive alteration of soil texture, which could bias root activity within the ingrowth cores. Splitting the sampling period into time steps allowed estimation of the amount of root material remaining uncollected in the soil sample after 40 minutes (for a detailed explanation see sections 2.3. and 7.2.3.).

7.2.3. Processing root samples

Root sub-samples were cleaned of residual dirt and detritus, and scanned (grey-scale scan, tiff image file, 600 dpi). Before scanning, roots were arranged on the scanner so that they overlapped as little as possible. The interval between removing roots from the soil and scanning was kept as short as possible (< 48 hours). Scanned images of roots were analyzed with commercially available software (WinRHIZO, Regent Instruments, Canada). The software allowed measurement of root length, surface area and volume. After scanning, root samples, together with organic litter samples, were dried at 70 ^{o}C to constant mass and weighed. Two mass measurements were made for organic litter: 1) fine litter (excluding un-decomposed fruit or twigs ≥ 5 mm diameter), and total litter. Root density was calculated (for use in rhizotron length-mass conversion, section 7.1.4.), by dividing root sample dry mass by sample volume. A maximum likelihood approach was used to fit a range of acceptable curves, based upon the observed cumulative increase in roots collected over 40 minutes for each sample together with estimates of measurement error around each data point (see error calculation method in section 7.2.4.), which predict root mass retrieval (± confidence intervals) beyond 40 minutes. The optimal parameters were found by minimizing the following objective function ($O(p)$):

$$O(p) = \sum_{i=1}^{n} \frac{1}{\sigma^2_{Yi}} \left[y_{i,meas}(x_i) - y_{i,\mathrm{mod}}(x_i : p) \right]^2$$

Where n is the total number of measurements, p is the number of model parameters, $y_{\mathrm{i,meas}}(x_{\mathrm{i}})$ is the measured value of output variable y at the value x_{i} of the driving variable x, $y_{\mathrm{i,mod}}(x_{\mathrm{i}} : p)$ is the modelled value of the output variable at the value x_{i} of the driving variable x given the parameters p, and σ^2_{yi} is the measurement error variance for each of the observations. The minimal sum-of-squares follows a chi-squared distribution with n-p degrees of freedom. A Monte-Carlo approach was used

to generate parameter confidence regions, varying the two unknown parameters at 100 points linearly arranged between specified maximum and minimum values ($8 < R_c < 80$ and $0.01 < k_r < 10$; $0.1 < a < 20$ and $0.0 < b < 100$). A chi-squared test was used to determine which of the 10000 combinations for each data-set lay within a 95 % confidence interval of the observations. The degrees of freedom was determined as $n - p$. It was possible to fit a range of different curves to the observed data (e.g.: logarithmic, power, saturation; see section 7.2.4. for a method of assessing the different curves).

7.2.4. Data calibration

It was necessary to test the reliability of root length, surface area and volume values provided by WinRHIZO software. To do this the following methodology was used. Fine electrical wire of three different diameters (e.g.: 0.5 mm, 1 mm, 2 mm) was cut up into different length segments. Segments were arranged and scanned following the same protocol and scanner settings as described in section 7.2.3. Multiple scans were taken (> 20) with a wide range of total lengths and various combinations of segments with different diameters. For each scan, the actual total wire length, and length of wire of each diameter category, was noted. Sample root lengths, surface areas and volumes calculated by WinRHIZO were compared to actual sample root lengths, surface areas and volumes. The difference between these multiple paired values was used to calculate mean and standard deviation of the software measurement error. To identify any confounding influence of changes in soil structure and chemistry within each ingrowth upon root dynamics, soil samples from each core and session were analyzed for C and N content. If changes in C and N content occur (which might be expected as root material is consistently removed from the ingrowth cores) and are causing changes in root dynamics, there should be a significant correlation. If there is no significant correlation between root growth and soil chemistry then it is probable that observed trends reflect real seasonal patterns. To estimate root collection

measurement error (to input into the maximum likelihood analysis, section 7.2.5.) the following technique was used. A soil core was extracted (diameter = 14 cm, depth = 30 cm), roots were removed with a sieve, and the soil was homogenized. Approximately 40 grams of wire segments of different colours, thicknesses and lengths were placed into the soil sample and thoroughly mixed in. Then the wire segments were manually removed from the soil over a period of 40 minutes, split into 10 minute time steps. Segments retrieved from each time step were weighed. At the end of the collection period, retrieved segments were mixed back into the soil, and the process was repeated a further nine times (ten iterations in total). This data was used to estimate mean ± measurement error of the cumulative mass of segments collected at each time step. The following experiment was used to assess which curve type best fits the observed pattern of cumulative root mass collection over time (to input into the maximum likelihood analysis, section 7.2.3.). Eight soil cores were extracted, and roots were manually removed over a period of 120 minutes, split into 10-minute time steps. Roots retrieved at each time step were cleaned of residual soil and detritus, dried at 70 ºC to constant mass and weighed. Cumulative dry root mass retrieved at each time step was plotted for each sample core. The accuracy of various curve types (logarithmic, power, saturation) was evaluated by fitting curves to the first 40 minutes of root collection for each sample, then using them to predict the pattern of retrieval up to 120 minutes. Predicted root mass collected between 50 - 120 minutes was then compared to the actual amount of root material manually collected over the same period

7.2.5. Key references

For a general review of methodologies for quantifying root dynamics, including ingrowth cores, see Vogt *et al*., (1998) and Hendricks *et al*., (2006). The following field studies provide information about potential biases of ingrowth cores: Flower-Ellis & Persson (1980), Friend *et al.* (1990), and Steingrobe *et al*., (2000). Bouma *et*

al., (2000) provide a detailed description of how to use WinRHIZO software to make measurements of root morphology. The following are examples of field studies which used the maximum likelihood approach: van Wijk *et al*., (2002), and Williams *et al*., (2006).

7.3. Standing crop soil cores

7.3.1. Core removal

Prior to core removal, supplementary measurements were made (see section 7.3.2.). Soil cores were then extracted (diameter ~ 14cm, depth ~ 30cm) with a cylindrical metal corer. Subsequently, each core was placed into a labelled plastic bag. The time of extraction for every core, and exact diameter and depth of each hole, was noted. Soil cores were not extracted until the last moment, to minimize the interval of time between core removal and root respiration measurements (see section 7.3.2.).

7.3.2. Supplementary measurements

Soil respiration was recorded directly above the soil cores with an infra-red gas analyzer (IRGA) system (e.g.: EGM-4 and SRC-1 chamber, PP Systems, Hitchin, U.K.). Respiration rate was calculated from the change in CO_2 concentration over time within the IRGA chamber according to:

$$Rs = M \frac{\Delta C}{\Delta T} \frac{Vch}{A},$$

Where M is the volume of one mole of gas (m^3), Vch is the total internal volume of the chamber (m^3), A is the ground area covered by the chamber (m^2) and $\Delta C / \Delta T$

represents the change in CO_2 within the chamber per unit time. Prior to respiration measurement a cylindrical collar was inserted into the soil, to enable a closer seal between the IRGA chamber and the soil. The collars increased the effective volume of the chamber, this was corrected for with:

$$Rsc = Rsuc\frac{A}{Vch}\frac{Vco + Vch}{A},$$

Where *Rsc* and *Rsuc* are corrected and uncorrected soil respiration respectively and *Vco* is the volume of the collar (m^3). Respiration measurement occurred only 5 minutes after collar insertion, to allow the effects of soil disturbance by collar insertion to subside. At each collar, soil respiration was recorded twice with the IRGA: once with surface organic litter and once without. Surface organic litter was defined as identifiable plant material on the ground surface which did not pass through a fine sieve (mesh aperture diameter = 0.1 cm). Organic litter removed from within each respiration collar was placed within a labelled plastic bag. The two IRGA measurements were separated by an interval of two minutes, to allow CO_2 levels near the soil surface to equilibrate with the atmosphere. At all respiration measurement locations, soil moisture (CS616 probe, Campbell Scientific, Loughborough, U.K.) and soil temperature (Testo 926 probe, Testo Ltd., Hampshire, U.K.) was recorded at a soil depth of 30 cm. The soil moisture probe output was converted to volumetric soil moisture (*VMC*) with:

$$VMC = -0.0663 - 0.0063P + 0.0007P^2$$

Where *P* is the probe output in microseconds, recorded with a digital multimeter. The area of soil measured by the IRGA was then extracted as a soil core (diameter = 12 cm, depth = 30 cm) using a cylindrical metal corer, and the roots were extracted following the technique described in section 7.3.1. Fresh roots from each core were

placed into a cuvette which was connected to an IRGA that measured the rate of CO_2 accumulation within the cuvette. The time interval between core extraction and root respiration measurement was noted. This was used to identify any effect of root excision upon respiration (see section 7.3.5.).

7.3.3. Extracting roots from soil

Roots were removed by hand for a period of 40 minutes per sample, but the sampling period was split into 10 minute time-steps. Whilst processing each sample, variation in sampling effort was minimized. Subsequently, all root sub-samples collected each time step were placed into labelled plastic bags. The purpose of sampling by hand instead of using sieves was to avoid excessive alteration of soil texture, which could bias root activity within the ingrowth cores. Splitting the sampling period into time steps allowed estimation of the amount of root material remaining uncollected in the soil sample after 40 minutes (for a detailed explanation see sections 2.3. and 7.3.4.).

7.3.4. Processing root samples

Root and litter samples were cleaned of inorganic detritus, dried at 70 ^{o}C to constant mass and weighed. Two mass measurements were made for root samples: 1) fine roots ($\leq$ 5 mm diameter), and 2) total roots. Two mass measurements were also made for organic litter: 1) fine litter (excluding un-decomposed fruit or twigs $\geq$ 5 mm diameter), and total litter. A maximum likelihood approach was used to fit a range of acceptable curves, based upon the observed cumulative increase in roots collected over 40 minutes for each sample together with estimates of measurement error around each data point (see error calculation method in section 7.3.5.), which predict root mass retrieval (± confidence intervals) beyond 40 minutes. The optimal parameters were found by minimizing the following objective function ($O(p)$):

$$O(p) = \sum_{i=1}^{n} \frac{1}{\sigma^2_{Yi}} \left[y_{i,meas}(x_i) - y_{i,\mathrm{mod}}(x_i : p) \right]^2$$

Where n is the total number of measurements, p is the number of model parameters, $y_{\mathrm{i,meas}}(x_{\mathrm{i}})$ is the measured value of output variable y at the value x_{i} of the driving variable x, $y_{\mathrm{i,mod}}(x_{\mathrm{i}} : p)$ is the modelled value of the output variable at the value x_{i} of the driving variable x given the parameters p, and σ^2_{yi} is the measurement error variance for each of the observations. The minimal sum-of-squares follows a chi-squared distribution with n-p degrees of freedom. A Monte-Carlo approach was used to generate parameter confidence regions, varying the two unknown parameters at 100 points linearly arranged between specified maximum and minimum values ($8 < R_{\mathrm{c}} < 80$ and $0.01 < k_r < 10$; $0.1 < a < 20$ and $0.0 < b < 100$). A chi-squared test was used to determine which of the 10000 combinations for each data-set lay within a 95 % confidence interval of the observations. The degrees of freedom was determined as $n - p$. It was possible to fit a range of different curves to the observed data (e.g.: logarithmic, power, saturation; see section 7.3.5. for a method of assessing the different curves).

Using the supplementary data it was possible to estimate organic litter respiration rate per unit mass (R_l, g g^{-1} hr^{-1}) with:

$$R_l = \frac{(R_s - R_{wl}) / M_{lf}}{1 / A_{xsc}}$$

Where R_s was soil respiration with organic litter (g m^{-2} hr^{-1}), R_{wl} was soil respiration without litter (g m^{-2} hr^{-1}), M_{lf} was fine leaf litter dry mass (g), and A_{xsc} was cross-sectional area of the respiration collar (m^2). Root respiration rate per unit mass (R_r, g g^{-1} hr^{-1}) was calculated with:

$$R_r = \frac{(R_{r0-10} - M_{r0-10})Mr}{1/A_{xsc}}$$

Where R_{r0-10} was respiration of standing crop roots collected during the first time step (g m^{-2} hr^{-1}), M_{r0-10} was the dry mass of standing crop roots collected during the first time step (g), M_r was total dry mass of standing crop roots (g). An alternative, less invasive method of estimating litter and root respiration is to plot total and/or fine litter/root mass against total soil respiration. If the relationship is linear, the y-intercept will represent an estimate of soil respiration at litter/root mass = 0. The change in respiration caused by litter/root mass can be calculated from the slope.

Soil organic matter respiration per unit mass cannot be calculated using the methods above. To present litter, root and soil organic matter respiration together it was necessary to calculate respiration per unit ground surface area (g m^{-2} hr^{-1}) per core with the following equations:

$$R_l = R_s - R_{wl}$$

$$R_r = \frac{R_{r0-10}}{M_{r0-10}} M_r$$

$$R_{som} = R_s - (R_l + R_r)$$

Where R_l, R_r and R_{som} are respiration per unit ground area from organic litter, roots and soil organic matter respectively.

7.3.5. Data calibration

Any influence of root excision upon root respiration was assessed by plotting values of root respiration against the time interval between excision and respiration measurement. If there is no clear change, it is likely that root respiration is not biased

by excision over the time-scale of measurement. To estimate root collection measurement error (to input into the maximum likelihood analysis, section 7.3.4.) the following technique was used. A soil core was extracted (diameter = 14 cm, depth = 30 cm), roots were removed with a sieve, and the soil was homogenized. Approximately 40 grams of wire segments of different colours, thicknesses and lengths were placed into the soil sample and thoroughly mixed in. Then the wire segments were manually removed from the soil over a period of 40 minutes, split into 10 minute time steps. Segments retrieved from each time step were weighed. At the end of the collection period, retrieved segments were mixed back into the soil, and the process was repeated a further nine times (ten iterations in total). This data was used to estimate mean ± measurement error of the cumulative mass of segments collected at each time step. The following experiment was used to assess which curve type best fits the observed pattern of cumulative root mass collection over time (to input into the maximum likelihood analysis, section 7.3.4.). Eight soil cores were extracted, and roots were manually removed over a period of 120 minutes, split into 10-minute time steps. Roots retrieved at each time step were cleaned of residual soil and detritus, dried at 70 ºC to constant mass and weighed. Cumulative dry root mass retrieved at each time step was plotted for each sample core. The accuracy of various curve types (logarithmic, power, saturation) was evaluated by fitting curves to the first 40 minutes of root collection for each sample, then using them to predict the pattern of retrieval up to 120 minutes. Predicted root mass collected between 50 - 120 minutes was then compared to the actual amount of root material manually collected over the same period.

7.3.6. Key references

For a general review of methodologies for partitioning soil respiration see Hanson *et al*., (2000) and Subke *et al.*, (2006). Law *et al*., (2001) use the methodology described here for measuring root respiration rate per unit mass. Davidson *et al*., (2002) provide

a general review of artefacts and biases inherent in chamber-based measurements of soil respiration. The following are examples of field studies which used the maximum likelihood approach: van Wijk *et al*., (2002), and Williams *et al*., (2006).

Chapter 8

8. References

Aber JD, Mellilo JM, Nadelhoffer KJ, McClaugherty CA, Pastor J. 1985. Fine root turnover in forest ecosystems in relation to quantity and form of nitrogen availability: a comparison of two methods. *Oecologia* **66**: 317-321.

Adachi, M, Bekku YS, Konuma A, Kadir WR, Okuda T, Koizumi H. 2005. Required sample size for estimating soil respiration rates in large areas of two tropical forests and of two types of plantation in Malaysia. *Forest Ecology and Management* **210**: 455-459.

Aerts R, Bakker C, de Caluwe H. 1992. Root turnover as a determinant of the cycling of C, N, and P in a dry heathland ecosystem. *Biogeochemistry* **15**: 175-190.

Agren GI, Axelsson B, Flower-Ellis J, Linder S, Persson H, Staaf H, Troeng E. 1980. Annual carbon budget for a young Scots pine. In: Persson, T, ed. *Structure and Function of Northern Coniferous Forests-an ecosystem study*. Stockholm, Sweden: Ecology Bulletin

Alvim PFT. 1960. Moisture stress as a requirement for flowering of coffee. *Science* **32**: 354.

Amthor JS. 1994. Plant respiratory responses to the environment and their effects on the carbon balance. In: Wilkinson RE, ed. *Plant-Environment Interactions*. New York: Marcel Dekker.

Amthor JS. 2000. The McCree-de Wit-Penning de Vries-Thornley respiration paradigms: 30 years later. *Annals of Botany* **86**: 1-20.

Anderson LJ, Comas LH, Lakso AN, Eissenstat DM. 2003. Multiple risk factors in root survivorship: a 4-year study in Concord grape. *New Phytologist* **158**: 489-501.

Andreae MO, Rosenfeld D, Artaxo P, Costa AA, Frank GP, Longo KM, Silva-Dias MAF. 2004. Smoking rain clouds over the Amazon. *Science* **303**: 1337–1342.

Aragão LEOC, Shimabukuro YE, Espírito Santo FDB, Williams M. 2005. Landscape pattern and spatial variability of leaf area index in Eastern Amazonia. *Forest Ecology and Management* **211**: 240-256.

Arunachalam A, Pandey HN, Tripathi RS, Maithani K. 1996. Biomass and production of fine and coarse roots during regrowth of a disturbed subtropical humid forest in north-east India. *Vegetatio* **123**: 73-80.

Asner GP, Keller M, Silva JNM. 2004. Spatial and temporal dynamics of forest canopy gaps following selective logging in the eastern Amazon. *Global Change Biology* **10**: 310-321.

Atkin OK, Edwards EJ, Loveys BR. 2000. Response of root respiration to changes in temperature and its relevance to global warming. *New Phytologist* **147**: 141-54.

Batjes NH. 2005. Organic carbon stocks in the soils of Brazil. *Soil Use and Management* **21**: 22-24.

Bengough AG, Bransby MF, Hans J, McKenna SJ, Roberts TJ, Valentine TA. 2006. Root responses to soil physical conditions; growth dynamics from field to cell. *Journal of Experimental Botany* **57**: 437-447.

Benjamin JG, Nielsen DC. 2004. A method to separate plant roots from soil and analyze root surface area. *Plant and Soil* **267**: 225-234.

Berish CW. 1982. Root biomass and surface area in three successional tropical forests. *Canadian Journal of Forest Research* **12**: 699-704.

Bernier PY, Robitaille G. 2004. A plane intersect method for estimating fine root productivity of trees from minirhizotron images. *Plant and Soil* **265**, 165-173.

Bernier PY, Robitaille G, Rioux D. 2005. Estimating the mass density of fine roots of trees for minirhizotron-based estimates of productivity. *Canadian Journal of Forest Research* **35**: 1708-1713.

Bingham IJ, Bengough AG. 2003. Morphological plasticity of wheat and barley roots in response to spatial variation in soil strength. *Plant and Soil* **250**: 273-282.

Black KE, Harbron CG, Franklin M, Atkinson D, Hooker JE. 1998. Differences in root longevity of some tree species. *Tree Physiology* **18**: 259-264.

Blanke MM. 1996. Soil respiration in an apple orchard. *Environmental and Experimental Botany*. **36**, 339-348.

Boone RD, Nadelhoffer KJ, Canary JD, Kaye JP. 1998. Roots exert a strong influence on the sensitivity of soil respiration. *Nature* **396**: 570-572.

Bormann FH, Berlyn G. 1981. *Age and growth rate of tropical trees: new directions for research*. New Haven, USA: Yale University Press.

Bouma TJ, Nielsen KL, Eissenstat DM, Lynch JP. 1997. Estimating respiration of roots in soil: Interactions with soil CO_2, soil temperature and soil water content. *Plant and Soil* **195**: 221-232.

Bowden RD, Nadelhoffer KJ, Boone RD, Mellillo JM, Garrisson JB. 1993. Contributions of above ground litter, below ground litter, and root respiration to total soil respiration in a temperate mixed hardwood forest. *Canadian Journal of Forestry Research* **23**: 1402-1407.

Bréda NJJ. 2003. Ground-based measurements of leaf area index: a review of methods, instruments and current controversies. *Journal of Experimental Botany* **54** 2403-2417.

Breitsprecher A, Bethel JS. 1990. Stem-growth periodicity of trees in a tropical wet forest of Costa Rica. *Ecology* **71**: 1156-1164.

Burke MK, Raynal DJ. 1994. Fine root growth phenology, production, and turnover in a northern hardwood forest ecosystem. *Plant and Soil* **162**: 135-146.

Burton AJ, Pregitzer KS, Zogg GP, Zak DR. 1998. Drought reduces root respiration in sugar maple forests. *Ecological Applications*, **8**, 771-778.

Cannell MGR, Dewar RC. 1994. Carbon allocation in trees: a review of concepts for modelling. *Advances in Ecological Research* **25**: 59-104.

Carpenter SR. 1996. Microcosm experiments have limited relevance for community and ecosystem ecology. *Ecology* **77**: 677-680.

Carswell FE, Costa AL, Palheta P, Malhi Y, Meir P, Costa J de PR, Leal L do SM, Costa JMN, Grace J. 2002. Seasonality in CO_2 and H_2O flux at an Eastern

Amazonian Rain Forest. *Journal Geophysical Research - Atmospheres* 107, 8076, doi: 10.1029/2000JD000284.

Cavelier J. 1992. Fine root biomass and soil properties in a semi deciduous and a lower montane rain forest in Panama. *Plant and Soil* **142**: 187-201.

Chambers JQ, Dos Santos J, Ribeiro RJ, Higuchi N. 2001. Tree damage, allometric relationships, and above-ground net primary production in central Amazon forest. *Global Change Biology* **152**: 73-84.

Chambers JQ, Schimel JP, Nobre AD. 2004a. Respiration from coarse wood litter in central Amazon forests. *Biogeochemistry* **52**: 115-131.

Chambers JQ, Tribuzy ES, Toledo LC, Crispim BF, Higuchi N, dos Santos J, Araujo AC, Kruijt B, Nobre AD, Trumbore SE. 2004b. Respiration from a tropical forest ecosystem: partitioning of sources and low carbon use efficiency. *Ecological Applications* **14**:72-88.

Chason JW, Baldocchi DD, Huston MA. 1991. A comparison of direct and indirect methods for estimating forest canopy leaf area. *Agricultural and Forest Meteorology* **57**: 107-128.

Cheng W, Coleman DC, Carroll CR, Hoffman CA. 1993. In situ measurement of root respiration and soluble C concentrations in the rhizosphere. *Soil Biology and Biochemistry* **25**: 1189-1196

Chotte JL, Laurent JY, Rossi JP. 1995. A modified hydropneumo-elutriation apparatus for quantitative root separation from large soil core samples. *Communications in Soil Science and Plant Analysis* **26**: 2703-2709.

Condit RS, Aguilar S, Hernandez A, Perez R, Lao S, Angehr GR, Hubbell SP, Foster RB. 2004. Tropical forest dynamics across a rainfall gradient and the impact of an El Niño dry season. *Journal of Tropical Ecology* **20**: 51-72.

Condit R, Hubbell SP, Foster RB. 1995. Mortality rates of 205 Neotropical tree and shrub species and the impact of a severe drought. *Ecological Monographs* **65**: 419-439.

Costa MH, Foley JA. 2000. Combined effects of deforestation and doubled atmospheric CO_2 concentrations on the climate of Amazonia. *Journal of Climate* **13**: 18–34.

Cox PM, Betts RA, Collins M, Harris P, Huntingford C, Jones CD. 2004. Amazon dieback under climate-carbon cycle projections for the 21st century. *Theoretical and Applied Climatology* **78**: 137-156.

Cox PM, Betts RA, Jones CD, Spall SA, Totterdell IJ. 2000. Acceleration of global warming due to carbon-cycle feedbacks in a coupled climate model. *Nature* **408**: 184-187.

Couteaux M, Bottner P, Berg B. 1995. Litter decomposition, climate and litter quality. *Trends in Ecology and Evolution* **10**: 63-66.

Coutinho LM, Lamberti A. 1971. Respiração edáfica e productividade primária numa comunidade Amazônica de mata de terra-firme. *Ciência e Cultura* **23**: 411-419.

Cramer W, Bondeau A, Woodward FI, Prentice IC, Betts RA, Brovkin V, Cox PM, Fisher V, Foley JA, Friend AD, Kucharik C, Lomas MR, Ramankutty N, Sitch S, Smith B, White A, Young-Molling C. 2001. Global response of terrestrial ecosystem structure and function to CO_2 and climate change: results from six dynamic global vegetation models. *Global Change Biology* **7**: 357-373.

Cubasch U, Meehl GA, Boer GJ, Stouffer RJ, Dix M, Noda A, Senior CA, Raper S, Yap KS. 2001. Projections of future climate change. In: Houghton JL, ed. Climate Change 2001: The Scientific Basis. Contribution of Working Group I to the Third Assessment Report of the Intergovernmental Panel on Climate Change, Cambridge, England: Cambridge University Press.

Cuevas E, Brown S, Lugo AE. 1991. Above- and below-ground organic matter storage and production in a tropical pine plantation and a paired broadleaf secondary forest. *Plant and Soil* **135**: 257-268.

Cuevas E, Medina E. 1988. Nutrient dynamics within Amazonian forests. 2. fine root–growth, nutrient availability and leaf litter decomposition. *Oecologia* **76**: 222–35.

Da Costa ML, Kern DC. 1999. Geochemical signatures of tropical soils with archeological black earth in the Amazon, Brazil. *Journal of Geochemical Exploration* **66**: 369-385.

Davidson EA, Belk E, Boone RD. 1998. Soil water content as independent or confounded factors controlling soil respiration in a temperate mixed hardwood forest. *Global Change Biology* **4**: 217-227.

Davidson EA, Ishida FY, Nepstad DC. 2004. Effects of an experimental drought on soil emissions of carbon dioxide, methane, nitrous oxide, and nitric oxide in a moist tropical forest. *Global Change Biology* **10**: 718-730.

Davidson EA, Janssens IA, Luo Y. 2006. On the variability of respiration in terrestrial ecosystems: moving beyond Q_{10}. *Global Change Biology* **12**: 154-164.

Davidson EA, Richardson AD, Savage KE, Hollinger DY. 2006. A distinct seasonal pattern of the ratio of soil respiration to total ecosystem respiration in a spruce-dominated forest. *Global Change Biology* **12**: 230-239.

Davidson EA, Savage K, Verchot LV, Navarro R. 2002. Minimizing artefacts and biases in chamber-based measurements of soil respiration. *Agricultural and Forest Meteorology* **113**: 21-37.

Davidson EA, Verchot LV, Cattanio JH, Ackerman IL, Carvalho JEM. 2000. Effects of soil water content on soil respiration in forests and cattle pastures of eastern Amazonia. *Biogeochemistry* **48**: 53-69.

Davis JP, Haines B, Coleman D, Hendrick R. Fine root dynamics along an elevational gradient in the southern Appalachian Mountains, USA. *Forest Ecology and Management* **187**: 19-34.

Dickman DI, Nguyen PV, Pregitzer KS. 1996. Effects of irrigation and coppicing on above-ground growth, physiology, and fine-root dynamics of two field-grown hybrid poplar clones. *Forest Ecology and Management* **80**: 163-174.

Dorr H, Munnich KO. 1987. Annual variation in soil respiration in selected areas of the temperate zone. *Tellus* **39B**: 114-121

Dufresne J, Friedlingstein P, Berthelot M, Bopp P, Ciais L, Fairhead H, Le Treut H, Monfray P. 2002. On the magnitude of positive feedback between future climate change and the carbon cycle. *Geophysical Research Letters*. **29** (10): 43-1.

Eissenstat DM, Wells CE, Yanai RD, Whitbeck JL. 2000. Building roots in a changing environment: implications for root longevity. *New Phytologist* **147**: 33-42.

Ellsworth DS. 1999. Atmospheric CO_2 enrichment in a maturing pine forest: is CO_2 and water status in canopy affected. *Plant, Cell and Environment* **53**: 167-172.

Fan S-M, Wofsy SC, Bakwin PS, Jacob DJ. 1990. Atmosphere-biosphere exchange of CO_2 and O_3 in the central Amazon forest. *Journal of Geophysical Research* **95**: 16851-16864.

Fang C, Moncrieff JB. 2001. The dependence of soil CO_2 flux on temperature. *Soil Biology and Biochemistry* **33**: 155-165.

Farquhar GD, von Caemmerer S. 1982. Modelling of photosynthetic response to the environment. In: Lange OL, Nobel, PS, Osmond CB, Ziegler, H, eds. *Physiological Plant Ecology II. Encyclopedia of Plant Physiology, New Series*. Berlin, Germany: Springer-Verlag, 549-587.

Farrish KW. 1991. Spatial and temporal fine-root distribution in three Louisiana forest soils. *Soil Science Society of America Journal* **55**: 1752-1757.

Fisher RA. 2005. *Understanding the response of rain forest to drought stress*. PhD Thesis. University of Edinburgh, U.K.

Fisher RA, Williams M, Lobo do Vale R, da Costa AL, Meir P. 2006. Evidence from Amazonian forests is consistent with isohydric control of leaf water potential. *Plant, Cell and Environment* **29**: 151-165.

Fisher RA, Williams M, Lola da Costa A, Da Costa R, Almeida S, Meir PW. 2006. The response of an Eastern Amazonian rain forest to drought stress: results

and modelling analyses from a through-fall exclusion experiment. In preparation.

Fitter AH, Heinemeyer A, Staddon PL. 2000. The impact of elevated CO_2 and global climate change on arbuscular mycorrhizas: a mycocentric approach. *New Phytologist* **147**: 179-187.

Flower-Ellis JGK, Persson H. 1980. Investigations of structural properties and dynamics of Scots pine stands. In: Persson T, ed. *Structure and Function of Northern Coniferous Forests-an ecosystem study*. Stockholm, Sweden: Ecology Bulletin.

Foley JA, Botta, A, Coe MT, Costa MH. 2002. El Nino-Southern Oscillation and the climate, ecosystems and rivers of Amazonia. *Global Biogeochemical Cycles* **16**: 79.1-79.20

Friedlingstein P, Dufresne J-L, Cox P, Rayner P. 2003. How positive is the feedback between climate change and the carbon cycle. *Tellus* **55B** (2): 692-700.

Friend, AL, Eide MR, Hinckley TM. 1990. Nitrogen stress alters root proliferation in Douglas fir seedlings. *Canadian Journal of Forestry Research* **20**: 1524-1529

Giardina CP, Ryan MJ, Binkley D, Fownes JH. 2003. Primary production and carbon allocation in relation to nutrient supply in a tropical experimental forest. *Global Change Biology* **9**: 1438-1450.

Gill RA, Jackson RB. 2000. Global patterns of root turnover for terrestrial ecosystems. *New Phytologist* **147**: 13-31.

Gordon AM, Schlentner RE, van Cleve K. 1987. Seasonal patterns of soil respiration and CO_2 evolution following harvesting in the white spruce forests of interior Alaska. *Canadian Journal of Forestry Research* **17**: 304-310

Gordon WS, Jackson RB. 2000. Nutrient concentrations in fine roots. *Ecology* **81**: 275-280.

Gosz JR, Likens GE, Bormann FH. 1972. Nutrient content of litter fall on the Hubbard Brook experimental forest, New Hampshire. *Ecology* **53**: 769-784.

Grace J, Lloyd J, McIntyre J, Miranda AC, Meir P, Miranda HS, Nobre C, Moncrieff J, Massheder J, Malhi Y, Wright I, Gash J. 1995. Carbon dioxide

uptake by an undisturbed tropical rain forest in southwest Amazonia, 1992 to 1993. *Science* **270**: 778-780.

Grace J, Malhi Y, Lloyd J, McIntyre J, Miranda AC, Meir P, Miranda HS. 1996. The use of eddy covariance to infer the net carbon dioxide uptake of Brazilian rain forest. *Global Change Biology* **2**: 209-217.

Greenland DJ, Kowal JML. 1960. Nutrient content of the moist tropical forest of Ghana. *Plant and Soil* **12**: 154-174.

Grogan P. 1999. Arctic Soil Respiration: Effects of Climate and Vegetation Depend on Season. *Ecosystems* **2**: 451-459.

Gulledge J, Schimel JP. 2000. Controls on soil carbon dioxide and methane fluxes in a variety of Taiga forest stands in interior Alaska. *Ecosystems* **3**: 269-282.

Gower ST. 1987. Relations between mineral nutrient availability and fine root biomass in two Costa Rican tropical wet forests: a hypothesis. *Biotropica* **19**: 171-175.

Hale SE, Edwards C. 2002. Comparison of film and digital hemispherical photography across a wide range of canopy densities. *Agricultural and Forest Meteorology* **112**: 51-56.

Hanson PJ, Edwards NT, Garten CT, Andrews JA. 2000. Separating root and soil microbial contributions to soil respiration: a review of methods and observations. *Biogeochemistry* **48**: 115-146.

Hammond R, McCullagh PS. 1978. *Quantitative techniques in geography*. London, UK: Clarendon Press.

Hayes DC, Seastedt TR. 1987. Root dynamics of tallgrass prairie in wet and dry years. *Canadian Journal of Botany* **65**: 787-791.

Hendrick RL, Pregitzer KS. 1992. The demography of fine roots in a northern hardwood forest. *Ecology* **73**: 1994-1104.

Hendrick R, Pregitzer KS. 1993. The dynamics of fine root length, biomass and nitrogen content in two northern hardwood ecosystems. *Canadian Journal of Forestry Research* **23**: 2507-2520.

Hendrick RL, Pregitzer KS. 1993. Patterns of fine root mortality in two sugar maple forests. *Nature* **361**: 59-61.

Hendrick RL, Pregitzer KS. 1996. Temporal and depth-related patterns of fine root dynamics in northern hardwood forests. *Journal of Ecology* **84**: 167-176.

Hendricks JJ, Hendrick RL, Wilson CA, Mitchell RJ, Pecot SD, Guo D. 2006. Assessing the patterns and controls of fine root dynamics: an empirical test and methodological review. *Journal of Ecology* **94**: 40-57.

Hendricks JJ, Nadelhoffer KJ, Aber JD. 1993. Assessing the role of fine roots in carbon and nutrient cycling. *Trends in Ecology and Evolution* **8**: 174-178.

Högberg P, Nordgren A, Buchmann N, Taylor AFS, Ekblad A, Högberg MN, Nyberg G, Ottosson-Löfvenius M, Read DJ. 2001. Large-scale forest girdling shows that current photosynthesis drives soil respiration. *Nature* **411**, 789-792.

Högberg P, Read DJ. 2006. Towards a more plant physiological perspective on soil ecology. *Trends in Ecology and Evolution* **21**: 548-554.

Hollinger DY, Goltz SM, Davidson EA, Lee JT, Tu K, Valentine HT. 1999. Seasonal patterns and environmental control of carbon dioxide and water vapour exchange in an ecotonal boreal forest. *Global Change Biology* **5**: 891-902.

Houghton RA, Lawrence KT, Hackler JL, Brown S. 2001. The spatial distribution of forest biomass in the Brazilian Amazon: a comparison of estimates. *Global Change Biology* **7**: 731-746.

House JI, Prentice IC, Ramankutty N, Houghton RA, Heimann M. 2003. Reconciling apparent inconsistencies in estimates of terrestrial CO_2 sources and sinks. *Tellus* **55B**: 345-363.

Huck MG, Hoogenboom G, Peterson CM. 1987. Soybean root senescence under drought stress. In: Taylor HM, ed. *Minirhizotron observation tubes: methods and applications for measuring rhizosphere dynamics*. Madison, USA: ASA Special Publication NO. 50.: Agronomy Society of America, 109-121.

Huete AR, Didan K, Shimabukuro YE, Ratana P, Saleska SR, Hutyra LR, Yang W, Nemani RR, Myneni R. 2006. Amazon rainforests green-up with sunlight in

dry season. *Geophysical Research Letters* **33**, L06405, doi: 10.1029/2005GL025583.

Hurlbert SH. 1984. Pseudoreplication and the design of ecological field experiments. *Ecological Monographs* **54**: 187-211.

Hurlbert SH. 2004. On misinterpretations of pseudoreplication and related matters: a reply to Oksanen. *Oikos* **104**: 591-597.

Huttel C. 1975. Root distribution and biomass in three Ivory Coast rain forest plots. In: Golley FB, Medina E, eds. *Tropical Ecological Systems*. New York, USA: Springer Heidelberg, 123-130.

Ingestad T, Agren GI. 1991. The influence of plant nutrition on biomass allocation. *Ecological Applications* **1**: 168-174.

Intergovernmental Panel for Climate Change. 2001. Climate Change 2001: the scientific basis. In: *Contribution of working group I to the third assessment report of the International Panel on Climate Change*. Cambridge University Press, U.K.

Itoh S. 1985. In situ measurement of rooting density by micro-rhizotron. *Soil Science and Plant Nutrition* **31**: 653-656.

Jackson G, Irvine J, Grace J. 1995. Xylem cavitation in Scots pine and Sitka spruce saplings during water stress. *Tree Physiology* **15**: 783-790.

Jackson RB, Canadell J, Ehleringer JR, Mooney HA, Sala OE, Schulze ED. 1996. A global analysis of root distributions for terrestrial biomes. *Oecologia* **108**: 389-411.

Jackson RB, Mooney HA and Schulze ED. 1997. A global budget for fine root biomass, surface area, and nutrient content. *Proceeding of the National Academy of Sciences, USA* **94**: 7362-7366.

Jackson RB, Sala OE, Paruelo JM, Mooney HA. 1998. Ecosystem water fluxes for two grasslands in elevated CO_2: a modelling analysis. *Oecologia* **113**: 537–546.

Janssens IA, Lankreijer H, Matteucci G, Kowalski AS, Buchmann N, Epron D, Pilegaard K, Kutsch W, Longdoz B, Grunwald T, Montagnani L, Dore S, Rebmann S, Moors EJ, Grelle A, Rannik U, Morgenstern K, Oltchev S,

Clement R, Gudmundsson J, Minerbi S, Berbigier P, Ibrom A, Moncrieff J, Aubinet M, Bernhofer C, Jensen NO, Vesala T, Granier A, Schulze E-D, Lindroth A, Dolman AJ, Jarvis PG, Ceulemans R, Valentini R. 2001. Productivity overshadows temperature in determining soil and ecosystem respiration across European forests. *Global Change Biology* **7**: 269-278.

Jones DL, Hodge A, Kuzyakov Y. 2004. Plant and mycorrhizal regulation of rhizodeposition. *New Phytologist* **163**: 459-480.

Jordan CF, Escalante G. 1980. Root productivity in an Amazonian rain forest. *Ecology* **61**: 14-18.

Joslin JD, Wolfe MH, Hanson PJ. 2000. Effects of altered water regimes on forest root systems. *New Phytologist* **147**: 117-129.

Keller M, Palace M, Asner GP, Pereira Jr R, Natalino J, Silva M. 2004. Coarse woody debris in undisturbed and logged forests in the eastern Brazilian Amazon. *Global Change Biology* **10**: 784-795.

King JS, Albaugh TJ, Lee Allen H, Buford M, Strain BR, Dougherty P. 2002. Below-ground carbon input to soil is controlled by nutrient availability and fine root dynamics in loblolly pine. *New Phytologist* **154**: 389-398.

King JS, Albaugh TJ, Allen HL, Kress LW. 1999. Stand-level allometry in *Pinus taeda* as affected by irrigation and fertilization. *Tree Physiology* **19**: 769-778.

Kinnaird MF, O'Brien TG. 1998. Ecological effects of wildfire on lowland rain forest in Sumatra. *Conservation Biology* **12**: 954-956.

Kirschbaum MUF. 2000. Will changes in soil organic carbon act as a positive or negative feedback on global warming? *Biogeochemistry* **48**: 21–51.

Klepper B, Taylor HM, Huck MG, Fiscus EL. 1973. Water relations and growth of cotton in drying soils. *Agronomy Journal* **54**: 307-310.

Klinge H. 1973. Root mass estimation in lowland tropical rain forests of central Amazonia, Brazil. I. Fine root masses of a pale yellow latosol and a giant humus podzol. *Tropical Ecology*. **14**: 29-38.

Klinge H, Herrera R. 1978. Root biomass studies in Amazon caatinga forest in southern Venezuela. I. Standing crop of composite root mass in selected stands. *Tropical Ecology*. **19**: 93-110.

Kummerow J, Castillanos J, Maas M, Larigauderie A. 1990. Production of fine roots and the seasonality of their growth in a Mexican deciduous dry forest. *Vegetatio* **90**: 73-80.

Kutsch WL, Staack A, Wotzel J, Middelhoff U, Kappen L. 2001. Field measurements of root respiration and total soil respiration in an alder forest. *New Phytologist*. **150**: 157-168

Lambers H. 1982. Cyanide-resistant respiration: a non-phosphorylating electron transport pathway acting as an energy overflow. *Physiologia Plantarum* **55**: 478-485.

Lambers H. 1997. Respiration and the alternative oxidase. In: Foyer CH, Quick P, eds. *A molecular approach to primary metabolism in plants*. London, UK: Taylor and Francis.

Laurance WF, Williamson GB. 2001. Positive feedbacks among forest fragmentation, drought, and climate change in the Amazon. *Conservation Biology* **15**: 1529-1535.

Laurance WF, Williamson GB, Delamonica P, Oliveira A, Lovejoy TE, Gascon C, Pohl L. 2001. Effects of a strong drought on Amazonian forest fragments and edges. *Journal of Tropical Ecology* **17**: 771-785.

Lavigne MB, Ryan MG, Anderson DE. 1997. Comparing nocturnal eddy covariance measurements to estimates of ecosystem respiration made by scaling chamber measurements at six coniferous boreal sites. *Journal of Geophysical Research* **102**: 28977-28986.

Law BE, Ryan MG, Anthoni PM. 1999. Seasonal and annual respiration of a ponderosa pine ecosystem. *Global Change Biology* **5**: 169-182.

Legendre P. 1993. Spatial autocorrelation: trouble or new paradigm? *Ecology* **74**: 1659-1673.

Lehman J, Zech W. 1998. Fine root turnover of irrigated hedgerow intercropping in northern Kenya. *Plant and Soil* **198**: 19-31.

Lehmann J, Kern DC, Glaser B, Woods WI. 2003. *Amazonian Dark Earths: Origin, Properties, Management.* Dordrecht, Netherlands: Kluwer Academic Publishers.

Lenton TM, Huntingford C. 2003. Global terrestrial carbon storage and uncertainties in its temperature sensitivity examined with a simple model. *Global Change Biology* **9**: 1333–1352.

Lewis SL, Malhi Y, Phillips OL. 2004. Fingerprinting the impacts of global change on tropical forests. *Philosophical Transactions of the Royal Society B: Biological Sciences* **359**: 437-462.

Liljeroth E, Kuikman P, Veen JA. 1994. Carbon translocation to the rhizosphere of maize and wheat and influence on the turnover of native soil organic matter at different soil nitrogen levels. *Plant and Soil* **161**: 233-240.

Lin G, Ehleringer JR, Rygiewicz PT, Johnson MG, Tingey DT. 1999. Elevated CO_2 and temperature impacts on different components of soil CO_2 efflux in Douglas fir terracosms. *Global Change Biology* **5**: 157-168

Lindroth A, Grelle A, Morén A. 1998. Long-term measurements of boreal forest carbon balance reveal large temperature sensitivity. *Global Change Biology* **4**: 443-450.

Livingston GP, Hutchinson GL. 1995. Enclosure-based measurement of trace gas exchange: applications and sources of error. In: Matson PA, Harriss RC, eds. *Biogenic Trace Gases: Measuring Emissions from Soil and Water.* Oxford, UK: Blackwell Scientific Publications.

Lloyd, J. 1999. The CO_2 dependence of photosynthesis, plant growth responses to elevated CO_2 concentrations and their interactions with soil nutrient status II. Temperate and boreal forest productivity and the combined effects of increasing CO_2 concentrations and increased nitrogen deposition at a global scale. *Functional Ecology* **13**: 439-459.

Lloyd J, Farquhar GD. 2000. Do slow-growing species and nutrient-stressed plants consistently respond less to elevated CO2? A clarification of some issues raised by Poorter (1998). *Global Change Biology* **6**: 871-876.

Lloyd J, Wong SC, Styles JM, Batten D, Priddle R, Turnbull C, McConchie CA. 1995. Measuring and modelling whole-tree gas exchange. *Australian Journal of Plant Physiology* **22**: 987-1000.

Loescher HW, Oberhauer SF, Gholz HL, Clark DB. 2003. Environmental controls on net ecosystem-level carbon exchange and productivity in a central American tropical wet forest. *Global Change Biology* **9**: 396-412.

Lopez R, Galinato GI. 2005. Deforestation and forest-induced carbon dioxide emissions in tropical countries: how do governance and trade openness affect the forest-income relationship? *The Journal of Environment & Development* **14**: 73-100.

Lussenhop J, Fogel R, Pregitzer K. 1991. A new dawn for soil biology: video analysis of root-soil-microbial faunal interactions. *Agriculture, Ecosystems and Environment* **34**: 235-249

Lugo AE. 1992. Comparison of tropical tree plantations with secondary forests of similar age. *Ecological Monographs* **62**: 1-41.

MacDicken D. 1997. *A guide to monitoring carbon storage in forestry and agroforestry projects*. Arlington, USA: Winrock International.

Malhi Y. 2005. The carbon balance of the tropical forest biome. In: Griffiths H, Jarvis PG, eds. *The carbon balance of forest biomes*. Oxford, UK: Taylor & Francis.

Malhi Y, Baker TR, Phillips OL, Almeida S, Alvarez E, Arroyo L, Chave J, Czimczik CI, Fiore A Di, Higuchi N, Killeen TJ, Laurance SG, Laurance WF, Lewis SL, Montoya LMM, Monteagudo A, Neill DA, Vargas PN, Patiño S, Pitman NCA, Quesada CA, Salomão R, Silva JNM, Lezama AT, Martínez RV, Terborgh J, Vinceti B, Lloyd J. 2004. The above-ground coarse wood

productivity of 104 Neotropical forest plots. *Global Change Biology* **10**: 563-591.

Malhi Y, Baldocchi DD, Jarvis PG. 1999. The carbon balance of tropical, temperate and boreal forests. *Plant, Cell and Environment* **22**: 715-740.

Malhi Y, Grace J. 2000. Tropical forests and atmospheric carbon dioxide. *Trends in Ecology and Evolution* **15**: 332-337.

Malhi Y, Iwata H, Lola da Costa AC, da Costa R, Meir P, Costa JMN, Athaydes J, Almeida S, Andrade V, Carswell F, Grace J. In preparation. Energy, water and carbon dioxide cycling in an eastern Amazonian rain forest.

Malhi Y, Nobre AC, Grace J, Kruijt B, Pereira MGP, Culf A, Scott S. 1998. Carbon dioxide transfer over a central Amazonian rain forest. *Journal of Geophysical Research* **103**, D24: 31,593-31,612.

Malhi Y' Phillips OL, Lloyd J, Baker T, Wright J, Almeida S, Arroyo L, Frederiksen T, Grace J, Higuchi N, Killeen T, Laurance WF, Leaño C, Lewis S, Meir P, Monteagudo A, Neill D, Núñez Vargas P, Panfil SN, Patiño S, Pitman N, Quesada CA, Rudas-Li A, Salomão R, Saleska S, Silva N, Silveira M, Sombroek WG, Valencia R, Vásquez Martínez R, Vieira ICG, Vinceti B. 2002. An international network to monitor the structure, composition, and dynamics of Amazonian forests (RAINFOR). *Journal of Vegetation Science* **13**: 439-450.

Malhi Y, Wright J. 2004. Spatial patterns and recent trends in the climate of tropical rain forest regions. *Philosophical transactions of the Royal Society B: Biological Sciences* **359**: 311-329.

Mann CC. 2002. The real dirt on rain forest fertility. *Science* **267**: 920.

Martins FR, Matthes LAF. 1978. Respiração edáfica e nutrientes na Amazônia (Região de Manaus): floresta arenícola, campinarana e campina. *Acta Amazonica* **8**: 233-244.

Majdi H, Ohrvik J. 2004. Interactive effects of soil warming and fertilization on root production, mortality, and longevity in a Norway spruce stand in northern Sweden. *Global Change Biology* **10**: 182-188.

Marland G, Boden T. 1993. The magnitude and distribution of fossil fuel related carbon releases. In: Heimann, M, ed. *The Global Carbon Cycle*. New York, USA: Springer Verlag.

Marschner H, Kirkby EA, Cakmak I. 1996. Effect of mineral nutritional status on root-shoot partitioning of photoassimilates and cycling of mineral nutrients. *Journal of Experimental Botany* **47**: 1255-1263.

Medhurst J, Parsby J, Linder S, Wallin G, Ceschia E, Slaney M. 2006. A whole-tree chamber system for examining tree-level physiological responses of field-grown trees to environmental variation and climate change. *Plant, Cell & Environment* **29**: 1853-1869.

Medina E, Klinge H, Jordan CF, Herrera R. 1980. Soil respiration in Amazonian rain forests in the Rio Negro basin. *Flora* **170**: 240-250.

Megonigal JP, Schlesinger WH. 1997. Enhanced CH_4 emissions from a wetland soil exposed to elevated CO_2. *Biogeochemistry* **37**: 77–88.

Meir P. 1996. *The exchange of carbon dioxide in tropical forest.* PhD thesis, University of Edinburgh, UK.

Meir P, Grace J. 2002. Scaling relationships for woody tissue respiration in two tropical rain forests. *Plant, Cell & Environment* **25**: 963-973.

Meir P, Grace J. 2005. The response to drought by tropical rain forest ecosystems. In: Malhi Y, Phillips O, eds. *Tropical forests and global atmospheric change*. Oxford, U.K: Oxford University Press, 75-84.

Meir P, Grace J, Miranda AC. 2001. Leaf respiration in two tropical rain forests: constraints on physiology by phosphorus, nitrogen and temperature. *Functional Ecology* **15**: 378-387.

Meir P, Grace J, Miranda A, Lloyd J. 1996. Soil respiration in a rain forest in Amazonia and in Cerrado in central Brazil. In: Gash JHC, Nobre CA, Roberts JM,

Victoria RL, eds. *Amazonian Deforestation and Climate*, West Sussex, UK: John Wiley & Sons Ltd, 319-329.

Meir P, Fisher RA, Costa ACL, Sotta ED, Vale R, Costa R, Tomasella J, Almeida S, Carvalho C, Maroco J, Chaves M, Veldkamp E, Malhi Y, Williams M, Grace J. 2006. Drought causes little or no carbon loss from an Amazon rain forest at the 1-2 year timescale. In preparation.

Melillo JM, Steudler PA, Aber JD, Newkirk K, Lux H, Bowles FP, Catricala C, Magill A, Ahrens T, Morrisseau S. 2002. Soil warming and carbon cycle feedbacks to the climate system. *Science* **298** 2173-2176

Mensah KOA, Jeník J. 1968. Root systems of tropical trees. 2. Features of the root system of Iroko. *Preslia* **40**: 21-27 .

Mooney HA, Winner WE, Pell EJ. 1991. *Response of plants to multiple stresses*. San Diego, USA: Academic Press, Inc.

Moraes JL, Volkoff B, Cerri CC, Bernoux M. 1996. Soil properties under Amazon forest and changes due to pasture installation in Rondonia, Brazil. *Geoderma* **70**: 63-81.

Moreira-Turcq P, Seyler P, Guyot JL, Etcheber H. 2003. Exportation of organic carbon from the Amazon river and its main tributaries. *Hydrological Processes* **17**: 1329-1344.

Nadelhoffer KJ, Raich JW. 1992. Fine root production estimates and belowground carbon allocation in forest ecosystems. *Ecology* **73**: 1139-1147.

Neill C, Piccolo MC, Cerri CC, Steudler PA, Melillo JM, Brito M. 1997. Net nitrogen mineralization and net nitrification rates in soils following deforestation for pasture across the southwestern Brazilian Amazon Basin landscape. *Oecologia* **110**: 243-252.

Neilson RP, Drapek RJ. 1998. Potentially complex biosphere responses to transient global warming. *Global Change Biology* **4**: 505–521.

Nepstad D, Carvalho G, Barros AC, Alencar A, Paulo Capobianco J, Bishop J, Lefebvre P, Lopes Silva U, Prins E.. 2001. Road paving, fire regime feedbacks, and the future of Amazon forests. *Forest Ecology and Management* **154**: 395-407.

Nepstad D, Lefebvre P, Lopes da Silva U, Tomasella J, Schlesinger P, Solorzano L, Moutinho P, Ray D, Guerreira Benito J. 2004. Amazon drought and its implications for forest flammability and tree growth: a basin-wide analysis. *Global Change Biology* **10**: 704-717.

Nepstad D, McGrath D, Alencar A, Barros AC, Carvalho G, Santilli M, Vera Cruz M del C. 2002. Frontier governance in Amazonia. *Science* **25**: 629-631.

Nepstad DC, de Carvalho CR, Davidson EA, Jipp PH, Lefebvre PA, Negreiros GH, da Silva ED, Stone TA, Trumbore SE. 1994. The role of deep roots in the hydrological and carbon cycles of Amazonian forests and pastures. *Nature* **372**: 666-669.

Nepstad DC, Moutinho P, Dias MB, Davidson E, Cardinot G, Markewitz D, Figueiredo R, Vianna N, Chambers J, Ray D, Guerreiros JB, Lefebvre P, Sternberg L, Moreira M, Barros L, Ishida FY, Tohlver I, Belk E, Kalif K, Schwalbe K. 2002. The effects of partial through fall exclusion on canopy processes, aboveground production and biogeochemistry of an Amazon forest. *Journal of Geophysical Research-Atmospheres* **107**: 1–18.

Nguyen C. 2003. Rhizodeposition of organic C by plants: mechanisms and controls. *Agronomy* **23**: 375-396.

Niinemets U, Kull O, Tenhunen JD. 1999. Variability in leaf morphology and chemical composition as a function of canopy light environment in coexisting deciduous trees. *International Journal of Plant Science* **160**: 837-848.

Nobre CA, Sellers PJ, Shukla J. 1991. Amazonian deforestation and regional climate change. *Journal of Climatology* **4**: 957-988

Norby RJ, Cotrufo MF, Ineson P, O'Neill EG, Canadell JG. 2001. Elevated CO_2, litter chemistry, and decomposition: a synthesis. *Oecologia* **127**: 153-165.

Norby RJ, Jackson RB. 2000. Root dynamics and global change: seeking an ecosystem perspective. *New Phytologist* **147**: 3-12.

Nordgren A, Ottosson Lofvenius M, Hogberg MN. 2003. Tree root and soil heterotrophic respiration as revealed by girdling of boreal Scots pine forest: extending observations beyond the first year. *Plant, Cell and Environment* **26**: 1287-1296.

Ometto JPHB, Nobre AD, Rocha HR, Artaxo P, Martinelli LA. 2005. Amazonia and the modern carbon cycle: lessons learned. *Oecologia* **143**: 483-500.

Orchard VA, Cook FJ. 1983. Relationship between soil respiration and soil moisture. *Soil Biology and Biochemistry* **15**: 447-453.

Osmond B, Ananyev G, Berry J, Langdon C, Kolber Z, Lin G, Monson R, Nichol C, Rascher U, Schurr U, Smith S, Yakir D. 2004. Changing the way we think about global change research: scaling up in experimental ecosystem science. *Global Change Biology* **10**: 393-407.

Pendall E, Bridgham S, Hanson PJ, Hungate B, Kicklighter DW, Johnson DW, Law BE, Luo Y, Megonigal JP, Olsrud M, Ryan MG, Wan S. 2004. Below-ground process responses to elevated CO_2 and temperature: a discussion of observations, measurement methods, and models. *New Phytologist* **162**: 311-322.

Phillips OL, Malhi Y, Higuchi N, Laurence WF, Nunez V, Vasquez MR, Laurance SG, Ferreira LV, Stern M, Brown S, Grace J. 1998. Changes in the carbon balance of tropical forests: evidence from long-term plots. *Science* **282**: 439-442.

Phillips OL, Vásquez R, Arroyo L, Baker TR, Killeen T, Lewis S, Malhi Y, Monteagudo A, Neill D, Núñez Vargas P, Alexiades M, Cerón C, Di Fiore A, Erwin T, Jardim A, Palacios W, Saldias M, Vinceti B. 2002. Increasing dominance of large lianas in Amazonian forests. *Nature* **418**: 770-774.

Prathapar SA, Meyer WS, Cook FJ. 1989. Effect of cultivation on the relationship between root length density and unsaturated hydraulic conductivity in a moderately swelling clay soil. *Australian Journal of Soil Research* **27**: 645-650.

Pregitzer KS, King JS, Burton AJ, Brown SS. 2000. Responses of tree fine roots to temperature. *New Phytologist* **147**: 105-115.

Prentice IC, Lloyd J. 1998. C-quest in the Amazon basin. *Nature* **396**: 619-620.

Priess J, Then C, Folster H. 1999. Litter and fine root production in three types of tropical premontane rain forest in SE Venezuela. *Plant Ecology* **143**: 171-187.

Rayment MB. 2000. Closed chamber systems underestimate soil CO_2 efflux. *European Journal of Soil Science* **51**: 107-110

Raich JW, Nadelhoffer. 1989. Belowground carbon allocation in forest ecosystems: global trends. *Ecology* **70**: 1346-1354.

Raich JW, Potter CS. 1995. Global patterns of carbon dioxide emissions from soils. *Global Biogeochemical Cycles* **9**: 23-26.

Raich JW, Potter CS, Bhagawati D. 2002. Interannual variability in global soil respiration, 1980 –94. *Global Change Biology* **8**: 800–812.

Raich JW, Schlesinger WH. 1992. The global carbon dioxide flux in soil respiration and its relationship to vegetation and climate. *Tellus* **44**: 81-89.

Reich PB, Borchert R. 1982. Phenology and ecophysiology of the tropical tree, *Tabebuia neachrysantha* (Bignoniaciae). *Ecology* **63**: 294-299.

Richey JE, Melack JM, Aufdenkampe AK, Ballester VM, Hess LL. 2002. Outgassing from Amazonian rivers and wetlands as a large tropical source of atmospheric CO2. *Nature* **416**: 617-620.

Robinson D. 1986. Compensatory changes in the partitioning of dry matter in relation to nitrogen uptake and optimal variations in growth. *Annals of Botany* **58**: 841-848.

Roderstein M, Hertel D, Leuschner C. 2005. Above- and below-ground litter production in three tropical montane forests in southern Ecuador. *Journal of Tropical Ecology* **21**: 483-492.

Rosenfeld D. 1999. TRMM observed first direct evidence of smoke from forest fires inhibiting rainfall. *Geophysical Research Letters* **26**: 3105-3108.

Ruivo MLP, Cunha ES, 2003. Mineral and organic components in archaeological black earth and yellow latosol in Caxiuanã, Amazon, Brazil. In: Tiezzi E, Brebbia CA, Uso JL, eds. *Ecosystems and Sustainable Development*. London, UK: WIT Press, 319-329.

Ruivo MLP, Quanz B, Pereira Baia S, Busseti EPC, Nagaishi TY. 2002. *The soils of the LBA experimental sites (Caxiuanã, Pará State, Brazil).* 17th WCSS, 14-21 August 2002, Thailand.

Rustad LE, Huntington TG, Boone RD. 2000. Controls on soil respiration: implications for climate change. *Biogeochemistry* **48**: 1-6

Rustad LE, Fernandez IJ. 1998. Experimental soil warming effects on CO_2 and CH_4 flux in a low elevation spruce-fir forest soil in Maine, USA. *Global Change Biology* **4**: 597-605.

Ryan MG, Hubbard RM, Pongracic S, Raison RJ, McMurtrie RE. 1996. Foliage, fine root, woody tissue, and stand respiration in *Pinus radiata* in relation to nitrogen status. *Tree Physiology* **16**: 333-343.

Ryan MG, Hunt ER, McMurtrie RE. 1996. Comparing models of ecosystem function for temperate conifer forest. I. Model description and validation. In: Breymeyer AI, Hall DO, Melillo JM, Agren GI, eds. *Global Change: effects on coniferous forests and grasslands.* Chichester, UK: Wiley

Sakai RK, Fitzjarrald DR, Moraes OLL, Staebler RM, Acevedo OC, Czikowsky MJ, da Silva R, Brait E, Miranda V. 2004. Land-use change effects on local energy, water and carbon balances in an Amazonian agricultural field. *Global Change Biology* **10**: 895-907.

Saleska SR, Miller SD, Matross DM, Goulden ML, Wofsy SC, da Rocha HR, de Camargo PB, Crill P, Daube BC, de Freitas HC, Hutyra L, Keller M, Kirchhoff V, Menton M, Munger JW, Pyle EH, Rice AH, Silva H. 2003. Carbon in Amazon forests: unexpected seasonal fluxes and disturbance-induced losses. *Science* **302**: 1554-1557.

Savage KE, Davidson EA. 2001. Interannual variation of soil respiration in two New England forests. *Global Biogeochemical Cycles* **0**: 1-14.

Schenk HJ, Jackson RB. 2002. The global biogeography of roots. *Ecological Monographs* **72**: 311-328.

Schlesinger WH. 1977. Carbon balance in terrestrial detritus. *Annual Review of Ecology and Systematics* **8**: 51-81.

Schoengart J, Junk WJ, Piedade MTF, Ayres JM, Huttermann A, Worbes M. 2004. Teleconnection between tree growth in the Amazonian floodplains and the Nino-Southern Oscillation effect. *Global Change Biology* **10**: 683-692.

Schwendenmann L, Veldkamp E, Brenes T, O'Brien T, Mackensen J. 2003. Spatial and temporal variation in soil CO_2 efflux in an old-growth neotropical rain forest, La Selva, Costa Rica. *Biogeochemistry* **64**: 111-128.

Schroth G, Zech W. 1995. Above- and below-ground biomass dynamics in a sole cropping and an alley cropping system with *Gliricidia sepium* in the semi-deciduous rain forest zone of west Africa. *Agroforestry Systems* **31**: 181-198.

Schwarz PA, Law BE, Williams M, Irvine J, Kurpius M, Moore D. 2004. Climatic versus biotic constraints on carbon and water fluxes in seasonally drought-affected ponderosa pine ecosystems. *Global Biogeochemical Cycles*. **18**, GB4006, doi: 10.1029/2004GB002227.

Shukla J, Nobre C, Sellers P. 1990. Amazon deforestation and climate change. *Science* **247**: 1322–1325.

Silva-Dias MAF, Rutledge S, Kabat P, Dias PLS, Nobre C, Fisch G, Dolman AJ, Zipser E, Garstang M, Manzi AO, Fuentes JD, Rocha HR, Marengo J, Plana-Fattori A, Sa LDA, Alvala RCS, Andreae MO, Artaxo P, Gielow R, Gatti L. 2002. Cloud and rain processes in a biosphere-atmosphere interaction context in the Amazon region. *Journal of Geophysical Research- Atmospheres* **107**: 8072–8084.

Silver WL, Neff J, McGroddy M, Veldkamp E, Keller M, Cosme R. 2000. Effects of soil texture on belowground carbon and nutrient storage in a lowland Amazonian forest ecosystem. *Ecosystems* **3**:193–209.

Silver WL, Thompson AW, Mcgroddy ME, Varner RK, Dias JD, Silva H, Crill PM, Keller M. 2005. Fine root dynamics and trace gas fluxes in two lowland tropical forest soils. *Global Change Biology* **11**: 290-306.

Silver WL, Vogt KA. 1993. Fine root dynamics following single and multiple disturbances in a subtropical wet forest ecosystem. *Journal of Ecology* **81**: 729-738.

Singh KP, Singh RP. 1981. Seasonal variation in biomass and energy of small roots in tropical dry deciduous forest, Varanasi, India. *Oikos* **37**: 88-92.

Soares-Filho B, Alencar A, Nepstad DC, Cerqueira G, Vera Diaz MdC, rivero S, Solorzano L, Voll E. 2004. Simulating the response of land-cover changes to road paving and governance along a major Amazon highway: the Santarem-Cuiaba corridor. *Global Change Biology* **10**: 745-764.

Sotta ED. 2006. *Soil carbon dioxide dynamics and nitrogen cycling in an eastern Amazonian rainforest, Caxiuana, Brazil*. PhD Thesis, Georg-August-University of Göttingen, Germany.

Sotta ED, Meir P, Malhi Y, Nobre AD, Hodnett M, Grace J. 2004. Soil CO_2 efflux in a tropical forest in the central Amazon. *Global Change Biology* **10**: 601-617.

Sotta E, Veldkamp E, Guimarães BR, Paixão RK, Ruivo MLP, Almeida SS. 2006. Landscape and climatic controls on spatial and temporal variation in soil CO2 efflux in an eastern Amazonian rain forest, Caxiuanã, Brazil. *Forest Ecology and Management* In press.

Spark JP, Black RA. 1999. Regulation of water loss in populations of *Populus trichocarpa*: the role of stomatal control in preventing xylem cavitation. *Tree Physiology* **19**: 453-459.

Sperry JS, Hacke UG, Oren R, Comstock JP. 2002. Water deficits and hydraulic limits to leaf water supply. *Plant, Cell and Environment* **25**: 251-263.

Steingrobe B, Schmid H, Claassen N. 2000. The use of the ingrowth core method for measuring root production of arable crops- influence of soil conditions inside the ingrowth core on root growth. *Journal of Plant Nutrition and Soil Science* **163**: 617-622.

Steingrobe B, Schmid H, Claassen N. 2001. The use of the ingrowth core method for measuring root production of arable crops – influence of soil and root disturbance during installation of the bags on root ingrowth into the cores. *European Journal of Agronomy* **15**: 143-151.

Strömgren M, Linder S. 2002. Effects of nutrition and soil warming on stemwood production in a boreal Norway spruce stand. *Global Change Biology* **8**: 1195–1204.

Subke JA, Inglima I, Cotrufo MF. 2006. Trends and methodological impacts in soil CO_2 efflux partitioning: A metaanalytical review. *Global Change Biology* **12**: 1-23.

Sullivan TJ. 1997. Ecosystem manipulation experimentation as a means of testing a biogeochemical model. *Environmental Management* **21**: 15-21.

Sulzman EW, Brant JB, Bowden RD, Lajtha K. 2005. Contribution of aboveground litter, belowground litter, and rhizosphere respiration to total soil CO_2 efflux in an old growth coniferous forest. *Biogeochemistry* **73**: 231-256.

Sword MA, Gravatt DA, Faulkner PL, Chambers JL. 1996. Seasonal branch and fine root growth of juvenile Loblolly pine five growing seasons after fertilization. *Tree Physiology* **16**, 899-904.

Taylor HM. 1987. *Minirhizotron Observation Tubes: methods and applications for measuring rhizosphere dynamics*. Madison, USA: ASA Special Publication NO. 50.: Agronomy Society of America.

Taylor HM, Huck MG, Klepper B, Lund ZF. 1970. Measurement of soil-grown roots in a rhizotron. *Agronomy Journal* **62**: 807-809.

Tewary CK, Pandey U, Singh JS. 1982. Soil and litter respiration rates in different microhabitats of a mixed oak-conifer forest and their control by edaphic conditions and substrate quality. *Plant and Soil* **65**: 233-238

Thornley JHM. 1972. A balanced quantitative model for root:shoot ratios in vegetative plants. *Annals of Botany* **36**: 431-441.

Tian H, Melillo JM, Kicklighter DW, McGuire DA, Helfrich JVK, Moore III B, Vorosmarty CJ. 1998. Effect of interannual variability on carbon storage in Amazonian ecosystems. *Nature* **396**: 664-667.

Tian HQ, Melillo JM, Kicklighter DW, McGuire AD, Helfrich J, Moore III B, Vörösmarty CJ. 2000. Climatic and biotic controls on annual carbon storage in Amazonian ecosystems. *Global Ecology and Biogeography* **9**: 315-336.

Timmerman A, Latif M, Bacher A, Oberhuber J, Roeckner E. 1999. Increased El Niño frequency in a climate model forced by future greenhouse warming. *Nature* **398**: 694-696.

Tingey DT, Phillips DL, Johnson MG. 2000. Elevated CO_2 and conifer roots: effects on growth, life span and turnover. *New Phytologist* **147**: 87-103.

Torreano SJ, Morris LA. 1998. Loblolly pine root growth and distribution under water stress. *Soil Science Society of America Journal* **62**: 818-827.

Trenberth KE, Hoar TJ. 1997. El Niño and climate change. *Geophysical Research Letters* **24**: 3057–3060.

Trumbore S, Da Costa ES, Nepstad DC, De Camargo PB, Martinelli LA, Ray D, Restom T, Silver W. 2006. Dynamics of fine root carbon in Amazonian tropical ecosystems and the contribution of roots to soil respiration. *Global Change Biology* **12**: 217-229.

Trumbore SE, Gaudinski JB. 2003. The secret lives of roots. *Science* **302**: 1344-1345.

Tudhope AW, Chilcott CP, McCulloch MT, Cook ER, Chappell J, Ellam RM, Lea DW, Lough JM, Shimmield GB. 2001. Variability in the El Nino-Southern Oscillation through a glacial-interglacial cycle. *Science* **291**: 1511-1517.

Valentini R, **Matteucci G**, **Dolman AJ**, **Schulze ED**, **Rebmann C**, **Moors EJ**, **Granier A**, **Gross P**, **Jensen NO**, **Pilegaard K**, **Lindroth A**, **Grelle A**, **Bernhofer C**, **Grunwald T**, **Aubinet M**, **Ceulemans R**, **Kowalski AS**, **Vesala T**, **Rannik U**, **Berbigier P**, **Loustau D**, **Gudmundsson J**, **Thorgeirsson H**, **Ibrom A**, **Morgenstern K**, **Clement R. 2000.** Respiration as the main determinant of carbon balance in European forests. *Nature* **404**: 861-865.

Van Wijk MT, Bouten W, Verstraten JM. 2002. Comparison of different modelling strategies for simulating gas exchange of a Douglas-fir forest. *Ecological Modelling* **158**: 63-81.

Vance ED, Nadkarni NM. 1992. Root biomass distribution in a moist tropical montane forest. *Plant and Soil* **142**: 31-39.

Vogt KA, Vogt DJ, Bloomfield J. 1998. Analysis of some direct and indirect methods of estimating root biomass and production of forests at an ecosystem level. *Plant and Soil* **200**, 71-89

Vogt KA, Persson H. 1991. Root methods. In: Lassoie JP, Hinckley TM, eds. *Techniques and Approaches in Forest Tree Ecophysiology*. Florida, USA: CRC Press.

Vose JM, Ryan MG. 2002. Seasonal respiration of foliage, fine roots, and woody tissues in relation to growth, tissue N, and photosynthesis. *Global Change Biology* **8**: 182-193.

Weber MG. 1990. Forest soil respiration after cutting and burning in immature aspen ecosystems. *Forest Ecology and Management* **31**: 1-14.

Werth D, Avissar R. 2002. The local and global effects of Amazon deforestation. *Journal of Geophysical Research* **107**: D20, 8087, doi: 10.1029/2001/JD000717

West JB, Espeleta JF, Donovan LA. 2003. Root longevity and phenology differences between two co-occurring savanna bunchgrasses with different leaf habits. *Functional Ecology* **17**: 20-28.

Whalley WR, Bengough AG, Dexter AR. 1998. Water stress induced by PEG decreases the maximum growth pressure of the roots of pea seedlings. *Journal of Experimental Botany* **49**: 1689-1694.

Wiant HV. 1967. Contribution of soils to forest soil respiration. *Advances in the Frontiers of Plant Science* **18**: 163-167.

Widen B, Majdi H. 2001. Soil CO_2 efflux and root respiration at three sites in a mixed pine and spruce forest: seasonal and diurnal variation. *Canadian Journal of Forestry Research* **31**: 786-796.

Wigley TML, Briffa KR, Jones PD. 1984. Predicting plant productivity and water resources. *Nature* **312**: 102-103.

Williams M, Malhi Y, Nobre AD, Rastetter EB, Grace J, Pereira MGP. 1998. Seasonal variation in net carbon exchange and evapotranspiration in a Brazilian rain forest: a modelling analysis. *Plant, Cell and Environment* **21**: 953-968.

Williams M, Rastetter EB. 1999. Vegetation characteristics and primary productivity along an arctic transect: implications for scaling-up. *Journal of Ecology* **87**: 885–98.

Williams M, Schwarz PA, Law BE, Irvine J, Kurpius M. 2005. An improved analysis of forest carbon dynamics using data assimilation. *Global Change Biology* **11**: 89-105.

Williams M, Shimabukuro YE, Herbert DA, Pardi Lacruz S, Renno, C, Rastetter, EB. 2002. Heterogeneity of soils in an eastern Amazonian rain forest: implications for scaling up biomass and production. *Ecosystems* **5**: 692-704.

Williams M, Street L, van Wijk MT, Shaver GR. 2006. Identifying differences in carbon exchange among arctic ecosystem types. *Ecosystems* **9**: 288-304.

Williamson GB, Laurance WF, Oliveira AA, Delamonica P, Gascon C, Lovejoy TE, Pohl L. 2000. Amazonian tree mortality during the 1997 El Niño drought. *Conservation Biology* **14**: 1538–1542.

Winkler JP, Cherry RS, Schlesinger WH. 1996. The Q10 relationship of microbial respiration in a temperate forest soil. *Soil Biology and Biochemistry* **28**: 1067-1072

Withington JM, Elkin AD, Bulaj B, Olesinski J, Tracy KN, Bouma TJ, Oleksyn J, Anderson LJ, Modrzynski J, Reich PB, Eissenstat DM. 2003. The impact of material used for minirhizotron tubes for root research. *New Phytologist* **160**: 533-544.

Wofsy SC, Harriss RC, Kaplan WA. 1988. Carbon dioxide in the atmosphere over the Amazon basin. *Journal of Geophysical Research* **93**: 1377-1387.

Woodwell GM. 1983. Biotic effects on the concentration of atmospheric carbon dioxide: a review and projection. In: Legget J, ed. *Changing Climate*. Washington DC, USA: National Academy Press.

Wright SJ, Calderon O. 2006. Seasonal, El Niño and longer term changes in flower and seed production in a moist tropical forest. *Ecology Letters* **9**: 35–44.

Wright SJ, Cornejo FH. 1990. Seasonal drought and leaf fall in a tropical forest. *Ecology* **71**: 1165-1175.

Xu M, DeBiase TA, QI Y. 2000. A simple technique to measure stem respiration using a horizontally orientated soil chamber. *Canadian Journal of Forest Research* **30**: 1555-1560.

Xu X, Enoki T, Hirata E, Tokashiki Y. 2003. Pattern and chemical composition of fine litterfall in a subtropical forest in northern Okinawa Island, Japan. *Basic and Applied Ecology* **4**: 229-237.

Xu M, Qi Y. 2001. Soil surface CO_2 efflux and its spatial and temporal variation in a young ponderosa pine plantation in California. *Global Change Biology* **7**: 667-677.

Yim MH, Joo SJ, Shutou K, Nakane K. 2003. Spatial variability of soil respiration in a larch plantation: estimation of the number of measurement points required. *Forest Ecology and Management* **175**: 585-588.

Zak DR, Pregitzer KS, King JS, Holmes WE. 2000. Elevated atmospheric CO_2, fine roots and the response of soil micro-organisms: a review and hypothesis. *New Phytologist* **147**: 201-222.

Zogg GP, Zak DR, Burton AJ, Pregitzer KS. 1996. Fine root respiration in northern hardwood forests in relation to temperature and nitrogen availability. *Tree Physiology* **16**: 719-725.